Solvent Resistant Nanofiltration Membranes

Szymon Dutczak

Solvent Resistant Nanofiltration Membranes

Szymon Dutczak

ISBN: 978-90-365-3277-8

SOLVENT RESISTANT NANOFILTRATION MEMBRANES

This work was financially supported by Dutch Technology Foundation (STW) project no 07349.

Graduation committee

Chairman	
Prof. Dr. G. van der Steenhoven	University of Twente
Promotor	
Prof. Dr. -Ing. M. Wessling	University of Twente
Assistant promotor	
Dr. D. Stamatialis	University of Twente
Prof. Dr. Ir. A. Nijmeijer	University of Twente
Prof. Dr. Ir. R.G.H. Lammertink	University of Twente
Prof. Dr. -Ing. V. Jordan	Fachhochschule Münster
Prof. I. Vankelecom	Katholieke Universiteit Leuven
Dr. Ir. F.P. Cuperus	SolSep BV - Apeldoorn

Solvent resistant nanofiltration membranes
Szymon M. Dutczak, PhD Thesis, University of Twente, The Netherlands
ISBN: 978-90-365-3277-8

Cover design by S.M. Dutczak, pictures by S.M. Dutczak

Printed by: Gildeprint Drukkerijen, Enschede, The Netherlands

SOLVENT RESISTANT NANOFILTRATION MEMBRANES

DISSERTATION

to obtain
the degree of doctor at the University of Twente,
on the authority of the rector magnificus,
Prof. Dr. H. Brinksma,
on account of the decision of the graduation committee,
to be publicly defended
on Friday the 11th of November 2011 at 12:45

by

Szymon Maria Dutczak

born on 2nd of June 1982
in Kraków, Poland

This dissertation has been approved by:

Prof. Dr. -Ing. M. Wessling

Dr. D. Stamatialis

“If your experiment needs statistics, then you ought to have done a better experiment.”

Ernest Rutherford

This thesis is dedicated to my family

Table of contents

Chapter I

Introduction

S.M. Dutczak, M. Wessling, D. Stamatialis

1. Nanofiltration

The beginning of nanofiltration (NF), a membrane process capable of efficient separation of molecules in the range of 200-1000 g mol^{-1}, dates back to the late 1950s when Loeb and Sourirajan developed the first reverse osmosis (RO) asymmetric membrane for sea water desalination [1, 2]. In fact, rapid development of RO and ultrafiltration (UF) membranes at that time, led quickly to preparation of membranes which filled the gap in separation performance between RO and UF. Over the years NF proved useful in many applications such as water softening [3-7], removal of pesticide and micro-pollutants from ground water [8-16], treatment of textile wastewater [17-20], virus and bacteria removal [21-24], decontamination and recycling of industrial wastewater [25-29], as feed pretreatment for desalination [30-36] and removal of heavy metal ions from ground water [37-40].

The success of NF in aqueous systems has triggered expansion to organic solvents. In fact, in the late 1990s a new spin-off of NF, solvent resistant nanofiltration (SRNF) emerged. The first reported successful separations in organic solvents [41-44] showed high potential of SRNF. Low energy consumption, compared to traditional techniques like distillation, and ease of combining with already existing processes made SRNF particularly attractive for industrial applications. Low process temperature minimizing thermal degradation of sensitive molecules opened up a wide range of applications in the pharmaceutical industry. The now feasible, low cost solvents recycle could contribute to decrease of hazardous chemicals discharges to the environment. A significant contribution to the growing interest in SRNF was a relative ease of up-scaling [45]. However, the use of first generation of NF membranes, designed almost exclusively for aqueous systems, presented a lot of difficulties in organic solvents. Due to excessive swelling or even dissolution of membrane forming material loss of selectivity was often observed [46, 47]. An urgent need of better membranes for SRNF arose.

2. Solvent resistant nanofiltration membranes

Over the past decade a significant progress in SRNF membranes has been made. Various polymeric and ceramic membranes were prepared and studied for the use in organic solvents. With regard to chemical, thermal and mechanical stability, the most robust are ceramic membranes. They are usually prepared from materials such as alumina (Al_2O_3), zirconia (ZrO_2) or titania (TiO_2). Indisputable advantages of ceramic membranes are good selectivity, long life time and ease of cleaning [48, 49]. However, their large-scale production and module construction are relatively difficult and expensive. Due to intrinsic hydrophilicity of ceramics and consequently low flux of non-polar solvents, these membranes are less versatile in applications. In order to increase the transport of organic solvents, the surface of inorganic membranes can however, be hydrophobized via silylation grafting [50, 51]. So far, only few ceramic SRNF membranes are commercially available. The best known (and probably most studied) is a sylilated TiO_2-based membrane HITK-T1 produced by Fraunhofer-Institut für Keramische Technologien und Systeme – IKTS (former HITK, Hermsdorf, Germany) [45, 52].

Nowadays the majority of SRNF membranes are based on polymers. The reasons for that are wide choice of materials, relatively easy processing (coating or phase inversion) and good reproducibility. It is also much easier to tailor polymeric membrane to the application compared to ceramic membranes. The general disadvantages of polymeric materials are usually limited solvent and thermal stability. One of the first and most studied type of SRNF membranes are thin film composites comprising of a thin, dense poly (dimethylsiloxane) (PDMS) selective layer on poly acrylonitrile (PAN) [53-60] or polyimide porous supports [61]. Although PAN shows good stability in organic solvents, the PDMS selective layer swells extensively in non-polar solvents decreasing the solute rejection [54, 60, 62-64]. In order to suppress swelling additional plasma crosslinking can be performed [53]. This approach however results in significant decrease of fluxes. Much better results are obtained with PDMS top layer filled with ceramic particles such as zeolites [61, 65] or zeolite hollow spheres [66].

Majority of SRNF membranes obtained by phase inversion process are made from polyimides (PI) [49, 67-69]. PIs are attractive for membrane fabrication because of their excellent film-forming and mechanical properties as well as good thermal and chemical resistance [67, 70-74]. However, these membranes are unstable in some strong aprotic solvents including methylene chloride (DCM), tetrahydrofuran (THF), dimethyl formamide (DMF) and *n*-methyl pyrrolidone (NMP) [69, 70, 72]. To improve the polymer stability, crosslinking can be performed via UV irradiation, thermal treatment or chemical reactions [70-72, 75-77].

PI crosslinking was originally developed to improve performance of gas separation membranes. For organic solvent filtration, unlike for gas separation, the stability of both selective and support layers of the membrane are equally important. This implies that uniform crosslinking over entire membrane must be achieved. For this purpose, photo-crosslinking which only results in crosslinked selective top layer cannot be utilized. Thermal crosslinking is also not preferred since high temperature treatment may result in the densification of the membrane leading to flux decrease. In order to achieve throughout crosslinking, without significant change of separation behaviour of the membrane, chemical crosslinking can be performed. Toh et al. [72] obtained SRNF membranes by immersing P84 PI porous films in methanolic solution containing bi-functional amines. The resulted membrane had good separation performance in DMF with permeability of 1-8 l m^{-2} h^{-1} bar^{-1} and a MWCO between 250 and 400 g mol^{-1}. These membranes also had good chemical stability across a wide range of organic solvents including polar aprotic solvents such as DCM, THF, NMP and DMF. Similar method was employed by Vanherck et al., who utilized p-xylylenediamine to crosslink Matrimid PI membranes [77]. The modified membrane were stable in DMF, NMP, DMA and dimetilsulfoxide (DMSO), with DMF permeability up to 5.4 l m^{-2} h^{-1} bar^{-1} and rejections of Bengal Rose (1017 g mol^{-1}) and Methyl Orange (327 g mol^{-1}) of >98% and >95%, respectively. Only recently, Vanherck et al. reported simultaneous crosslinking and coagulation of P84 PI membranes using diamines [70]. This simplification of the crosslinking method, compared to the conventional post treatment process, can result in cheaper and simpler membrane fabrication.

Most of earlier mentioned literature is focussed on fabrication of SRNF flat membranes [45, 70, 72, 77]. In fact, there are only few publications on the fabrication of hollow fiber (HF) membranes. Loh et al. [78], developed polyaniline (PANi) HF membrane stable in acetone and DMF having acetone flux of 9 l m^{-2} h^{-1} and MWCO of approximately 350 g mol^{-1}. Kopeć et al. [79] reported a novel HF preparation method called “chemistry in a spinneret” which integrates crosslinking and membrane formation in a single step process. The prepared HF (P84 based, crosslinked with poly(ethyleneimine)) were insoluble in NMP, however no filtration of organic solvents was performed. Despite clear advantages of HF, such as a high surface to volume ratio, no need of spacers and much simpler construction of modules, all commercial SRNF membranes are exclusively available in flat sheet form or spiral-wound modules. Moreover, the choice of suppliers of these membranes is limited only to a few suppliers including Evonik (DuraMem and PuraMem P84 polyimide membranes) and SolSep BV (polyamide-imide and PDMS type membranes) occupying the most prominent places at the market [80].

It is evident that there is an urgent need of new SRNF membranes in order to cope with increasing separation demands in organic solvents. The development of novel flat membranes, more robust and better tailored to the applications as well as HF for higher efficiency is essential to make SRNF more attractive and more competitive separation technique.

3. MWCO of the membrane in organic solvents

A proper selection of a membrane for particular solvent/solute system is essential. To this end one needs a consistent and reliable method of molecular weight cut off (MWCO) characterization in organic solvents. Several procedures have been proposed including filtration of solutions containing alkanes [81], organic dyes [82, 83], various molecules of increasing weight such as polynuclear aromatic and organometallic compounds or quaternary ammonium salts [84-86], sugars or lipids [87], polyethylene glycols [54, 88] and polyisobutylenes [56]. The major drawback of the proposed methods is the fact that the test solutions contain a single solute. Consequently it is not possible to obtain a complete retention curve in one filtration experiment. Moreover, very often the proposed solutes have different chemical natures (e.g. various charges), thus different interactions with a membrane. All these issues may lead to complications in the interpretation of results of retention measurements. A more efficient method seems to be filtration of a mixture of homologues molecules of different molecular weight (MW). Voigt et.al [89] proposed filtration of mixture of narrow low-MW fractions of styrene oligomers dissolved in toluene. The use of neutral oligomers minimizes electrostatic interactions with the membrane, allowing more accurate retention measurements. Later, the concept was further developed by See Toh et al. [90]. Due to relatively high price of commercial mono-disperse styrene oligomers the method was limited to rather small, lab scale filtrations. In order to test large size membrane modules Zwijnenberg et al. [91] proposed synthesis of a broad range PS by n anionic living polymerization. Despite more than fifteen years of research on organic solvent filtration (OSF) there is currently no universal protocol for determination of the MWCO in organic solvents. The most promising and the most widely use one seems to be the filtration of solutions containing polystyrene oligomers. In Chapter 3 of this thesis, we will discuss critical issues related to the MWCO determination of membranes in organic solvents.

4. Applications of solvent resistant nanofiltration

Classical separations such as distillation, extraction, crystallization and chromatography are energy and solvent intensive. In the era of rapidly increasing energy costs end environmental concerns, it is important to develop more efficient processes generating less hazardous discharge. SRNF has potential to solve both issues. It offers substantial cost savings by lower energy consumption and significant reduction of waste by easy solvent recycle.

The petrochemical industry has already recognized the potential of SRNF. In the late 1990s ExxonMobil implemented an industrial scale (5800 m^3/day) installation for the recovery of dewaxing solvents (methyl ethyl ketone and toluene) from dewaxing lube oil filtrates [92-94]. Since then, other successful applications in petrochemical industry have been reported: enrichment of aromatic compounds in refinery streams [95], desulfurization of gasoline [96, 97] and deacidification of crude oil [98]. Recently Othman et al. demonstrated usefulness of organic solvent stable membranes in different separation and purification stages in the biodiesel production process [99].

Besides petrochemical industry, SRNF membranes have high potential in chemical synthesis. They were successfully applied for the recovery of organometallic complexes from organic solvents [100], separation of phase transfer catalyst (PTC) from toluene [101, 102] and for separation of homogeneous catalyst (MW > 450 g mol^{-1}) from reaction products [103, 104]. The recovery of homogeneous catalyst has been recently improved to 100% [105].

Synthesis of pharmaceuticals usually requires several changes of reaction medium, which is very often an organic solvent. This solvent exchange can be easily accomplished utilizing SRNF. In fact practical demonstration of this technique has been already reported by Sheth et al. and Lin et al. [97, 106]. Since membrane separations do not require elevated temperature, SRNF also seems to be ideal concentration and isolation technique for heat-sensitive bio-compounds. One example is the recovery of 6-aminopenicilannic acid (MW = 216 g mol^{-1}), an intermediate in the enzymatic manufacturing of synthetic penicillin [98, 107].

The benefits of SRNF implementation in the food industry, especially in the production of edible oil are also substantial. The membrane technology could potentially reduce oil loss of 75% saving at the same time 15-22 trillion kJ per year in the USA alone [45]. The efficiency of SRNF in edible oil processing has been by now demonstrated practically in vegetable oil and sunflower oil processing [108-111]. Moreover, as shown by Darnoko et al., SRNF as a non-destructive separation technique can create valuable by-products like carotenoids useful in cosmetics [45, 112].

Despite all the advantages and already proved large scale application [93, 96] the chemical industry is often reluctant to adopt SRNF. The general hesitation of process engineers in implementing new separation technologies, together with limited choice of membranes, which are often not robust enough, hampers the advance of SRNF. With this end in view further development of membranes, focusing on improvement of chemical resistance, long term stability and separation performance is critical. The development and characterization of new membranes is the main scope of this thesis.

5. Scope and structure of the thesis

This thesis describes preparation and characterization of membranes for separations in organic solvents. Chapters 2-4 focus more on development and characterization of SRNF membranes, whereas chapter 5 describes spinning relatively open integrally skinned polyimide hollow (HF) fibers for OSF.

In **Chapter 2** the preparation and characterization of capillary α-alumina / poly(dimethylsiloxane) (PDMS) composite membranes is described. The composites are prepared by coating a tailor made PDMS coating solution on a ceramic support.

In **Chapter 3** effects of solvent, solute, membrane properties, and the applied process conditions, on molecular weight cut off (MWCO) characterization in organic solvents is studied. For this two membranes are selected; a rigid porous (hydrophobized zirconia) and a rubbery dense (α-alumina / PDMS composite homemade hollow fiber). The retention behavior of two solutes a stiff (polystyrene) and a flexible one (polyisobutylene) in two solvents toluene and n-hexane) are studied.

In **Chapter 4** a new crosslinking method of polyamide-imide NF membranes is developed. The prepared membranes are characterized by filtration experiments in acetone and N-methyl pyrrolidone (NMP) which is a solvent of the non crosslinked polyamine - imide membrane.

In **Chapter 5** we use “chemistry in a spinneret” for fabricating membranes for organic solvent filtration (OSF). The interplay between crosslinking and phase inversion during membrane formation is studied by systematic variations of bore liquid composition including solvent / non-solvent ratio and crosslinker (PEI) concentration. The crosslinking of the membranes is evaluated by ATR-FTIR and immersion tests in NMP. The performance of selected membranes (MWCO and permeance) is evaluated by filtration of toluene / PS and ethanol / PEG solutions.

Finally, in **Chapter 6** general conclusions and reflections on various challenges encountered during this this thesis are discussed and an outlook is given on future directions in development of membranes for filtration of organic solvents.

References

[1] S. Loeb, The Loeb-Sourirajan Membrane: How It Came About, in: Synthetic Membranes:, American Chemical Society, 1981, pp. 1-9.

[2] A. Schaefer, A. Fane, T. Waite, Nanofiltration - Principles and Applications, Elsevier, Oxford, 2005.

[3] R.A. Bergman, Membrane softening versus lime softening in Florida: A cost comparison update, Desalination, 102 (1995) 11-24.

[4] R.A. Bergman, Cost of membrane softening in Florida, J. Am. Water. Works. Assoc., 88 (1996) 32-43.

[5] J. Schaep, B. Van Der Bruggen, S. Uytterhoeven, R. Croux, C. Vandecasteele, D. Wilms, E. Van Houtte, F. Vanlerberghe, Remvoal of hardness from groundwater by nanofiltration, Desalination, 119 (1998) 295-302.

[6] H.D.M. Sombekke, D.K. Voorhoeve, P. Hiemstra, Environmental impact assessment of groundwater treatment with nanofiltration, Desalination, 113 (1997) 293-296.

[7] B.M. Watson, C.D. Hornburg, Low-energy membrane nanofiltration for removal of color, organics and hardness from drinking water supplies, Desalination, 72 (1989) 11-22.

[8] P. Berg, G. Hagmeyer, R. Gimbel, Removal of pesticides and other micropollutants by nanofiltration, Desalination, 113 (1997) 205-208.

[9] G. Ducom, C. Cabassud, Interests and limitations of nanofiltration for the removal of volatile organic compounds in drinking water production, Desalination, 124 (1999) 115-123.

[10] Y. Kiso, A. Mizuno, R.A.A.B. Othman, Y.J. Jung, A. Kumano, A. Ariji, Rejection properties of pesticides with a hollow fiber NF membrane (HNF-1), Desalination, 143 (2002) 147-157.

[11] Y. Kiso, Y. Nishimura, T. Kitao, K. Nishimura, Rejection properties of non - phenylic pesticides with nanofiltration membranes, J. Membr. Sci., 171 (2000) 229-237.

[12] T. Montovay, M. Assenmacher, F.H. Frimmel, Elimination of pesticides from aqueous solution by nanofiltration, Magy. Kem. Foly., 102 (1996) 241-247.

[13] B. Van der Bruggen, K. Everaert, D. Wilms, C. Vandecasteele, The use of nanofiltration for the removal of pesticides from groundwater: An evaluation, Wa. Sci. Technol., 1 (2001) 99-106.

[14] B. Van Der Bruggen, K. Everaert, D. Wilms, C. Vandecasteele, Application of nanofiltration for removal of pesticides, nitrate and hardness from ground water: Rejection properties and economic evaluation, J. Membr. Sci., 193 (2001) 239-248.

[15] B. Van Der Bruggen, J. Schaep, W. Maes, D. Wilms, C. Vandecasteele, Nanofiltration as a treatment method for the removal of pesticides from ground waters, Desalination, 117 (1998) 139-147.

[16] E. Wittmann, P. Cote, C. Medici, J. Leech, A.G. Turner, Treatment of a hard borehole water containing low levels of pesticide by nanofiltration, Desalination, 119 (1998) 347-352.

[17] C. Tang, V. Chen, Nanofiltration of textile wastewater for water reuse, Desalination, 143 (2002) 11-20.

[18] I. Voigt, M. Stahn, S. Wöhner, A. Junghans, J. Rost, W. Voigt, Integrated cleaning of coloured waste water by ceramic NF membranes, Sep. Purif. Technol., 25 (2001) 509-512.

[19] R. Weber, H. Chmiel, V. Mavrov, Characteristics and application of new ceramic nanofiltration membranes, Desalination, 157 (2003) 113-125.

[20] A. Bes-Pia, J.A. Mendoza-Roca, L. Roig-Alcover, A. Iborra-Clar, M.I. Iborra-Clar, M.I. Alcaina-Miranda, Comparison between nanofiltration and ozonation of biologically treated textile wastewater for its reuse in the industry, Desalination, 157 (2003) 81-86.

[21] P. Laurent, P. Servais, D. Gatel, G. Randon, P. Bonne, J. Cavard, Microbiological quality before and after nanofiltration, J. Am. Water. Works. Assoc., 91 (1999) 62-72.

[22] M.T. Yahya, C.B. Cluff, C.P. Gerba, Virus removal by slow sand filtration and nanofiltration, Water Sci. Technol., 27 (1993) 445-448.

[23] M. Otaki, K. Yano, S. Ohgaki, Virus removal in a membrane separation process, Water Sci. Technol., 37 (1998) 107-116.

[24] T. Urase, K. Yamamoto, S. Ohgaki, Effect of pore structure of membranes and module configuration on virus retention, J. Membr. Sci., 115 (1996) 21-29.

[25] M. Afonso, R. Yaez, Nanofiltration of wastewater from the fishmeal industry, Desalination, 139 (2001) 429.

[26] R. Rautenbach, T. Linn, High-pressure reverse osmosis and nanofiltration, a "zero discharge" process combination for the treatment of waste water with severe fouling/scaling potential, Desalination, 105 (1996) 63-70.

[27] R. Rautenbach, T. Linn, L. Eilers, Treatment of severely contaminated waste water by a combination of RO, high-pressure RO and NF - Potential and limits of the process, J. Membr. Sci., 174 (2000) 231-241.

[28] V. Geraldes, M.N. De Pinho, Process water recovery from pulp bleaching effluents by an NF/ED hybrid process, J. Membr. Sci., 102 (1995) 209-221.

[29] B. Schlichter, V. Mavrov, H. Chmiel, Study of a hybrid process combining ozonation and membrane filtration - Filtration of model solutions, Desalination, 156 (2003) 257-265.

[30] A.M. Hassan, M.A.K. Al-Sofi, A.S. Al-Amoudi, A.T.M. Jamaluddin, A.M. Farooque, A. Rowaili, A.G.I. Dalvi, N.M. Kither, G.M. Mustafa, I.A.R. Al-Tisan, A new approach to membrane and thermal seawater desalination processes using nanofiltration membranes (Part 1), Desalination, 118 (1998) 35-51.

[31] M.A.K. Al-Sofi, A.M. Hassan, G.M. Mustafa, A.G.I. Dalvi, M.N.M. Kither, Nanofiltration as a means of achieving higher TBT of ≥ 120°C in MSF, Desalination, 118 (1998) 123-129.

[32] M. Abdul-Kareem Al-Sofi, Seawater desalination - SWCC experience and vision, Desalination, 135 (2001) 121-139.

[33] A.M. Hassan, A.M. Farooque, A.T.M. Jamaluddin, A.S. Al-Amoudi, M.A. Al-Sofi, A.F. Al-Rubaian, N.M. Kither, I.A.R. Al-Tisan, A. Rowaili, Demonstration plant based on the new NF-SWRO process, Desalination, 131 (2000) 157-171.

[34] A. Criscuoli, E. Drioli, Energetic and exergetic analysis of an integrated membrane desalination system, Desalination, 124 (1999) 243-249.

[35] M.S. Mohsen, J.O. Jaber, M.D. Afonso, Desalination of brackish water by nanofiltration and reverse osmosis, Desalination, 157 (2003) 167.

[36] M. Pontie, C. Diawara, M. Rumeau, D. Aureau, P. Hemmery, Seawater nanofiltration (NF): Fiction or reality?, Desalination, 158 (2003) 277-280.

[37] N. Hilal, H. Al-Zoubi, N.A. Darwish, A.W. Mohammad, M. Abu Arabi, A comprehensive review of nanofiltration membranes: Treatment, pretreatment, modelling, and atomic force microscopy, Desalination, 170 (2004) 281-308.

[38] A.G. Pervov, E.V. Dudkin, O.A. Sidorenko, V.V. Antipov, S.A. Khakhanov, R.I. Makarov, RO and NF membrane systems for drinking water production and their maintenance techniques, Desalination, 132 (2000) 315-321.

[39] O. Raff, R.D. Wilken, Removal of dissolved uranium by nanofiltration, Desalination, 122 (1999) 147-150.

[40] T. Urase, J.I. Oh, K. Yamamoto, Effect of pH on rejection of different species of arsenic by nanofiltration, Desalination, 117 (1998) 11-18.

[41] K. Ebert, P. Cuperus, Solvent resistant nanofiltration membranes in edible oil processing, Membr. Technol., (1999) 5-8.

[42] D.R. MacHado, D. Hasson, R. Semiat, Effect of solvent properties on permeate flow through nanofiltration membranes. Part I: Investigation of parameters affecting solvent flux, J. Membr. Sci., 163 (1999) 93-102.

[43] H.J. Zwijnenberg, A.M. Krosse, K. Ebert, K.V. Peinemann, F.P. Cuperus, Acetone-stable nanofiltration membranes in deacidifying vegetable oil, J. Am. Oil Chem. Soc., 76 (1999) 83-87.

[44] D.R. Machado, D. Hasson, R. Semiat, Effect of solvent properties on permeate flow through nanofiltration membranes. Part II: Transport model, J. Membr. Sci., 166 (2000) 63-69.

[45] P. Vandezande, L.E.M. Gevers, I.F.J. Vankelecom, Solvent resistant nanofiltration: Separating on a molecular level, Chem. Soc. Rev., 37 (2008) 365-405.

[46] S. Darvishmanesh, J.C. Jansen, F. Tasselli, E. Tocci, P. Luis, J. Degrčve, E. Drioli, B. Van der Bruggen, Novel polyphenylsulfone membrane for potential use in solvent nanofiltration, J. Membr. Sci., In Press, Corrected Proof.

[47] B. Van der Bruggen, J. Geens, C. Vandecasteele, Influence of organic solvents on the performance of polymeric nanofiltration membranes, Sep. Sci. Technol., 37 (2002) 783-797.

[48] M. Mulder, Basic principles of membrane technology, second ed., Kluwer Academic Publishers, The Netherlands, 1997.

[49] A.V. Volkov, G.A. Korneeva, G.F. Tereshchenko, Organic solvent nanofiltration: prospects and application, Russ. Chem. Rev., 77 (2008) 983-993.

[50] T. Tsuru, M. Miyawaki, H. Kondo, T. Yoshioka, M. Asaeda, Inorganic porous membranes for nanofiltration of nonaqueous solutions, Sep. Purif. Technol., 32 (2003) 105-109.

[51] B. Verrecht, R. Leysen, A. Buekenhoudt, C. Vandecasteele, B.V.d. Bruggen, Chemical surface modification of γ-Al2O3 and TiO2 toplayer membranes for increased hydrophobicity, Desalination, 200 (2006) 385.

[52] J. Geens, K. Boussu, C. Vandecasteele, B.V.d. Bruggen, Modelling of solute transport in non - aqueous nanofiltration, J. Membr. Sci., 281 (2006) 139-148.

[53] S. Aerts, A. Vanhulsel, A. Buekenhoudt, H. Weyten, S. Kuypers, H. Chen, M. Bryjak, L.E.M. Gevers, I.F.J. Vankelecom, P.A. Jacobs, Plasma-treated PDMS - membranes in solvent resistant nanofiltration: Characterization and study of transport mechanism, J. Membr. Sci., 275 (2006) 212.

[54] K. Ebert, J. Koll, M.F.J. Dijkstra, M. Eggers, Fundamental studies on the performance of a hydrophobic solvent stable membrane in non - aqueous solutions, J. Membr. Sci., 285 (2006) 75-80.

[55] N. Stafie, Poly(dimethyl siloxane) – based composite nanofiltration membranes for non-aqueous applications, Ph.D. thesis, University of Twente, Enschede, The Netherlands, (2004).

[56] N. Stafie, D.F. Stamatialis, M. Wessling, Insight into the transport of hexane-solute systems through tailor - made composite membranes, J. Membr. Sci., 228 (2004) 103-116.

[57] N. Stafie, D.F. Stamatialis, M. Wessling, Effect of PDMS cross-linking degree on the permeation performance of PAN/PDMS composite nanofiltration membranes, Sep. Purif. Technol., 45 (2005) 220-231.

[58] D.F. Stamatialis, N. Stafie, K. Buadu, M. Hempenius, M. Wessling, Observations on the permeation performance of solvent resistant nanofiltration membranes, J. Membr. Sci., 279 (2006) 424-433.

[59] E.S. Tarleton, J.P. Robinson, C.R. Millington, A. Nijmeijer, M.L. Taylor, The influence of polarity on flux and rejection behaviour in solvent resistant nanofiltration - Experimental observations, J. Membr. Sci., 278 (2006) 318-327.

[60] E.S. Tarleton, J.P. Robinson, M. Salman, Solvent - induced swelling of membranes - Measurements and influence in nanofiltration, J. Membr. Sci., 280 (2006) 442-451.

[61] L.E.M. Gevers, S. Aldea, I.F.J. Vankelecom, P.A. Jacobs, Optimisation of a lab - scale method for preparation of composite membranes with a filled dense top-layer, J. Membr. Sci., 281 (2006) 741-746.

[62] J.P. Robinson, E.S. Tarleton, C.R. Millington, A. Nijmeijer, Solvent flux through dense polymeric nanofiltration membranes, J. Membr. Sci., 230 (2004) 29-37.

[63] J.P. Robinson, E.S. Tarleton, C.R. Millington, A. Nijmeijer, Evidence for swelling - induced pore structure in dense PDMS nanofiltration membranes, Filtration, 4 (2004) 50-56.

[64] E.S. Tarleton, J.P. Robinson, S.J. Smith, J.J.W. Na, New experimental measurements of solvent induced swelling in nanofiltration membranes, J. Membr. Sci., 261 (2005) 129-135.

[65] L.E.M. Gevers, I.F.J. Vankelecom, P.A. Jacobs, Zeolite filled polydimethylsiloxane (PDMS) as an improved membrane for solvent-resistant nanofiltration (SRNF), Chem. Commun., (2005) 2500-2502.

[66] K. Vanherck, A. Aerts, J. Martens, I. Vankelecom, Hollow filler based mixed matrix membranes, Chem. Commun., 46 (2010) 2492-2494.

[67] C. Ba, J. Langer, J. Economy, Chemical modification of P84 copolyimide membranes by polyethylenimine for nanofiltration, J. Membr. Sci., 327 (2009) 49-58.

[68] J. Ren, Z. Li, F.-S. Wong, Membrane structure control of BTDA-TDI/MDI (P84) co-polyimide asymmetric membranes by wet-phase inversion process, J. Membr. Sci., 241 (2004) 305-314.

[69] A.G. Livingston, Y.H. See-Toh, Asymmetric membranes for use in nanofiltration, in: P.A. Publication (Ed.), Imperial Innovations Limited, United States, 2010.

[70] K. Vanherck, A. Cano-Odena, G. Koeckelberghs, T. Dedroog, I. Vankelecom, A simplified diamine crosslinking method for PI nanofiltration membranes, J. Membr. Sci., 353 (2010) 135-143.

[71] W. Albrecht, B. Seifert, T. Weigel, M. Schossig, A. Hollander, T. Groth, R. Hilke, Amination of poly(ether imide) membranes using di- and multivalent amines, Macromol. Chem. Phys., 204 (2003) 510-521.

[72] Y.H.S. Toh, F.W. Limb, A.G. Livingston, Polymeric membranes for nanofiltration in polar aprotic solvents, J. Membr. Sci., 301 (2007) 3-10.

[73] Y. Liu, R. Wang, T.-S. Chung, Chemical cross - linking modification of polyimide membranes for gas separation, J. Membr. Sci., 189 (2001) 231-239.

[74] D.T. Clausi, W.J. Koros, Formation of defect - free polyimide hollow fiber membranes for gas separations, J. Membr. Sci., 167 (2000) 79-89.

[75] H. Kita, T. Inada, K. Tanaka, K.-I. Okamoto, Effect of photocrosslinking on permeability and permselectivity of gases through benzophenone - containing polyimide, J. Membr. Sci., 87 (1994) 139-147.

[76] A. Bos, I. Punt, H. Strathmann, M. Wessling, Suppression of gas separation membrane plasticization by homogeneous polymer blending, AIChE Journal, 47 (2001) 1088-1093.

[77] K. Vanherck, P. Vandezande, S.O. Aldea, I.F.J. Vankelecom, Cross-linked polyimide membranes for solvent resistant nanofiltration in aprotic solvents, J. Membr. Sci., 320 (2008) 468–476.

[78] X.X. Loh, M. Sairam, J.H.G. Steinke, A.G. Livingston, A. Bismarck, K. Li, Polyaniline hollow fibres for organic solvent nanofiltration, Chem. Commun., (2008) 6324-6326.

[79] K.K. Kopec, S.M. Dutczak, M. Wessling, D.F. Stamatialis, Chemistry in a spinneret - On the interplay of crosslinking and phase inversion during spinning of novel hollow fiber membranes, J. Membr. Sci., (2011).

[80] A. Verhoef, A. Figoli, B. Leen, B. Bettens, E. Drioli, B. Van der Bruggen, Performance of a nanofiltration membrane for removal of ethanol from aqueous solutions by pervaporation, Sep. Purif. Technol., 60 (2008) 54-63.

[81] L.S. White, Transport properties of a polyimide solvent resistant nanofiltration membrane, J. Membr. Sci., 205 (2002) 191-202.

[82] D. Bhanushali, S. Kloos, D. Bhattacharyya, Solute transport in solvent - resistant nanofiltration membranes for non - aqueous systems: Experimental results and the role of solute-solvent coupling, J. Membr. Sci., 208 (2002) 343-359.

[83] X.J. Yang, A.G. Livingston, L. Freitas Dos Santos, Experimental observations of nanofiltration with organic solvents, J. Membr. Sci., 190 (2001) 45-55.

[84] J. Geens, A. Hillen, B. Bettens, B. Van der Bruggen, C. Vandecasteele, Solute transport in non - aqueous nanofiltration: Effect of membrane material, J. Chem. Technol. Biotechnol., 80 (2005) 1371-1377.

[85] E. Gibbins, M. D'Antonio, D. Nair, L.S. White, L.M. Freitas dos Santos, I.F.J. Vankelecom, A.G. Livingston, Observations on solvent flux and solute rejection across solvent resistant nanofiltration membranes, Desalination, 147 (2002) 307-313.

[86] E.S. Tarleton, J.P. Robinson, C.R. Millington, A. Nijmeijer, Non-aqueous nanofiltration: Solute rejection in low - polarity binary systems, J. Membr. Sci., 252 (2005) 123-131.

[87] J. Kwiatkowski, M. Cheryan, Performance of nanofiltration membranes in ethanol, Sep. Sci. Technol., 40 (2005) 2651-2662.

[88] T. Tsuru, T. Sudoh, T. Yoshioka, M. Asaeda, Nanofiltration in non-aqueous solutions by porous silica-zirconia membranes, J. Membr. Sci., 185 (2001) 253-261.

[89] I. Voigt, P. Puhlfürß, T. Holborn, G. Dudziak, M. Mutter, A. Nickel, Ceramic nanofiltration membranes for applications in organic solvents, in: 9th Aachen Membrane Colloquium, Aachen, Germany, 2003, pp. pOP 20-21-OP 20-11.

[90] Y.H. See Toh, X.X. Loh, K. Li, A. Bismarck, A.G. Livingston, In search of a standard method for the characterisation of organic solvent nanofiltration membranes, J. Membr. Sci., 291 (2007) 120-125.

[91] H.J. Zwijnenberg, A standardized characterization method for solvent resistant nanofiltration membrane modules, in: ICOM Presentation, 2005.

[92] R.M. Gould, A.R. Nitsch, Lubricating oil dewaxing with membrane separation of cold solvent, in, 1996.

[93] L.S. White, A.R. Nitsch, Solvent recovery from lube oil filtrates with a polyimide membrane, J. Membr. Sci., 179 (2000) 267-274.

[94] N.A. Bhore, R.M. Gould, S.M. Jacob, P.O. Staffeld, D, P.H. Smiley, C.R. Wildemuth, New membrane process debottlenecks solvent dewaxing unit, Oil Gas J., 97 (1999) 67.

[95] L.S. White, C.R. Wildemuth, Aromatics Enrichment in Refinery Streams Using Hyperfiltration, Ind. Eng. Chem. Res., 45 (2006) 9136-9143.

[96] L.S. White, Development of large - scale applications in organic solvent nanofiltration and pervaporation for chemical and refining processes, J. Membr. Sci., 286 (2006) 26-35.

[97] J.C.T. Lin, A.G. Livingston, Nanofiltration membrane cascade for continuous solvent exchange, Chem. Eng. Sci., 62 (2007) 2728-2736.

[98] M. Kyburz, W. Meindersma, in: A.I. Schafer, A.G. Fane, T.D. White (Eds.) Nanofiltration. Principles and Applications, Elsevier, 2005, pp. 329–361.

[99] R. Othman, A.W. Mohammad, M. Ismail, J. Salimon, Application of polymeric solvent resistant nanofiltration membranes for biodiesel production, J. Membr. Sci., 348 (2010) 287-297.

[100] J.T. Scarpello, D. Nair, L.M. Freitas dos Santos, L.S. White, A.G. Livingston, The separation of homogeneous organometallic catalysts using solvent resistant nanofiltration, J. Membr. Sci., 203 (2002) 71-85.

[101] A. Livingston, L. Peeva, S. Han, D. Nair, S.S. Luthra, L.S. White, L.M. Freitas Dos Santos, Membrane Separation in Green Chemical Processing, Ann. N. Y. Acad. Sci., 984 (2003) 123-141.

[102] S.S. Luthra, X. Yang, L.M. Freitas dos Santos, L.S. White, A.G. Livingston, Homogeneous phase transfer catalyst recovery and re-use using solvent resistant membranes, J. Membr. Sci., 201 (2002) 65-75.

[103] A. Livingston, L. Peeva, S. Han, D. Nair, S.S. Luthra, L.S. White, L.M.F.D. Santos, Membrane Separation in Green Chemical Processing: Solvent Nanofiltration in Liquid Phase Organic Synthesis Reactions, Ann. Ny. Acad. Sci., 984 (2003) 123–141.

[104] N.J. Ronde, D. Vogt, in: D.J.C.-H.a.R.P. Tooze (Ed.) Catalysis by Metal Complexes. Catalyst Separation, Recovery and Recycling, Chemistry and Process Design, Springer, The Netherlands, pp. 73–104.

[105] A.G. Livingston, Organic Solvent nanofiltration - emerging technology, in: ICOM 2011, Amsterdam, The Netherlands, 2011.

[106] J.P. Sheth, Y. Qin, K.K. Sirkar, B.C. Baltzis, Nanofiltration-based diafiltration process for solvent exchange in pharmaceutical manufacturing, J. Membr. Sci., 211 (2003) 251-261.

[107] X. Cao, X.Y. Wu, T. Wu, K. Jin, B.K. Hur, Concentration of 6-aminopenicillanic acid from penicillin bioconversion solution and its mother liquor by nanofiltration membrane, Biotechnol. Bioprocess Eng., 6 (2001) 200-204.

[108] S.S. Koseoglu, D.E. Engelgau, Membrane applications and research in the edible oil industry: An assessment., J. Am. Oil Chem. Soc., 67 (1990) 239–249.

[109] G. Bargeman, M. Timmer, C.v.d. Horst, Nanofiltration in the food industry, in: A. I. Schafer, A.G. Fane, T.D. White (Eds.) Nanofiltration. Principles and Applications, Elsevier Advanced Technology, 2005, pp. 306-328.

[110] L. Lin, K.C. Rhee, S.S. Koseoglu, Bench - scale membrane degumming of crude vegetable oil: Process optimization, J. Membr. Sci., 134 (1997) 101-108.

[111] R. Subramanian, K.S.M.S. Raghavarao, H. Nabetani, M. Nakajima, T. Kimura, T. Maekawa, Differential permeation of oil constituents in nonporous denser polymeric membranes, J. Membr. Sci., 187 (2001) 57-69.

[112] D. Darnoko, M. Cheryan, Carotenoids from red palm methyl esters by nanofiltration, J. Am. Oil Chem. Soc., 83 (2006) 365-370.

Chapter II

Composite capillary membrane for solvent resistant nanofiltration

S.M. Dutczak, M.W.J. Luiten-Olieman, H.J. Zwijnenberg, L.A.M. Bolhuis-Versteeg,

L. Winnubst, M.A. Hempenius, N.E. Benes, M. Wessling, D. Stamatialis

Dutczak, S.M. et al. J. Membr. Sci. 2011. 372(1-2): p. 182-190.

Abstract

Solvent resistant nanofiltration (SRNF) is a membrane separation process allowing for an efficient separation of small molecules of 200-1000 g mol^{-1} from organic solvents. The application of SRNF in industry applications is currently hindered by a limited choice of SRNF membranes and configurations. Despite clear advantages of capillary membranes (high surface to volume ratio, no spacers required and therefore more compact and simpler modules can be built), commercial SRNF membranes are almost exclusively produced in a spiral wound form. In this work, we prepare and study SRNF composite capillary membranes made of an α-alumina support and a selective poly(dimethylsiloxane) (PDMS) top layer. We combine the advantages of a ceramic support such as high mechanical, thermal and chemical stability with very good separation properties of the PDMS coating. All composite membranes are systematically investigated including: permeation experiments (permeance / molecular weight cut – off, MWCO) using a high pressure set-up and study of morphology using SEM imaging. The prepared composite capillary membranes are stable for at least 40 h in toluene and have MWCO of 500 g mol^{-1}.

1. Introduction

Solvent resistant nanofiltration (SRNF) is an energy-efficient separation process with high potential in many branches of industry, ranging from petro-chemistry [1] to pharmaceuticals [2-6]. SRNF is a relatively new membrane process capable of effective separation of molecules in the range of 200-1000 g mol^{-1} in various organic solvents. Most of the SRNF membranes reported in the literature are either asymmetric integrally skinned made of polyimides (PI) [7] or composites comprising of a thin poly(dimethylsiloxane) (PDMS) separating layer on a polyacrylonitrile (PAN) [8-15] or PI porous support [16]. In order to improve chemical resistance of PI membranes to organic solvents, a diamine crosslinking step has been applied, too [17, 18]. The crosslinking can be performed as a post casting process or be incorporated into the phase inversion process itself [19].

In the industry, the majority of the organic solvent nanofiltration processes use commercial polymeric membranes which are exclusively in a spiral wound form (e.g. SolSep NF 030306; MET Starmem™). The MPS-50 has been applied for example in pharmaceutical manufacturing for solvent exchange [4] or for the recovery of organometallic complexes from organic solvents [20] but it is not available any more (its production was discontinued a few years ago). The Starmem™ PI membranes have been used to separate phase transfer catalyst (PTC) from toluene [21, 22] and for the recovery of dewaxing solvents (e.g. toluene) from dewaxed lube oil filtrates in petrochemistry [23]. A recent publication also showed, that SolSep membranes can be successfully used in different separation and purification stages in the biodiesel production process [24].

It is well known that a membrane in hollow fiber (HF) or capillary form has some advantages over membranes in a flat sheet configuration. A capillary/HF membrane provides a high surface to volume ratio, does not require spacers and thus enables the design of more compact and much simpler modules. Unfortunately, there are neither SRNF hollow fibers nor capillary membranes commercially available and literature reports very little on this topic. Only recently X. Loh et al. developed polyaniline (PANI) hollow fibers with good stability in dimethylformamide and acetone [25].

It is obvious, that there is need to develop SRNF hollow fiber / capillary membranes to make SRNF a more attractive and more competitive separation technique. To this end, in this work we prepare composite capillary membranes, made of a commercial Hyflux InoCep M20 α-alumina capillary support and a selective poly(dimethylsiloxane) (PDMS) top layer. In contrast to polymeric support membranes [6, 26] ceramic materials do not compact at high pressures and are inert to virtually all organic solvents making them excellent candidates for membrane supports. As a separation layer we chose PDMS due to its well established position in SRNF. To the best of our knowledge, this work is the first reporting composite α-alumina/PDMS capillary membranes for SRNF. Other studies developed capillary/hollow fibers or tubular membranes based on a PDMS selective layer but only for pervaporation or VOC removal [27-30]. All composite membranes are systematically investigated including permeation experiments (permeance / MWCO) using a high pressure cross flow set-up and study of morphology using SEM imaging.

1. Experimental

1.1. Materials

InoCep™ M20 ceramic capillaries (I.D. 2.8 mm, O.D. 3.8 mm) made of α-alumina were purchased from HyFlux Ltd. (The Netherlands). The pore size on the inside of the capillary was 20 nm and 800 nm on the outside (as reported by the manufacturer). Toluene (for analysis) was purchased from Merck (The Netherlands), styrene (ReagentPlus ≥99%), *sec*-buthyllithium solution (1.4 M in cyclohexane), were purchased from Sigma Aldrich (The Netherlands) and used as supplied. General Electric PDMS RTV 615 kit was purchased from Permacol B.V. (The Netherlands). The silicone kit consisted of two components; a vinyl terminated pre-polymer (RTV-A) and a Pt-catalyzed cross-linker (RTV-B) containing a polyhydrosilane component. A two component epoxy resin Araldite® 2014-1 obtained from Viba (The Netherlands) was used as potting in module preparation with membranes having the selective layer on the outside of the capillary.

Sauereisen electrical cement No. DW-30 was purchased from Sepp Zeug Gmbh & Co. Kg Adhesive Cements (Germany), and used as a potting material for modules where the selective layer was on the inside of the capillary.

1.2. Preparation of the coating solution

RTV 615 pre-polymer (RTV-A) was dissolved in toluene. The solution was first brought to 60°C under reflux and stirring, and then the crosslinking component (RTV-B) was added. The concentration of PDMS solution was 15% (w/w). After addition of the RTV-B component, the exact timing of the crosslinking reaction was started. The crosslinking reaction was carried out in three steps. In the first step, the temperature of the reaction was kept at 60°C for 150 min and then the temperature was decreased to 50°C. The reaction continued till the solution reached a viscosity of about 100 mPa s. In the next step, the viscous solution was diluted with toluene to 7.5% (w/w) and the crosslinking was continued at 60°C till the solution reached a viscosity of about 100 mPa s. Finally in step 3, the solution was diluted with toluene to 3.7% (w/w) and reaction was continued at 60°C until a desired viscosity was reached. The solution of the pre-crosslinked PDMS was cooled down in an ice bath to stop the reaction. All viscosity measurements were performed at 25°C using a Brookfield DV-II+ Pro viscometer using a spindle nr-61 (ø18.9 mm) and glass cylinder (ø26 mm).

1.3. Composite membrane preparation

The composite membranes were prepared in an ISO-6 class dust free room. The membranes with the selective layer on the outside of the support were prepared by dip-coating in the pre-crosslinked PDMS/toluene solution. The coating was performed using an automated set-up adjusted to an immersion / pull up velocity of 0.9 cm/s and a contact time of 30 s. The membranes with the selective layer on the inside of the support were prepared using a communicating vessel principle. The capillary support was fixed in a vertical position and its bottom end was connected by a flexible (polyurethane) hose with the bottom part of a vessel

containing a PDMS coating solution. The change of the level of the PDMS coating solution inside the capillary support was regulated by rising-lowering the vessel with the PDMS coating solution. The filling/emptying velocity and the contact time were controlled by the automated set-up at 0.9 cm/s and at 30 s respectively. In both cases, a single coating was performed after which the membranes were left at room temperature for 30 min to evaporate the solvent. Subsequently, the coated tubes were put into an oven at 60°C for 8 h to complete the crosslinking reaction. The produced membranes coated on the outside are named M800/X whereas those coated on the inside M20/X, where X is the viscosity (in mPa s) of PDMS solution used for coating.

1.4. Module preparation

The composite membranes were potted in cross-flow stainless steel modules. Each module contained one capillary of 155 mm active length. The membrane area of each M800/X module was 1.86×10^{-3} m^2 and of the M20/X was 1.36×10^{-3} m^2. Araldite® 2014-1 was used as a potting material for membranes M800/X. The resin was allowed to set at room temperature for minimum 24 h before using the module for permeation experiments. The M20/X membranes were potted with Sauereisen electrical cement No. DW-30 cured at room temperature for minimum 48 h. If the Araldite® 2014-1 is used there, the membranes crack due to the mechanical stress caused by the slight swelling of the potting in toluene. For the M800/X membranes, it seems that the PDMS layer (coating) between Araldite® and the α-alumina capillary absorbs the mechanical stress due to resin swelling thus preventing membrane cracking.

1.5. MWCO determination

1.5.1. Polystyrene synthesis

Polystyrene (PS) of broad molecular weight (MW) was synthesized by anionic living polymerization. The polymerization was carried out in a 2 l three neck round bottom flask equipped with magnetic agitator, dropping funnel, vertical

condenser and a rubber septum. To ensure an oxygen and moisture free reaction environment, the set up was purged continuously with a slow stream of dry nitrogen. The temperature of the polymerizing solution was maintained below 30°C all the time.

In the reaction flask, containing 500 g of toluene, 200 ml of 1.4 M sec-butyllithium (0.28 mol) was injected through the septum. Next, 71.8 g (0.69 mol) styrene dissolved in 90 g of toluene was added within 8 minutes into the *sec*-butyllithium toluene solution. The reaction mixture was stirred for 4 minutes and afterwards, 8.4 ml (0.21 mol) of methanol was injected to quench 75% of the growing polymer chains. Directly afterwards 71.8 g (0.69 mol) styrene dissolved in 90 g of toluene was added during 3.5 minutes to the polymerizing solution. The PS solution was stirred for an additional 2 h at room temperature and quenched with 10 ml of methanol.

After quenching, the synthesised PS was purified by partial evaporation of solvents in a rotary evaporator followed by removal of the lithium metoxide by washing the PS oligomers with distilled water. The washing was repeated several times until the water phase reached neutral pH (removal of LiOH). To complete the purification process, the rest of the solvent was evaporated first in a rotary evaporator and next in a nitrogen box at room temperature. A 0.3% (w/w) broad range MW PS solution in toluene was used for the filtration experiments to obtain MWCO curves.

1.5.2. Determination of PS oligomers retention

The concentration of the PS oligomers as a function of MW in the feed and permeate stream was determined by GPC chromatography. For this we used “Agilent Technologies 1200 Series” GPC system equipped with the refractive index detector “Shodex RI-71”. The column used for separation of PS oligomers was PSS SDV with porosity 1000 Å. As a mobile phase analytical grade toluene was used.

Similar to the method developed by Schock et al. for measurement of the MWCO of ultrafiltration membranes [31], the GPC analysis resulted in a single

lumped peak for both permeate and feed samples. The data was then processed by the GPC software (Win GPC Unity) in order to obtain retention curves. The membrane retention R, for the PS oligomers was calculated from permeate and feed samples with the following equation:

$$R_{i-PS}(\%) = \left(1 - \frac{C_{P,i}}{C_{F,i}}\right) \times 100\% \quad (1)$$

where $C_{P,i}$ and $C_{F,i}$ are the concentrations of the individual PS oligomers in the permeate and the feed stream, respectively.

1.6. Scanning Electron Microscopy (SEM) characterization

Composite membranes were fractured in liquid nitrogen. The samples were then mounted in holders, dried in vacuum oven at 30°C for 12 h and sputtered with gold using a Blazers Union SCD 040 sputtering device (4 min, current 13 mA). SEM micrographs were taken using a Jeol JSM5600LV scanning electron microscope at 5 kV.

1.7. Gas permeation measurements and determination of PDMS layer thickness

Gas permeation measurements of the composite capillary membranes were performed in an automized constant volume / variable pressure set up (see details elsewhere [32]). The gas permeance values were calculated based on a pressure increase in a calibrated constant volume at the permeate side. The temperature during all measurements was maintained at 30°C. From gas permeation values the effective PDMS layer thickness (l_{eff}) was calculated. It was assumed that PDMS intrinsic permeability of N_2 equals 280 Barrers and CO_2 3200 Barrers [33]. The obtained l_{eff} was compared with the PDMS thickness obtained by SEM observation (l_{SEM}) to estimate the extent of the pore intrusion (l_{intr}):

$$l_{intr} = l_{eff} - l_{SEM} \quad (2)$$

The l_{SEM} was obtained from SEM images of cross sections of at least three different membranes per case. The average PDMS thickness was obtained from five SEM images per cross section.

1.8. Permeation experiments

All permeation experiments were performed in a custom made cross-flow high pressure permeation set up (Fig. 1) in a total recycle mode. The set-up was equipped with an HPLC pump which pressurizes the system up to 40 bar. A gear pump was used for circulation and equipped with frequency inverter allowing precise control over the cross flow velocity. All permeation experiments were performed at a crossflow velocity of the feed solution above 2 m s^{-1}. The membranes M800/X have been tested outside-in and the M20/X inside-out. The temperature of the feed solution was controlled at 18°C. The flux through the membrane (J, in l $m^{-2}h^{-1}$) was calculated using the following equation:

$$J = \frac{V}{A \times t} \quad (3)$$

where V is the permeate volume (l), A the membrane area (m^2) and t is the permeation time (h). The permeance coefficient, P (l $m^{-2}h^{-1}bar^{-1}$), was calculated from the slope of the flux versus trans membrane pressure (TMP) graph:

$$P = \frac{J}{\Delta P} \quad (4)$$

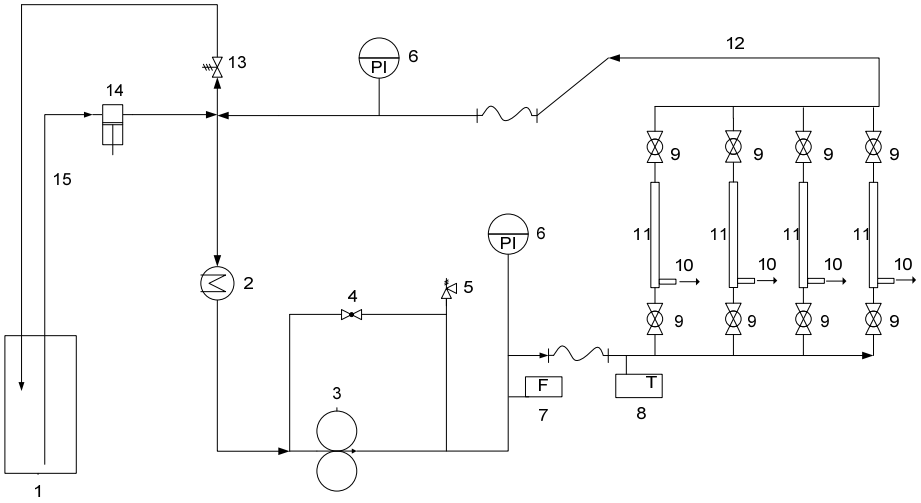

Figure 1 High pressure permeation set up: 1) feed vessel, 2) heat exchanger, 3) gear pump, 4) bypass ball valve, 5) pressure relief, 6) pressure indicator, 7) flow meter, 8) temperature controller, 9) ball valves, 10) permeate line, 11) membrane modules, 12) retentate line, 13) back pressure valve, 14) HPLC pump, 15) feed line.

2. Results and discussion

2.1. Preparation of PDMS coating solutions

In order to prepare a good quality composite membrane it is crucial to prepare a PDMS coating solution of well-defined properties. It is generally known that using lower concentrations one can fabricate thin selective layers, however, the viscosity of the PDMS solution should be sufficient to make a defect free coating. Diluted PDMS solutions have very low viscosity and are not suitable to be applied directly as coatings. To achieve a high solution viscosity at low PDMS concentrations it is necessary to pre-crosslink the coating solution [11]. Following the pre-crosslinking procedure described by Stafie et al. [10, 12] we prepared several 15% (w/w) toluene/PDMS solutions. Figure 2a shows viscosity changes as a function of crosslinking reaction time for three different factory batches of GE RTV615 silicone. Our results suggest that although all three batches are within the factory specification, the behavior during crosslinking reaction varies greatly. One can see that for Batch I and Batch II the time difference where a sharp increase in viscosity occurs, is as much as 150 min. Despite such significant variations between batches it is possible to obtain PDMS solutions of desired viscosity by tuning the reaction time for each batch separately. Figure 2b presents the change of the viscosity of a 15% (w/w) PDMS coating solution versus crosslinking time for different reaction conditions. All curves presented in Figure 2b were obtained using the silicone batch I (see Fig.2a, batch I). Case 1 shows the change of viscosity of the PDMS solution, cross-linked at constant 60^{o}C. Here, the viscosity increases up to 6 times in only 20 minutes between 170 and 190 min of the reaction time. In case 2 after 150 minutes of crosslinking at 60^{o}C we decreased the temperature to 55^{o}C. As a result the viscosity increase occurs later and is somewhat less sharp.

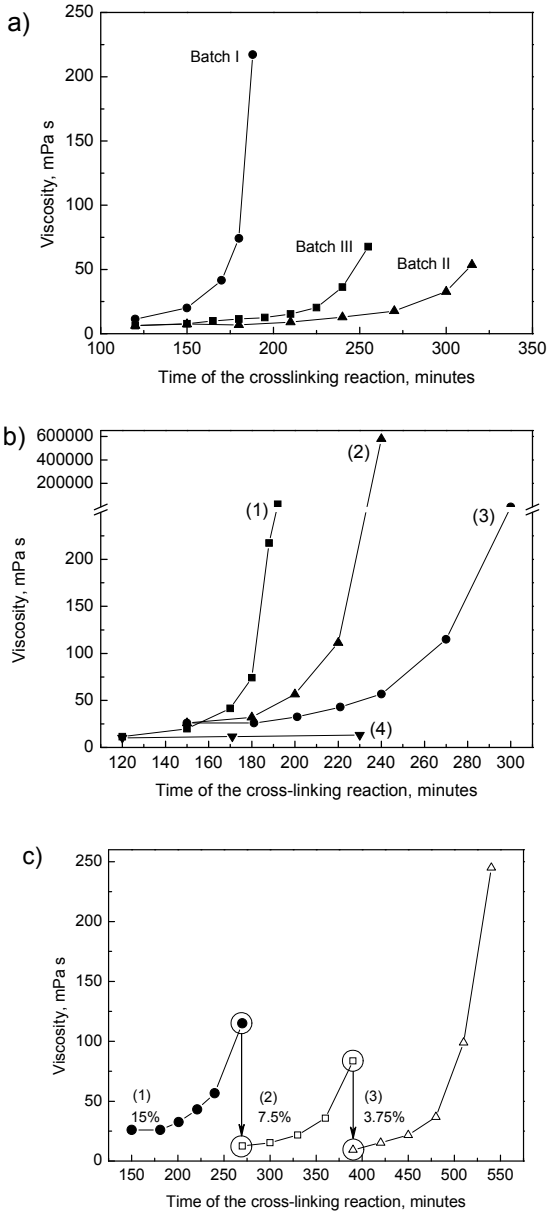

Figure 2 Crosslinking of PDMS coating solutions: (a) difference between PDMS batches – 15%w/w toluene solution, (b) influence of temperature on viscosity of PDMS coating solution – 15%w/w toluene solutions: (1) constant T=60°C, (2) 150 minutes at T=60°C then the temperature lowered to T=55°C, (3) 150 minutes at T=60°C then the temperature lowered to T=50°C, (4) 150 minutes at T=60°C then the temperature lowered to T=40°C (c) effect of dilution on viscosity of PDMS coating solution: (1) - 15%, (2) - 7.5%, (3) - 3.75%. The measurement error for all results presented in figures a) b) and c) is less than 10%.

When after 150 minutes of crosslinking at 60^{o}C the temperature is decreased to 50^{o}C (Fig.2b, case 3) the change of viscosity is less dramatic. If one decreases the crosslinking reaction temperature earlier than 150 min, or uses temperatures lower than 50^{o}C, the PDMS viscosity stays below 20 mPa s for more than 300 min (see Fig.2b, case 4). Since controlling the viscosity of a coating solution is very important to obtain a good coating quality, it seems that a better control of viscosity can be achieved at a temperature around 50^{o}C.

After some preliminary coating experiments with 15 % (w/w) solution, we found that when the coating solution viscosity is high, we obtain a thick PDMS layer whereas when the viscosity is low we obtain membranes with high pore intrusion and defects. It is desirable to have a solution with relatively low PDMS concentration, to obtain thin selective layer, but of relatively high viscosity, to avoid pore intrusion and defects. Figure 2c presents the viscosity change in three different phases of the crosslinking reaction. Phase (1) presents the viscosity of 15% (w/w) solution first crosslinked for 150 min at 60^{o}C and subsequently for 120 min at 50^{o}C. Next, the solution was diluted with toluene to 7.5% (w/w) and crosslinking was continued at 60^{o}C for 120 min (Fig.2c, phase 2). After that the solution was again diluted with toluene to 3.75% (w/w) and the reaction continued at 60^{o}C (Fig.2c, phase 3). These results show that one can tailor precisely the viscosity of diluted solutions, even at 60^{o}C.

Our crosslinking results show that we can control the viscosity of the PDMS coating solution independent of the concentration. In fact, a pre-crosslinking procedure with gradual dilution enables preparation of carefully tailored PDMS solutions of various concentrations and of any viscosity between 10-300 mPa s. Based on the above results we selected cross-linked 3.75% (w/w) PDMS/toluene solutions with viscosities: 55, 69, 100 and 245 mPa s for the preparation of composite membranes.

2.2. Characterization of InoCep M20 Hyflux ceramic support

Figure 3a presents a SEM image of the cross section of the Hyflux InoCep M20 support. In Figure 3b one can see the ~5 μm denser ceramic coating with 20 nm pore size (as reported by the manufacturer) on the inside of the capillary. The outside layer of the capillary has larger pores of 800 nm pore size (as reported by the manufacturer) (see Figure 3c).

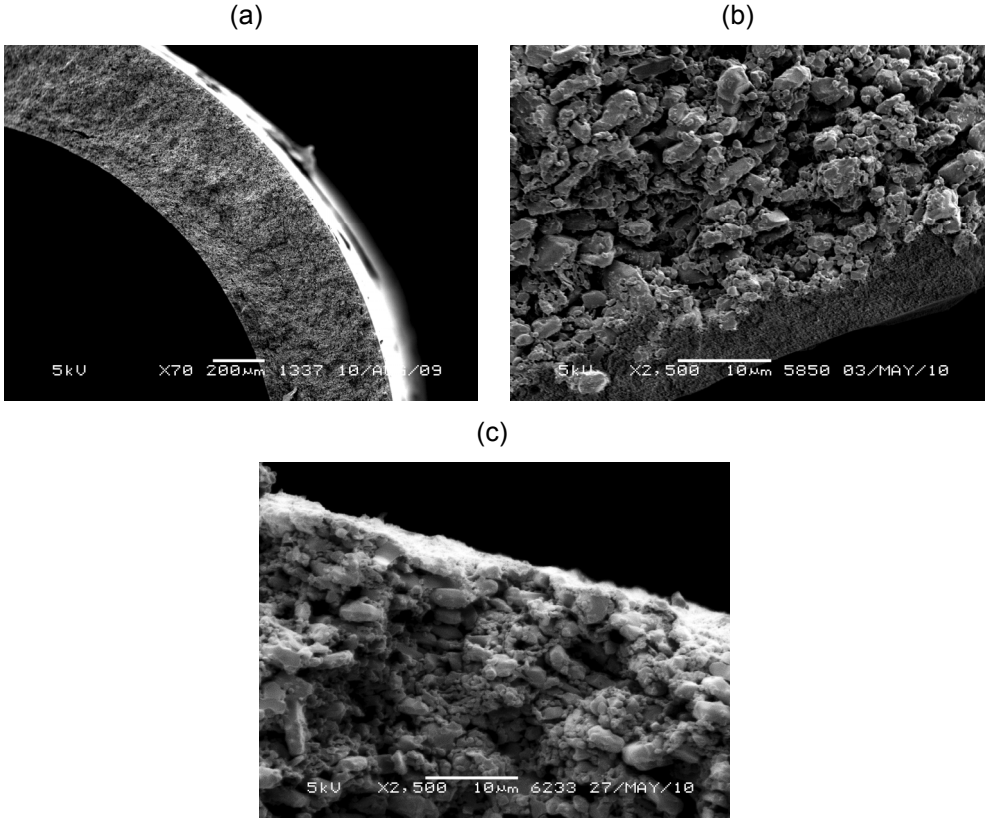

Figure 3 Scanning electron microscopy (SEM) images of Hyflux InoCep M20 capilary support: (a) Wall cross-section, (b) cross-section of the inner layer (20 nm pore size), (c) cross-section of the outer layer (800 nm pore size).

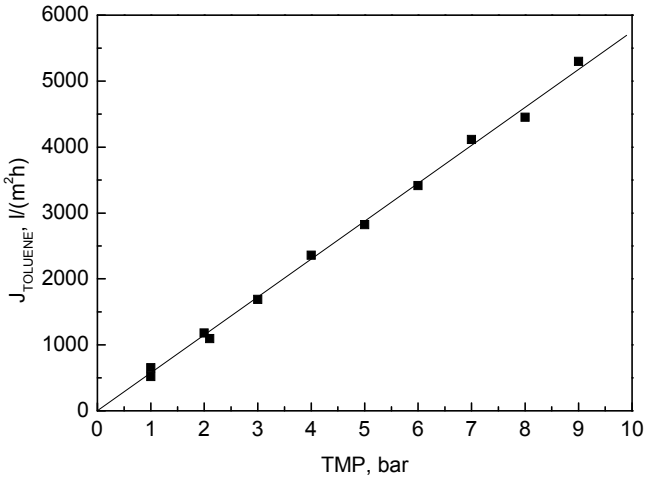

Figure 4 Transport of toluene through Hyflux Inocep M20 support.

Figure 4 presents the flux of toluene as a function of transmembrane pressure (TMP). Within the studied pressure range (0-9 bar) the line remains straight indicating that no compaction occurs. Because of the very high flux of toluene through InoCep M20 support we were not able to apply higher pressures in our experimental set up. The toluene permeance of the M20 capillary is 575 ± 5 l $m^{-2}h^{-1}bar^{-1}$.

2.3. Optimization of ceramic/PDMS hollow fiber membrane

2.3.1. Coating on the outside (M800/X)

Table 1 presents an overview of the coating experiments. The first series of the composite membranes were prepared by dip coating on the outside of the support. In order to investigate the influence of PDMS solution viscosity on pore intrusion we used 3.75% (w/w) PDMS solutions with three different viscosities: 69, 100 and 245 mPa s (tailored as described in Figure 2c). SEM images of cross-sections of those membranes are presented in Figure 5a, 5b and 5c, respectively.

Table 1 Characteristics of membranes and results of permeation measurements.

Code	PDMS, w/w %	Viscosity, mPa s	Support pore size, nm	l_{SEM}, µm	l_{eff}, µm	Estimated Pore Intrusion, µm	Selectivity $\alpha_{CO2/N2}$	Toluene permeance, l $m^{-2}h^{-1}bar^{-1}$
M20	-	-	20	-	-	-	-	575 ± 5
M800/69	3.75%	69	800	6±3	51±1	45	10.6±0.1	0.07 ± 0.01
M800/100	3.75%	100	800	10±1	28±1	18	10.0±0.2	0.22 ± 0.02
M800/245	3.75%	245	800	18±3	32±6	14	10.3±0.3	0.14 ± 0.02
M20/245	3.75%	245	20	16±4	16±1	0	8.4±0.1	0.9 ± 0.6
M20/55	3.75%	55	20	7.3±0.3	7.1±0.2	0	8.4±0.1	1.6 ± 0.1

The thickness of the PDMS on top of the 800 nm pore size support layer (l_{SEM}) was 6 µm for the M800/69, 10 µm for M800/100 and 18 µm for M800/245 membrane. The l_{eff}, as calculated based on N_2 permeance measurements, was 51 µm, 28 µm and 32 µm for M800/69, M800/100 and M800/245 respectively. For all prepared membranes we also calculated $\alpha_{CO2/N2}$ in order to check the quality of the PDMS layer.

(a) M800/69

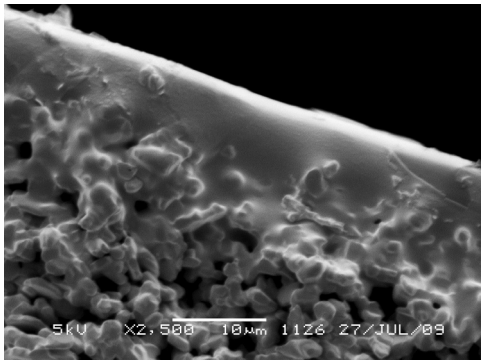

(b) M800/100

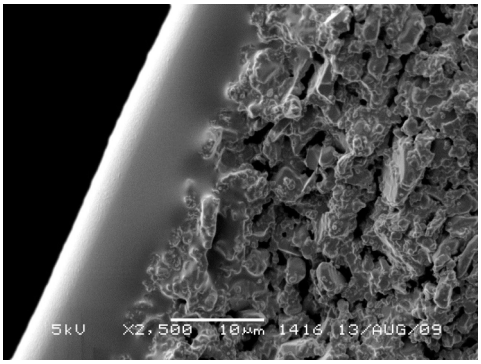

(c) M800/245

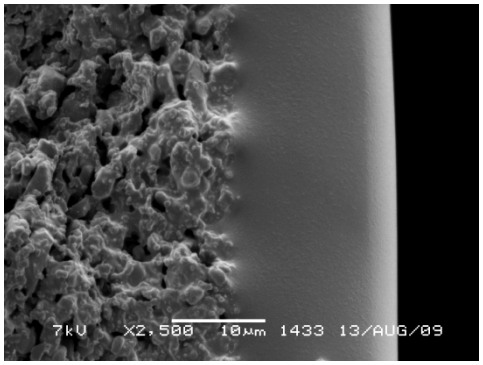

(d) M20/245

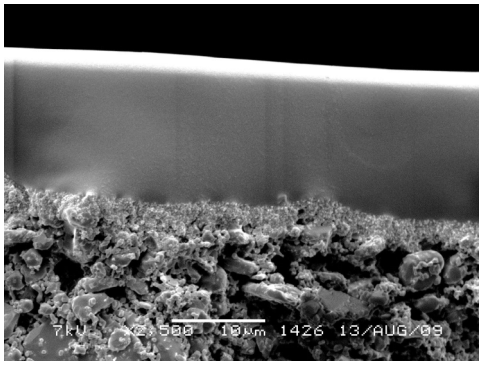

(e) M20/55

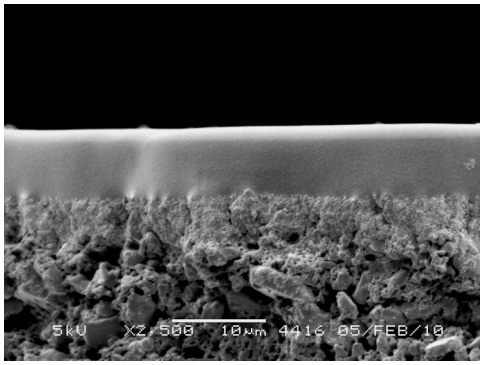

Figure 5 Hyflux InoCep M20/PDMS composite capillary membranes: (a) M800/69, (b) M800/100, (c) M800/245, (d) M20/245, (e) M20/55.

For all M800/X membranes the $\alpha_{CO2/N2}$ was above 10 (the ideal $\alpha_{CO2/N2}$ is 11.3 [11]) showing a very good quality of the coating (see Table 1). When the coating solution viscosity was increased the coating thickness on top of the support also increased from 6 to 18 μm, whereas the estimated pore intrusion decreased from 45 to 14 μm.

Figure 6 presents the flux of toluene as a function of pressure for the composite membranes. The error bars represent deviation between the samples of the composite membranes from the same batch. The error of the permeation measurement itself is less than 1%. All M800/X membranes have relatively low toluene permeance. The M800/69 membrane has the largest pore intrusion resulting in the highest l_{eff} and therefore has the lowest toluene permeance. The M800/100 membrane with the lowest l_{eff} has the highest permeance. The PDMS thickness measured from SEM images for M800/100 and M800/245

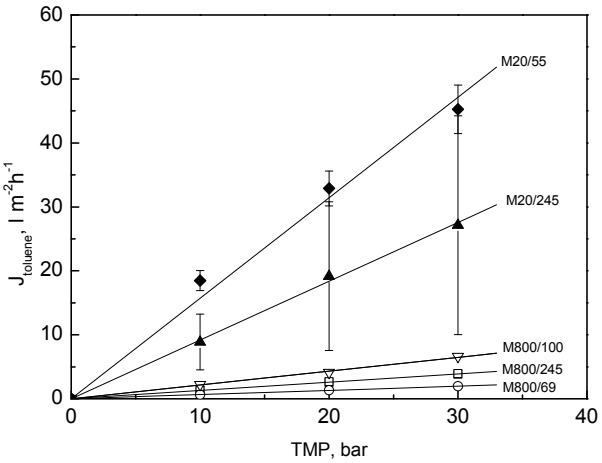

Figure 6 Transport of toluene through alumina / PDMS hollow fiber membranes.

(compare Fig.5b and Fig.5c) is 10 μm and 18 μm respectively and is consistent with the trend of toluene permeance for both membranes. It seems that further increase of the coating solution viscosity above 245 mPa s would produce a membrane with even lower permeance of toluene.

The results above suggest that in order to obtain a thinner PDMS layer it is necessary to use a support with smaller pore size. InoCep M20 capillaries have 20 nm pore size on the inner side, allowing the use of the same support for further optimization of composite membranes, by coating the inner surface of the capillaries.

2.3.2. Coating on the inside (M20/X)

Figure 5d presents a cross section of a composite capillary membrane (M20/245), prepared by coating a 3.75% (w/w) PDMS toluene solution of a viscosity of 245 mPa s on the inside of the support membrane. A close examination of the SEM image does not reveal pore intrusion. The l_{eff} and l_{SEM} are in close agreement, also indicating that no significant pore intrusion occurred (see Table 1). It is nonetheless important to point out that for this membrane the $\alpha_{CO2/N2}$ was ~8.4 (ideal 11.3 [34]) indicating some defects in the separation layer. One must be aware that those defects influence the gas permeation measurements leading to a slightly lower calculated PDMS thickness.

Figure 6 presents the flux of toluene as a function of pressure for membrane M20/245. The permeance of toluene, P_{tol}, was 0.9 ± 0.6, l $m^{-2}h^{-1}bar^{-1}$. The low reproducibility of this membrane is probably due to a combination of two factors, high viscosity of the coating solution and applied coating technique (communicating vessel system). It seems that due to the high viscosity of the PDMS solution, control over the contact time and coating velocity is not precise, resulting in membranes with high and low permeances.

In order to obtain a better composite membrane with a thinner and reproducible coating we used a 3.75% (w/w) PDMS toluene solution with a viscosity of 55 mPa s. Figure 5e presents a cross-section of this composite (M20/55) membrane. A close examination of the SEM image suggests no pore intrusion. Also, l_{eff} and l_{SEM} are similar and about 7 μm (see Table 1). The $\alpha_{CO2/N2}$ of the M20/55 membranes is ~8.4 suggesting the presence of some defects in the PDMS layer. The toluene permeance of this membrane is 1.6 ± 0.1, l $m^{-2}h^{-1}bar^{-1}$, even higher than for the best sample of membrane M20/245. The reproducibility of

the M20/55 composite membranes is considerably better as demonstrated by the small thickness deviation between the samples (see Table 1). The less viscous coating solution allows better control over the coating process resulting in much better composite membranes. The thickness of the PDMS layer of our membrane M20/55 is 7 μm and is lower than that reported for other capillary membranes for pervaporation (~10 μm) [28] and hollow fibers for VOC removal (15.4 μm) [27].

In conclusion, based on the above results, the M20/55 is the best membrane developed in this study, having low pore intrusion and the highest toluene permeance.

2.3.3. Molecular Weight Cut-Off determination

In order to characterize the retention behavior of the nanofiltration (NF) membranes in organic solvents one needs a series of solutes of increasing molecular weight (MW). It is also important that all the molecules have the same chemical properties and are well soluble in the solvent used. Voigt et al. [35] proposed a filtration of mixture of narrow low-MW fractions of styrene oligomers dissolved in toluene as a method for MWCO characterization of ceramic NF membranes. Later, the concept was further developed by See Toh et al. [36]. The disadvantage of the use of a mixture of commercial PS is the relatively high price of these styrene oligomers. Zwijnenberg et al. [37] proposed therefore a method of synthesis of a broad range PS to be used for NF module testing. Since the amount of solution needed for our experiments was quite significant, we performed the synthesis of broad MW PS in our lab by means of the anionic living polymerization of styrene. This method is rather simple, leads to high yields (~95% after purification) and by varying the styrene to *sec*-butyllithium ratio allows simple adjustment of the MW of the final product. Figure 7a (dotted line - feed) presents MW distribution of the obtained PS. The addition of small amounts of methanol, which terminates partially the growth of the chains, also results in preparation of PS fractions of 300 and 400 g mol^{-1}, thus increasing polydispersity.

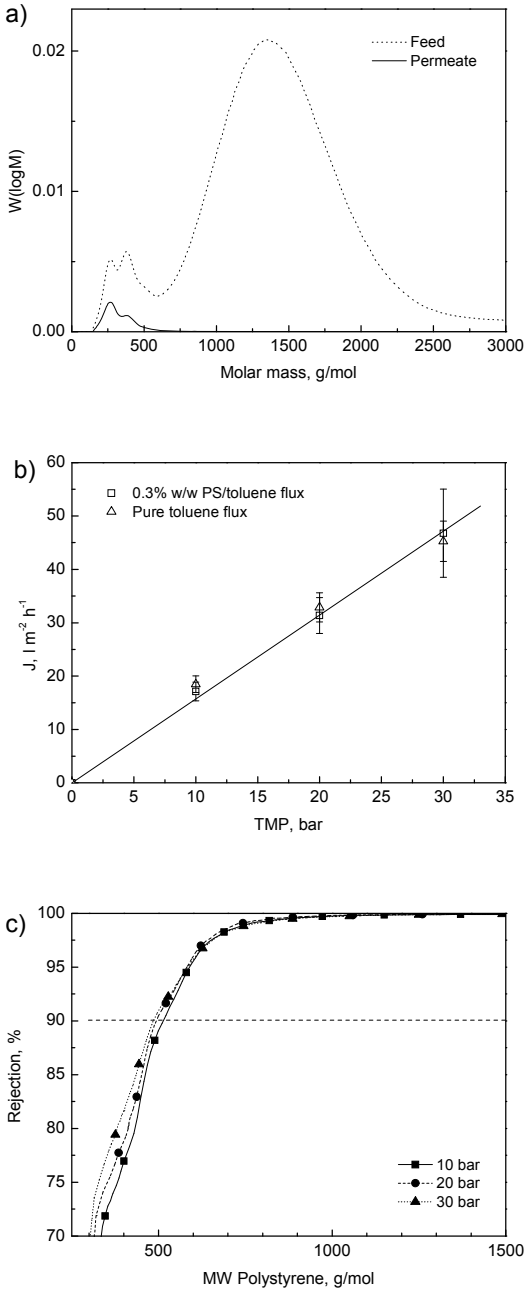

Figure 7 Transport through M20/55 membrane: (a) Molecular weight distribution of PS oligomers in the feed solution and permeate solution (b) toluene and toluene-PS transport through the membrane, (c) PS oligomer retention by the membrane.

The membrane M20/55, as the best one of all the membranes prepared in this study was chosen for MWCO characterization. For the retention measurements we used a 0.3% (w/w) solution of the synthesized PS oligomers. Examples of the GPC chromatograms of the feed and permeate samples are presented in the Figure 7a. Figure 7b presents a comparison of pure toluene and toluene/PS oligomers flux as a function of TMP for this membrane. For the chosen concentration of PS oligomers and filtration parameters (cross-flow velocity above 2 m/s, stage cut below 10%) the PS oligomers/toluene flux does not differ from the pure toluene flux indicating no concentration polarization phenomena. In this pressure range no compaction occurs either. Figure 7c presents the rejection of PS oligomers by the M20/55 membrane and shows its MWCO at about 500 g mol^{-1}. For this experiment, pure toluene permeation was performed for around 20 h followed by 20 h of toluene / oligostyrene filtration in a total recycle mode. The data presented in both Figure 7b and 7c are obtained using the same membrane samples.

The best composite capillary membrane developed in this study, M20/55, has a toluene permeance of 1.6 ± 0.1 l $m^{-2}h^{-1}bar^{-1}$ and MWCO 500 Da, and has similar permeation performance to other laboratory made silicone based composite membranes. A polyacrylonitrile-polyester/PDMS (PAN-PE/PDMS) composite reported by Vankelecom et al. [26] had a toluene permeance of 1.2 l $m^{-2}h^{-1}bar^{-1}$ and the PAN/PDMS composite membrane prepared by Stafie [10] had a toluene permeance of 2.0 l $m^{-2}h^{-1}bar^{-1}$. Comparing to commercial silicone based membranes, the MPF-50 (Koch) [6] had a toluene permeance of 1.3 l $m^{-2}h^{-1}bar^{-1}$ and MWCO about 700 g mol^{-1}, although this membrane suffers from compaction [26] which may deteriorate membrane performance [6, 38]. The permeance of our membrane is lower than an experimental PAN/PDMS membrane which was reported to have a toluene permeance of 8.2 l $m^{-2}h^{-1}bar^{-1}$ and 90% retention of PEG 900 [9].

When comparing to non-silicone NF membranes, a cross-linked polyimide membrane developed by See Toh et al. had a toluene permeance 3.2 l $m^{-2}h^{-1}bar^{-1}$

and MWCO 400 g mol^{-1}, based on PS oligomers rejection [17], whereas a polyimide Starmem™ membrane had a toluene permeance 1.8 l $m^{-2}h^{-1}bar^{-1}$ and MWCO 220 g mol^{-1}, based on 90% rejection of n-alkanes [6, 13]. It is also important to note that the toluene permeance of our M20/55 membrane is similar to a zeolite filled PDMS mixed matrix membrane reported by Gevers et al., (toluene permeance of 1.15, l·$m^{-2}h^{-1}bar^{-1}$ and 78% rejection of the Wilkinson catalyst (952 g mol^{-1})) [39]. The same authors reported that after optimization of the coating parameters and correct pretreatment of the support (Polyimide-Matrimid®) it was possible to achieve toluene permeance of 3.3 l $m^{-2}h^{-1}bar^{-1}$ and 98 % rejection of the Wilkinson catalyst [16].

3. Conclusions

In this work, we investigated the preparation of composite capillary membranes comprising of commercial Hyflux InoCep M20 α-alumina support and selective tailor made PDMS top layer. Our results showed that PDMS coatings on α-alumina support of 800 nm pore size did not provide a good composite membrane. Due to the large pore size, the coating solution intrudes significantly in the porous support blocking pores and decreases the toluene permeance considerably.

The best composite membrane M20/55 was prepared by coating PDMS on the inside of the α-alumina support. This membrane has stable performance for over 40 h in toluene, toluene permeance of 1.6 l $m^{-2}h^{-1}bar^{-1}$ and MWCO of ~500 g mol^{-1}. Despite the relatively thick PDMS layer of 7 μm, this membrane has comparable toluene permeance with respect to various laboratory PAN/PDMS membranes with thinner PDMS layers. Further development of the composite membrane will focus on coating a PDMS layer on tailor made ceramic hollow fibers which would further improve the surface to volume ratio of the resulting module.

4. Acknowledgments

Dutch Technology Foundation (STW) (project no 07349) is gratefully acknowledged for the financial support.

5. References

[1] L.S. White, Development of large-scale applications in organic solvent nanofiltration and pervaporation for chemical and refining processes, J. Membr. Sci., 286 (2006) 26.

[2] X. Cao, X.Y. Wu, T. Wu, K. Jin, B.K. Hur, Concentration of 6-aminopenicillanic acid from penicillin bioconversion solution and its mother liquor by nanofiltration membrane, Biotechnol. Bioprocess Eng., 6 (2001) 200-204.

[3] J.C.T. Lin, A.G. Livingston, Nanofiltration membrane cascade for continuous solvent exchange, Chem. Eng. Sci., 62 (2007) 2728-2736.

[4] J.P. Sheth, Y. Qin, K.K. Sirkar, B.C. Baltzis, Nanofiltration-based diafiltration process for solvent exchange in pharmaceutical manufacturing, J. Membr. Sci., 211 (2003) 251-261.

[5] D. Shi, Y. Kong, J. Yu, Y. Wang, J. Yang, Separation performance of polyimide nanofiltration membranes for concentrating spiramycin extract, Desalination, 191 (2006) 309-317.

[6] P. Vandezande, L.E.M. Gevers, I.F.J. Vankelecom, Solvent resistant nanofiltration: Separating on a molecular level, Chem. Soc. Rev., 37 (2008) 365-405.

[7] Y.H. See-Toh, F.C. Ferreira, A.G. Livingston, The influence of membrane formation parameters on the functional performance of organic solvent nanofiltration membranes, J. Membr. Sci., 299 (2007) 236-250.

[8] S. Aerts, A. Vanhulsel, A. Buekenhoudt, H. Weyten, S. Kuypers, H. Chen, M. Bryjak, L.E.M. Gevers, I.F.J. Vankelecom, P.A. Jacobs, Plasma-treated PDMS-membranes in solvent resistant nanofiltration: Characterization and study of transport mechanism, J. Membr. Sci., 275 (2006) 212.

[9] K. Ebert, J. Koll, M.F.J. Dijkstra, M. Eggers, Fundamental studies on the performance of a hydrophobic solvent stable membrane in non-aqueous solutions, J. Membr. Sci., 285 (2006) 75-80.

[10] N. Stafie, Poly(dimethyl siloxane) – based composite nanofiltration membranes for non-aqueous applications, Ph.D. thesis, University of Twente, Enschede, The Netherlands, (2004).

[11] N. Stafie, D.F. Stamatialis, M. Wessling, Insight into the transport of hexane-solute systems through tailor-made composite membranes, J. Membr. Sci., 228 (2004) 103-116.

[12] N. Stafie, D.F. Stamatialis, M. Wessling, Effect of PDMS cross-linking degree on the permeation performance of PAN/PDMS composite nanofiltration membranes, Sep. Purif. Technol., 45 (2005) 220-231.

[13] D.F. Stamatialis, N. Stafie, K. Buadu, M. Hempenius, M. Wessling, Observations on the permeation performance of solvent resistant nanofiltration membranes, J. Membr. Sci., 279 (2006) 424-433.

[14] E.S. Tarleton, J.P. Robinson, C.R. Millington, A. Nijmeijer, M.L. Taylor, The influence of polarity on flux and rejection behaviour in solvent resistant nanofiltration - Experimental observations, J. Membr. Sci., 278 (2006) 318-327.

[15] E.S. Tarleton, J.P. Robinson, M. Salman, Solvent-induced swelling of membranes - Measurements and influence in nanofiltration, J. Membr. Sci., 280 (2006) 442-451.

[16] L.E.M. Gevers, S. Aldea, I.F.J. Vankelecom, P.A. Jacobs, Optimisation of a lab-scale method for preparation of composite membranes with a filled dense top-layer, J. Membr. Sci., 281 (2006) 741-746.

[17] Y.H. See Toh, F.W. Lim, A.G. Livingston, Polymeric membranes for nanofiltration in polar aprotic solvents, J. Membr. Sci., 301 (2007) 3-10.

[18] K. Vanherck, P. Vandezande, S.O. Aldea, I.F.J. Vankelecom, Cross-linked polyimide membranes for solvent resistant nanofiltration in aprotic solvents, J. Membr. Sci., 320 (2008) 468-476.

[19] K. Vanherck, A. Cano-Odena, G. Koeckelberghs, T. Dedroog, I. Vankelecom, A simplified diamine crosslinking method for PI nanofiltration membranes, J. Membr. Sci., 353 (2010) 135-143.

[20] J.T. Scarpello, D. Nair, L.M. Freitas dos Santos, L.S. White, A.G. Livingston, The separation of homogeneous organometallic catalysts using solvent resistant nanofiltration, J. Membr. Sci., 203 (2002) 71-85.

[21] A. Livingston, L. Peeva, S. Han, D. Nair, S.S. Luthra, L.S. White, L.M. Freitas Dos Santos, Membrane Separation in Green Chemical Processing, Ann. N. Y. Acad. Sci., 984 (2003) 123-141.

[22] S.S. Luthra, X. Yang, L.M. Freitas dos Santos, L.S. White, A.G. Livingston, Homogeneous phase transfer catalyst recovery and re-use using solvent resistant membranes, J. Membr. Sci., 201 (2002) 65-75.

[23] L.S. White, C.R. Wildemuth, Aromatics enrichment in refinery streams using hyperfiltration, Ind. Eng. Chem. Res., 45 (2006) 9136-9143.

[24] R. Othman, A.W. Mohammad, M. Ismail, J. Salimon, Application of polymeric solvent resistant nanofiltration membranes for biodiesel production, J. Membr. Sci., 348 (2010) 287-297.

[25] X.X. Loh, M. Sairam, J.H.G. Steinke, A.G. Livingston, A. Bismarck, K. Li, Polyaniline hollow fibres for organic solvent nanofiltration, Chem. Commun., (2008) 6324-6326.

[26] I.F.J. Vankelecom, K. De Smet, L.E.M. Gevers, A. Livingston, D. Nair, S. Aerts, S. Kuypers, P.A. Jacobs, Physico-chemical interpretation of the SRNF transport mechanism for solvents through dense silicone membranes, J. Membr. Sci., 231 (2004) 99-108.

[27] S. Liu, W.K. Teo, X. Tan, K. Li, Preparation of PDMS^{vi}-Al_2O_3 composite hollow fibre membranes for VOC recovery from waste gas streams, Sep. Purif. Technol., 46 (2005) 110-117.

[28] F. Xiangli, Y. Chen, W. Jin, N. Xu, Polydimethylsiloxane (PDMS)/Ceramic Composite Membrane with High Flux for Pervaporation of Ethanol-Water Mixtures, Ind. Eng. Chem. Res., 46 (2007) 2224-2230.

[29] F. Xiangli, W. Wei, Y. Chen, W. Jin, N. Xu, Optimization of preparation conditions for polydimethylsiloxane (PDMS)/ceramic composite pervaporation membranes using response surface methodology, J. Membr. Sci., 311 (2008) 23-33.

[30] G.O. Yahaya, Separation of volatile organic compounds (BTEX) from aqueous solutions by a composite organophilic hollow fiber membrane-based pervaporation process, J. Membr. Sci., 319 (2008) 82-90.

[31] G. Schock, A. Miquel, R. Birkenberger, Characterization of ultrafiltration membranes: Cut-off determination by gel permeation chromatography, J. Membr. Sci., 41 (1989) 55-67.

[32] S.R. Reijerkerk, M.H. Knoef, K. Nijmeijer, M. Wessling, Poly(ethylene glycol) and poly(dimethyl siloxane): Combining their advantages into efficient CO_2 gas separation membranes, J. Membr. Sci., 352 (2010) 126-135.

[33] R. Baker, Membrane Technology and Applications, 2nd Edition John Wiley & Sons, Ltd, 2004.

[34] M. Mulder, Basic Principles of Membrane Technology, Kluwer Academic Publishers, Dodrecht / Boston / London, 2000.

[35] I. Voigt, P. Puhlfürß, T. Holborn, G. Dudziak, M. Mutter, A. Nickel, Ceramic nanofiltration membranes for applications in organic solvents, in: 9th Aachen Membrane Colloquium, Aachen, Germany, 2003, pp. pOP 20-21-OP 20-11.

[36] Y.H. See Toh, X.X. Loh, K. Li, A. Bismarck, A.G. Livingston, In search of a standard method for the characterisation of organic solvent nanofiltration membranes, J. Membr. Sci., 291 (2007) 120-125.

[37] H.J. Zwijnenberg, A standardized characterization method for solvent resistant nanofiltration membrane modules, in: ICOM Presentation, 2005.

[38] X.J. Yang, A.G. Livingston, L. Freitas Dos Santos, Experimental observations of nanofiltration with organic solvents, J. Membr. Sci., 190 (2001) 45-55.

[39] L.E.M. Gevers, I.F.J. Vankelecom, P.A. Jacobs, Zeolite filled polydimethylsiloxane (PDMS) as an improved membrane for solvent-resistant nanofiltration (SRNF), Chem. Commun., (2005) 2500-2502.

Chapter III

Important factors influencing molecular weight cut-off determination of membranes in organic solvents

H.J. Zwijnenberg[*], S.M. Dutczak[*], M.E. Boerrigter, M.A. Hempenius,

M.W.J. Luiten-Olieman, N.E. Benes, M. Wessling, D. Stamatialis

[*] Both authors contributed equally to this chapter

Submitted for publication in J. Membr. Sci.

Abstract

In solvent resistant nanofiltration (SRNF), sensible selection of a membrane for a particular solvent / solute system is recognized as challenging. Prospective methods for suitability analysis of membranes include molecular weight cut off (MWCO) characterization. However, insufficient understanding of the interrelated effects of solvent, solute, membrane properties, and the applied process conditions often complicates interpretation of MWCO data. This study demonstrates and discusses such effects with respect to transport mechanism. To this end very different SRNF systems have been selected: a rigid porous membrane (hydrophobized zirconia) versus a rubbery dense membrane (polydimethylsiloxane); a low flux solvent (toluene) versus high flux solvent (n-hexane); and a stiff solute (polystyrene) versus a flexible solute (polyisobutylene). The results indicate that, for the applied conditions, the MWCO of the dense membrane is predominantly affected by solute-membrane and solvent-membrane interactions. For the rigid porous membrane a significant effect of applied pressure is observed, in particular for the flexible solute. The non-linear relation between flux and pressure and the variations in MWCO with pressure indicate combined effects of concentration polarization and shear induced deformation of the flexible solute. The results unmistakably show that the interpretation of MWCO is heavily dependent on the system under study.

1. Introduction

In solvent resistant nanofiltration (SRNF) recently significant improvements have been achieved in the development of solvent stable membranes [1, 2]. An increasing number of successful applications have been reported in catalysis, the petrochemical industry, and the pharmaceutical industry. These applications include recovery of solvents (e.g. toluene) from dewaxed lube oil filtrates [3], solvent exchange [4], recovery of the organometallic complexes from various organic solvents [5], separation of phase transfer catalyst (PTC) from toluene [6, 7], deacidification of vegetable oils [8, 9] and concentration of pharmaceuticals [10-12].

Amongst others, application of SRNF membranes is hampered by the complications involved in selecting appropriate membranes for each distinct separation [12]. The choice for a particular membrane can be based on its MWCO, however, MWCO analysis in SRNF is less developed and more complicated as compared to aqueous systems [13-20]. The complexity of MWCO in SRNF arises from pronounced effects of process conditions, inherent properties of the membrane, and solvent- solute- membrane interactions.

Currently there is no universal protocol for determining the MWCO of SRNF membranes. A promising method is the filtration of a mixture of a homologues series of neutral polystyrene oligomers in toluene, as proposed by Voigt et al. [21]. This method was systematically further developed by Zwijnenberg et al. [22], See Toh et al. [23] and Dutczak et al. [24]. Based on this approach, the present work investigates the effect of process conditions and the interrelated and inherent properties of different components.

To this end different SRNF systems have been selected:

- Membrane: rigid and porous (zirconia) versus rubbery and dense (polydimethylsiloxane).
- Solvent: low flux (toluene) versus high flux (n-hexane).
- Solute: stiff solute (polystyrene) versus a flexible solute (polyisobutylene).

The choice of membranes represents two extremes in SRNF. Solvent fluxes through the porous membrane will be much higher as compared to the dense membrane. Consequently, for the porous membrane, concentration polarization effects and shear-induced deformation of the solutes [25] are expected to be more pronounced. In contrast to the rigid porous membrane, the rubbery dense membrane can exhibit pronounced swelling due to sorption of the solvent. Solvent selection is based on anticipated differences in flux. Compared to toluene, higher fluxes have been observed for n-hexane [16-18, 26] corresponding to more pronounced effects of flow-induced solute deformation and concentration polarization. In addition, solvent-solute interactions will be different. Selected solutes, polystyrene (PS) and polyisobutylene (PIB) are homologous oligomer mixtures, allowing for a broad molecular weight distribution. Crucial differences between these solutes are their shape and flexibility; compared to PS, PIB can be considered a long thin and flexible molecule.

This study aims at giving a practical display of the effects on MWCO originating from:

- Process conditions and phenomena such as concentration polarization.
- Interactions between solvent, solute, and membrane.
- Shape and flexibility of solute.

In that respect it focuses on the resulting difference in transport mechanism rather than on the characterization of the membranes.

2. Experimental

2.1. Materials

Toluene, n-hexane, methanol and tetrahydrofuran (THF), all analytical grades, were purchased from Merck (The Netherlands). Styrene (Reagent Plus ≥99%) and sec-butyllithium solution (1.4 M in cyclohexane) were purchased from Sigma Aldrich (The Netherlands). The polyisobutylene (PIB), Glissopal® of 550, 1000, 1300, and 2300 g mol^{-1} were kindly provided by BASF - Germany and the PIB of 350 g mol^{-1} by Janex S.A. - Switzerland. All chemicals were used as supplied without additional purification. General Electric polydimethylsiloxane (PDMS) RTV 615 kit was purchased from Permacol B.V. (The Netherlands). A two component epoxy resin Araldite® 2014-1 obtained from Viba (The Netherlands) was used as potting for modules containing PDMS/α-alumina HF composite membranes. Powders used for preparation of the hollow fiber α-alumina support were AKP 15 (particle size 0.6 μm) and AKP 50 (particle size 0.2 μm) purchased from Sumitomo Chemicals Co LTD. Poly(ethersulfone) (PES, Ultrason, 6020P) was used as polymer binder, N-methylpyrrolidone (NMP, 99,5 % (w/w), Aldrich) as solvent, deionized water as non-solvent. The α-alumina powder and PES were dried before use; all other chemicals were used without further treatment. A commercial multichannel porous silanized, hydrophobized zirconia membrane, referred to as zirconia, was kindly supplied by Fraunhofer-Institut für Keramische Technologien und Systeme – IKTS (former HITK, Hermsdorf, Germany). The selective layer of this membrane was produced by formation of a thin sol-gel derived zirconia coating with a pore size of 3 nm, followed by silanization to form a hydrophobic surface. The resulting pore size was therefore well below the 3 nm resulting in a membrane with true NF properties.

2.2. Composite hollow fiber membrane preparation

2.2.1. Preparation of an α-alumina hollow fiber support

Hollow fibers were prepared via a dry-wet spinning process followed by heat treatment, as described in detail elsewhere [27]. Two spinning mixtures were prepared for the preparation of the inner and the outer layer (see Table 1). The alumina powder was added to a NMP or in a NMP / H_2O mixture followed by stirring for 15 min and ultrasonic treatment for 15 min to decrease the amount of agglomerates in the alumina powder. PES was added in three steps with a time interval of two hours followed by stirring overnight. The NMP/PES ratio was kept constant (1/4), while the concentration of α-alumina was varied. The concentration of α-alumina particles was lowered in spinning mixture of the outer layer to achieve a thinner layer and water was added to improve the morphology of the layer. Prior to spinning the mixtures were degassed by applying vacuum for 30 min and left for 16 h under dry air.

Table 1 Spinning dope compositions for the fabrication of the alumina support.

Spinning dope	Composition					
	PES % (w/w)	NMP % (w/w)	AKP 15 % (w/w)	AKP 50 % (w/w)	H_2O % (w/w)	PVP %(w/w)
Inner (support layer)	10	39	49	-	-	2
Outer (separating layer)	12	52	-	33	3	0

Spinning experiments were performed with a bore liquid flow of 7 ml min^{-1}, air gap of 3 cm and pressure differences of 1 and 2.5 bar for the inner and outer layer, respectively. The spinning mixtures (see Table 1) were pressurized in a stainless

steel vessel, and consequently pressed through a spinneret (inner and outer diameter of 0.8 mm / 2.0 mm for inner layer and 2.2 mm / 2.5 mm for outer layer). After spinning, the fiber was immersed in a water bath for further solvent exchange for 1 day followed by drying and stretching (0.5 cm per m) for 1 day to straighten the fiber. The removal of PES was performed at 400 °C for 120 min (heating rate 1°C min^{-1}) and the fibers were sintered at 1500°C for 300 min (heating rate 1°C min^{-1}, cooling rate 5°C min^{-1}) in air.

2.2.2. PDMS coating on an α-alumina hollow fiber support

Composite α-alumina/PDMS hollow fiber membranes (referred to here as PDMS membranes) were prepared in an ISO-6 class dust free room. The membranes were prepared by dip-coating in the 3.2% (w/w) pre-crosslinked PDMS/toluene solution of viscosity 175 mPa s at the outside of the fiber. Pre-crosslinking was carried out in order to prevent significant pore intrusion of the PDMS in support. The coating was performed using an automated set-up adjusted to an immersion/pull up velocity of 0.9 cm/s and a contact time of 30 s. The pre-crosslinked PDMS coating solution was prepared in three steps, starting from 15% (w/w) PDMS solution in toluene. First, the solution was crosslinked at 60°C for 150 min then at 50°C till it reached 100 mPa s viscosity. In the next step, it was diluted to 7.5 % (w/w) and the reaction continued at 60°C till again the solution reached 100 mPa s viscosity. Finally, the solution was diluted to 3.2 % (w/w) and brought to a viscosity of 175 mPa s by crosslinking at 60°C. Detailed descriptions of pre-crosslinking of the PDMS solution as well as the coating procedure can be found elsewhere [24].

2.2.3. HF Module preparation

The composite membranes were potted in cross-flow stainless steel modules. Each module contained one fiber of 155 mm active length. Araldite® 2014-1 was used as a potting material. The resin was allowed to set at room temperature for minimum 24 h before using the module for permeation experiments.

2.3. MWCO determination

2.3.1. Polystyrene synthesis

PS of broad molecular weight distribution 300-6000 g mol^{-1} was synthesized by anionic living polymerization in a similar way as described in prior work [24] but with intermediate termination of part of the living chains.

In the reaction flask, containing toluene (500 g), 1.4 M *sec*-butyllithium (200 ml, 0.28 mol) was injected through the septum. The subsequent addition of a toluene-styrene solution to the *sec*-butyllithium dissolved in toluene was performed in three steps:

1) Styrene (42.8 g, 0.41 mol) in toluene (90 g) was added within 2 minutes. After 5 minutes of stirring, MeOH (1.1 ml, 0.03 mol) was injected into the reaction solution in order to quench 10% of growing chains. 2) Styrene (228.1 g, 2.18 mol) and MeOH (9.4 ml, 0.23 mol) in toluene (480 g) was added dropwise during 3 h 45 minutes into the polymerization mixture. 3) Directly afterwards, styrene (14.3 g, 0.14 mol) dissolved in toluene (30 g) was added within 1 minute to the polymerization solution. The temperature of the reaction mixture was maintained below 30 °C at all times. The polymer solution was stirred for an additional 2 h at room temperature and quenched with methanol (4 ml).

The resulting oligomer mixture had an average MW of about 1950 g mol^{-1}, see Figure 1 for the GPC results.

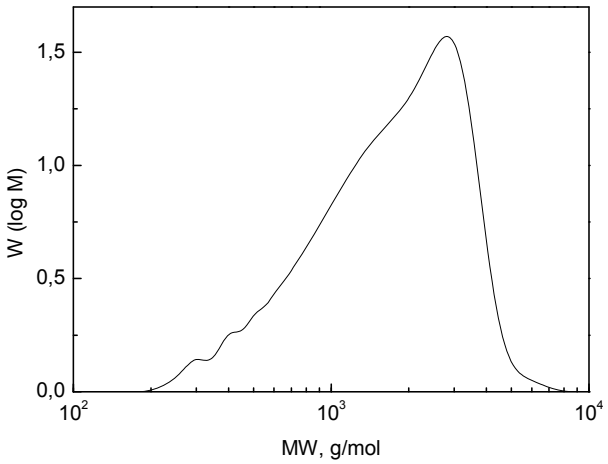

Figure 1 Molecular weight distribution of the synthesized polystyrene.

In order to ensure a sufficient concentration of high and low MW fractions of PS, the synthesized PS was mixed together in 1:1:1 w:w ratio with a PS batch of 1000 g mol^{-1} and one of 10000 g mol^{-1} PS. This particular mixture was chosen to obtain the rejection behaviour of the membranes above 1000 g mol^{-1} and check for leakages.

2.3.2 Permeation experiments

All permeation experiments were performed in a custom made cross-flow high pressure permeation set up [24]. The setup was equipped with a pressure and a circulation pump to adjust both pressure and circulation speed independently of each other. All permeation experiments were performed in a total recycle mode at a cross-flow velocity of the feed solution of 2,4 m s^{-1} for the PDMS membrane and 4.0 m s^{-1} for the zirconia membrane. These velocities corresponded to Reynold numbers of approximately 20000 for toluene and 31000 for hexane. The temperature of the feed solution was controlled at 25°C. All zirconia permeation experiments were performed using one module of 626.7 $x10^{-4}$ m^2. Each measurement was performed in triplicate. For the PDMS permeation studies we

used three membrane modules of 7.1 $x10^{-4}$ m^2, each. The average of the three membranes is reported here.

Before starting the flux or MWCO measurement, each membrane module was pressurized at the test pressure for minimum 2 h to reach the steady state conditions. The permeance coefficient, P (l $m^{-2}h^{-1}bar^{-1}$), was calculated from the slope of the flux (J, in l $m^{-2}h^{-1}$) versus trans membrane pressure (TMP) graph. Determination of the pure solvent permeance coefficients was always carried out first. Afterwards, the permeation of 0.3% (w/w) PS mixture, with MW distribution ranging from 300 to 20000 g mol^{-1}, was performed in order to obtain MWCO curves. Next a PIB mixture of 1:1:1:1:1 (w/w) of five fractions: 350, 550, 1000, 1300, and 2300 g mol^{-1}, all having a broad MW distribution, was dissolved in toluene at a total polymer concentration of 0.3% (w/w). The MW of the PIB oligomer mixture ranged from 200-20.000 g mol^{-1}. It was used to determine MWCO curves for all tested membranes in the toluene-PIB system. The same composition and concentration of PIB was used for tests in the n-hexane-PIB system. In order to ensure that separation performance of the membranes was not changed during filtration experiments, permeation of PS-toluene solution was repeated and compared to the initial results. The concentration of PS and PIB oligomers in the feed and permeate stream was determined by GPC chromatography. For PS a PSS SDV 1000 Å column was used with analytical grade toluene as a mobile phase. In the case of PIB, tandem columns PSS SDV 100 Å and PSS SDV 1000 Å were used with analytical grade THF as a mobile phase. The GPC analysis is described in detail elsewhere [24].

3. Results and discussion

3.1. PDMS membrane fabrication

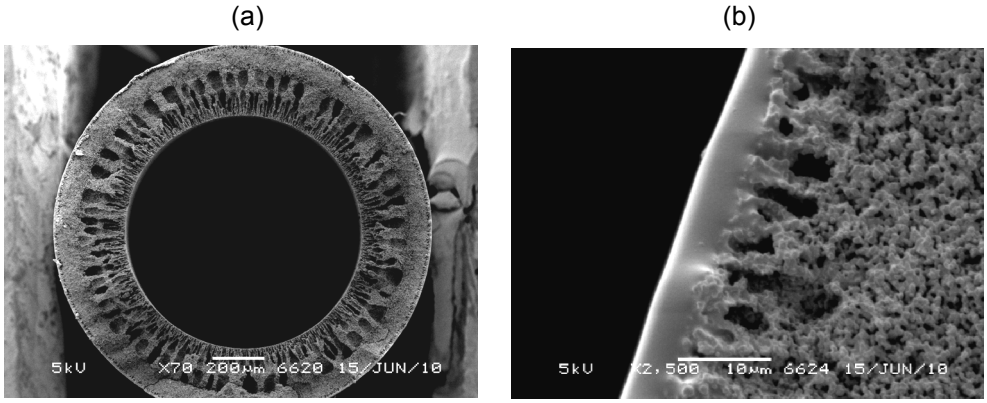

Figure 2. SEM pictures of composite α-alumina/PDMS hollow fiber: (a) Cross-section (magnification 75x) and (b) Cross-section (magnification 2500x).

Figure 2 presents SEM images of the cross section of the composite PDMS/α-alumina membrane. The outer diameter of the fiber was ~ 1.5 mm and the wall thickness ~ 0.28 mm. The cross section image reveals a distinct PDMS layer on a support consisting of two α-alumina layers with different particle size. The layers adhere very well. The inner α-alumina layer has relatively large pores in between particles combined with a noticeable macrovoid volume, corresponding to low resistance to mass transport. The outer α-alumina layer exhibits less macrovoids and has smaller interparticle pores, to prevent infiltration of the PDMS top layer. Dutczak et al. [24] described the importance of having small pores in the top layer on the support. The thickness of the PDMS layer was estimated to be 6 ± 1 µm with pore intrusion ~2 µm, using a procedure described elsewhere [24].

3.2. Permeance and MWCO

3.2.1. Effects of the solute

Figure 3a presents the flux of pure toluene and PS / toluene and PIB / toluene mixtures as function of pressure for both membranes whereas Figures 3b and 3c present the PS and PIB retention curves of the membranes. Please note that whereas in figure 3a the symbols represent actual experimental values, the symbols in figure 3b and 3c only serve to guide the eye between the different lines resulting from the gel permeation chromatograph analysis. For the PDMS membrane there is a linear relation between toluene flux and pressure that is not significantly affected by the presence of PS or PIB (Figure 3a). The membrane permeance coefficient is relatively low (P_{tol}=1.1, l $m^{-2}h^{-1}bar^{-1}$). The PS and PIB retention curves of PDMS (Figure 2b) reveal that the MWCO obtained with PIB is almost double (900 g mol^{-1}) as compared to that obtained with PS (500 g mol^{-1}). Since the flux through the PDMS membrane is unaffected by the presence of the solutes and the extent of membrane swelling is dominated by the solvent (the toluene volume fraction in the membrane is $\Phi_{toluene}$ = 0.73 [26]), the difference in retention must be a consequence of differences in molecular properties of the solutes. The lower retention of PIB is probably due to a combination of higher solubility and higher diffusivity in the membrane. A higher solubility can be justified based on the small difference between solubility parameters of PIB and PDMS ($\Delta\delta_{PDMS\text{-}PIB} \approx 0.4$), as compared PS and PDMS ($\Delta\delta_{PDMS\text{-}PS} \approx 3.0\text{-}2.3$ MPa $^{1/2}$) [28, 29].

It can be noted that although this highly swollen membrane consists for almost 3/4 of toluene, the larger radius of gyration for PIB in toluene, does not result in a higher retention. Apparently, the interaction of the solute with the PDMS network still dominates the transport. A higher diffusivity can be expected based on the smaller chain diameter and higher flexibility of PIB in comparison to PS [30], see Table 2. The smaller and more flexible PIB will be more mobile in the swollen PDMS, which according to Tarleton et al. could even be envisioned as an ill-defined porous structure with the pore size in the range of 1.0-1.5 nm [33, 34].

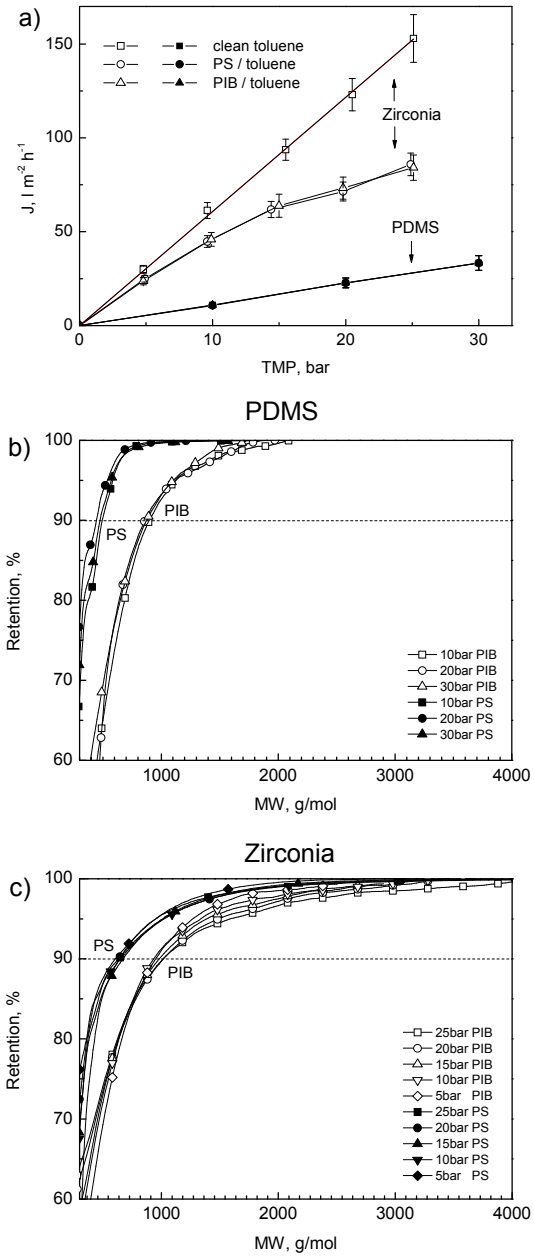

Figure 3 Transport properties of the zirconia and PDMS membranes: (a) Flux of toluene, PIB/toluene and PS/toluene as a function of transmembrane pressure. Retention curves of PIB and PS in toluene for (b) composite PDMS hollow fiber membrane (c) zirconia multichannel membrane. In Figure 3b and 3c the depicted symbols present an optical guide to distinguish between the experimental curves derived from the GPC analysis.

Table 2 Properties of solvents and solutes.

	PIB	PS
Static stiffness parameter λ^{-1}, nm [30]	1.27	2.35
Chain diameter d_b, nm [30]	0.64	1.01
Radius of gyration, nm [31, 32]	MW=854 (n-heptane) 0.79	MW=904 (toluene) 0.598

Figure 3b shows that there is no influence of pressure on the retention of PIB and PS oligomers by the PDMS membrane, similar to earlier observations [24]. This is a strong indication that the fluxes of solvent and solute through the PDMS are not directly coupled, i.e., via a solvent-solute friction term probably due to the low solute concentration (0.3% w/w). Stafie et al. investigated retention of oil in n-hexane by a PDMS/PAN membrane and reported an increase in retention with flux increase, at higher oil concentrations. The change of retention with flux was reduced at lower oil concentrations and was negligible below 8% (w/w) oil in n-hexane. In this work we used 0.3% (w/w) concentration of oligomers.

For the PDMS membrane, pressure independent solute retention combined with the linear relation between the flux and the pressure indicate that concentration polarization derived effects are not relevant. A quantitative analysis of concentration polarization is complicated by the uncontrolled turbulent hydrodynamics in the membrane module and the vibrations of the fiber. However, a relatively high mass transfer coefficient can be expected which combined with a low membrane flux corresponds to a rather small Peclet number. This indicates that the difference in concentration of oligomers in the liquid bulk and at the membrane surface will only be small.

The pure toluene flux through the porous zirconia increases linearly with pressure (Figure 3a). The permeance coefficient (6.1 ± 0.1, l $m^{-2}h^{-1}bar^{-1}$) is much higher as compared to the PDMS membrane. In the presence of PIB or PS the

permeance is not constant anymore but decreases with increasing pressure. The decrease in permeance is reversible; after washing the membrane with pure toluene for several hours the permeance recovers to its initial value. This non-linear relation between flux and pressure can be indicative of concentration polarization derived effects. For this system concentration polarization modulus was estimated to be approximately 11, according to the following equation [35]:

$$\frac{c_{i0}}{c_{ib}} = \frac{\exp(J_v \delta / D_i)}{1 + E_0[\exp(J_v \delta / D_i) - 1]} \quad (1)$$

The corresponding Peclet number is ~ 2 ($Pe_{PS/toluene} \approx Pe_{PIB/toluene} \approx 2$), indicating that there is moderate enhancement in concentration of oligomers at the surface of the membrane and low osmotic pressure difference ($\Delta\Pi < 1$ bar). The non-linear relation is probably due to the presence of oligomers in the membrane pores, hindering the transport through the membrane. This also complies with the relatively long time (~hours) required for recovery of the permeability. In order to restore the flux to its original behavior only permeation with pure solvent was used. In the experiments no influence of the history of the experiments was found, which is a strong indication that fouling or irreversible phenomena did not occur.

The PS retention curves for the zirconia membrane reveal MWCO of 650 g mol^{-1} (Figure 3c), in agreement with the specifications given by the manufacturer. The MWCO obtained with PIB (950 g mol^{-1}) is much higher. The lower PIB retention is probably due to its shape and flexibility: the thinner and more flexible PIB passes easier through the pores than the more rigid PS. Interestingly, the retention curves of PIB show a slight dependence on the pressure; for higher pressures a lower retention is observed. The reduced retention cannot be related to concentration polarization in a straightforward manner, because this phenomenon would in fact be more pronounced for the PS molecules (similar Peclet number, higher retention). The lower retention at higher pressures may indicate shear-induced deformation of the PIB molecules, allowing higher transport rate of these oligomers through the rigid pores. This effect will be unimportant for the rigid, non-deformable PS molecules.

3.2.2. Effect of solvent

This section deals with the influence of the solvent on the rejection of the PIB oligomers. Due to very limited solubility of PS in n-hexane, retention measurements could not be performed for PS/hexane.

Figure 4a depicts the fluxes of pure hexane and a PIB/hexane mixture for both membranes. The general trends are the same as in the case of toluene (compare with Figure 3). For the PDMS composite membrane, the flux of pure n-hexane and the PIB/n-hexane mixture are similar, and linearly proportional to the pressure. Despite comparable swelling of the membrane in toluene and n-hexane ($\Phi_{v/v}$=0.73-0.77 [26]) the flux of n-hexane is much higher as compared to toluene. The permeance coefficient is sufficiently low (P_{tol}=1.8 ± 0.1, l $m^{-2}h^{-1}bar^{-1}$) to assume that concentration polarization effects are negligible. Figure 4b depicts the PIB retention curves of the PDMS membrane using toluene or n-hexane as solvent. For both solvents the PIB retention is almost independent of pressure. The MWCO of PIB in toluene is much higher (900 g mol^{-1}) than in n-hexane (650 g mol^{-1}). The main reason for the difference in MWCO is the higher permeance of n-hexane, resulting in a lower concentration of PIB in the permeate. These observations suggest that there is no direct coupling between the fluxes of solvent and solute.

For the zirconia porous membrane the flux of pure hexane increases linearly with transmembrane pressure (Figure 4a). The permeance coefficient (17.2 ± 0.3, l $m^{-2}h^{-1}bar^{-1}$) is much larger than that of toluene. The presence of PIB results in a non-linear relation

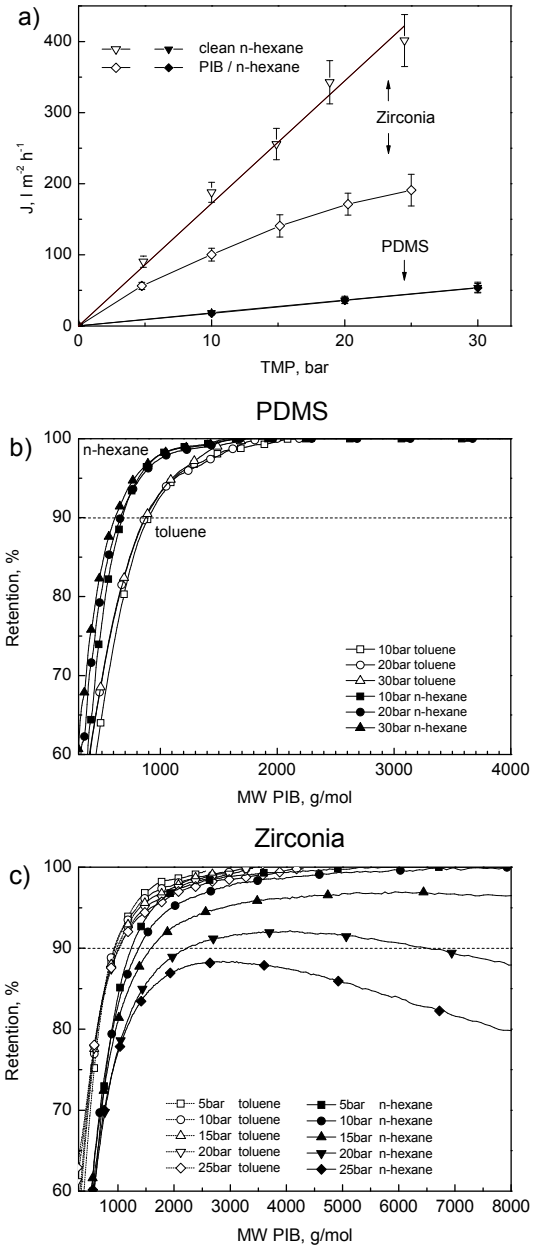

Figure 4 Transport properties of the zirconia and PDMS membranes: (a) Flux of n-hexane and PIB/n-hexane as a function of trans membrane pressure. (b) Retention curves of PIB for PDMS. Solvents: toluene and n-hexane. (c) Retention curves of PIB for zirconia membrane. Solvents: toluene and n-hexane. In Figure 4b and 4c the depicted symbols present an optical guide to distinguish between the experimental curves derived from the GPC analysis.

between flux and pressure, in fact at higher pressures the permeance decreases with increasing pressure. Also in this case, the estimated Peclet number is ~ 3 [35] and the osmotic pressure difference is low ($\Delta\Pi$ < 2 bar) indicating that concentration polarization induced osmotic effects cannot explain the drop in permeance. Similarly in this case, presence of PIB molecules in the pores seems to obstruct the flow. The retention of PIB by the zirconia membrane in the two solvents is in contrast with that of PDMS (Figure 4c). The MWCO obtained with PIB in toluene is much lower (950 g mol^{-1}) than in n-hexane (higher than 1200 g mol^{-1}). Notably, the retention curves in n-hexane show very pronounced pressure dependence. At high pressures the retention initially increases with MW until a maximum value and then decreases (see Figure 4c). The initial increase in retention corresponds to enhanced size exclusion of larger molecules. The decrease in retention with MW for the larger molecules is typically attributed to concentration polarization and was found to be reversible. The effect can be estimated calculating the concentration polarization modulus as a function of MW. It shows in particular that larger molecules diffuse at a lower rate from the membrane surface back to the liquid bulk, causing an increase of high-MW PIB concentration in the boundary layer. A higher concentration gradient of large oligomers over the membrane surface results in higher flux of these molecules through the membrane and hence a lower retention. Superimposed effects can be an increase of the partitioning coefficient of the high MW oligomers [36] and the shear induced deformation of PIB molecules in the pores, similar to that reported by Beerlage et al. for polyimide UF membranes with ethyl acetate / high MW polystyrene (96000 g mol^{-1}) [25]. As suggested by Beerlage, a higher trans-membrane pressure, and corresponding larger flow through the pore, increases the frictional force on the solute molecules. The enhanced frictional force causes the polymer coil to unroll into more elongated conformations, which are smaller than the original polymer coil and pass through the pores more easily. It should be noted that in the present study the higher flux of n-hexane is due to the lower viscosity, and in a macroscopic description of the flow the shear forces inside the liquid would remain unchanged for a given pressure drop. However, given the

comparable nanometer scale dimensions of the pores and oligomers, for the system under study such a macroscopic description is probably not valid.

Finally, it is important to point out that after all permeation experiments, filtration of PS / toluene was repeated for both membranes. No significant changes in retention were observed in comparison to the initial results suggesting that the membrane transport properties were not compromised during the study.

3.4 Conclusions

To summarize our observations, Figure 4 shows the retention of 1500 g mol^{-1} PS and PIB as a function of total permeate flux for the dense rubber PDMS membrane and the rigid porous zirconia membrane.

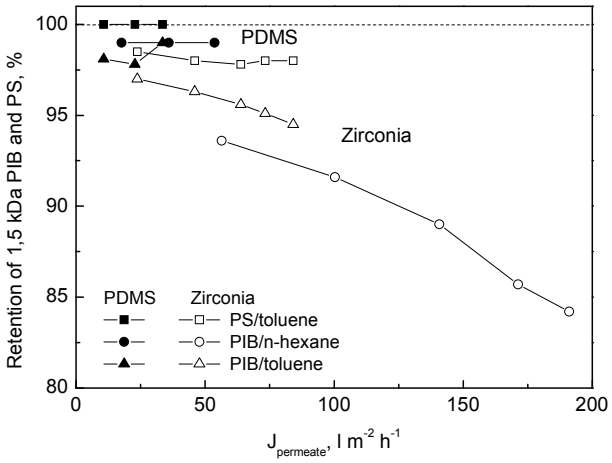

Figure 5 Retention of 1500 g mol^{-1} rigid PS and flexible PIB by the PDMS (full symbols) and zirconia (open symbols) membranes. Solvents: n-hexane and toluene.

In the case of the PDMS membrane there is very little effect of flux on retention. For this membrane the solvent and solute are transported independently through the membrane and solvent-membrane and solute-membrane determine retention behavior. For the zirconia membrane the retention of flexible PIB decreases dramatically at higher fluxes, whereas retention of the more rigid PS stays relatively constant. For this porous membrane there is direct coupling between the solvent

and solute fluxes and the superimposed effects concentration polarization and shear induced solute deformation are considerable. The presented observations point out that the selection of the proper solvent - solute system and the process conditions for the MWCO determination as well as the interpretation of MWCO data in organic solvents requires extreme caution.

Acknowledgments

We would like to gratefully acknowledge the Dutch Technology Foundation (STW) (project no 07349) for the financial support. Authors also would like to thank Nadia Vleugels and Lydia Bolhuis-Versteeg for the help with permeation measurements and Clemens Padberg for the help with GPC analysis.

References

[1] Y.H. See Toh, F.W. Lim, A.G. Livingston, Polymeric membranes for nanofiltration in polar aprotic solvents, J. Membr. Sci., 301 (2007) 3-10.

[2] K. Vanherck, P. Vandezande, S.O. Aldea, I.F.J. Vankelecom, Cross-linked polyimide membranes for solvent resistant nanofiltration in aprotic solvents, J. Membr. Sci., 320 (2008) 468-476.

[3] L.S. White, C.R. Wildemuth, Aromatics enrichment in refinery streams using hyperfiltration, Ind. Eng. Chem. Res., 45 (2006) 9136-9143.

[4] J.P. Sheth, Y. Qin, K.K. Sirkar, B.C. Baltzis, Nanofiltration-based diafiltration process for solvent exchange in pharmaceutical manufacturing, J. Membr. Sci., 211 (2003) 251-261.

[5] J.T. Scarpello, D. Nair, L.M. Freitas dos Santos, L.S. White, A.G. Livingston, The separation of homogeneous organometallic catalysts using solvent resistant nanofiltration, J. Membr. Sci., 203 (2002) 71-85.

[6] A. Livingston, L. Peeva, S. Han, D. Nair, S.S. Luthra, L.S. White, L.M. Freitas Dos Santos, Membrane Separation in Green Chemical Processing, Ann. N. Y. Acad. Sci., 984 (2003) 123-141.

[7] S.S. Luthra, X. Yang, L.M. Freitas dos Santos, L.S. White, A.G. Livingston, Homogeneous phase transfer catalyst recovery and re-use using solvent resistant membranes, J. Membr. Sci., 201 (2002) 65-75.

[8] V. Kale, S.P.R. Katikaneni, M. Cheryan, Deacidifying rice bran oil by solvent extraction and membrane technology, J. Am. Oil. Chem. Soc., 76 (1999) 723-727.

[9] H.J. Zwijnenberg, A.M. Krosse, K. Ebert, K.V. Peinemann, F.P. Cuperus, Acetone-stable nanofiltration membranes in deacidifying vegetable oil, J. Am. Oil. Chem. Soc., 76 (1999) 83-87.

[10] J.C.T. Lin, A.G. Livingston, Nanofiltration membrane cascade for continuous solvent exchange, Chem. Eng. Sci., 62 (2007) 2728-2736.

[11] D. Shi, Y. Kong, J. Yu, Y. Wang, J. Yang, Separation performance of polyimide nanofiltration membranes for concentrating spiramycin extract, Desalination, 191 (2006) 309-317.

[12] P. Vandezande, L.E.M. Gevers, I.F.J. Vankelecom, Solvent resistant nanofiltration: Separating on a molecular level, Chem. Soc. Rev., 37 (2008) 365-405.

[13] J.A. Whu, B.C. Baltzis, K.K. Sirkar, Nanofiltration studies of larger organic microsolutes in methanol solutions, J. Membr. Sci., 170 (2000) 159-172.

[14] D. Bhanushali, S. Kloos, D. Bhattacharyya, Solute transport in solvent-resistant nanofiltration membranes for non-aqueous systems: Experimental results and the role of solute-solvent coupling, J. Membr. Sci., 208 (2002) 343-359.

[15] D. Bhanushali, S. Kloos, C. Kurth, D. Bhattacharyya, Performance of solvent-resistant membranes for non-aqueous systems: Solvent permeation results and modelling, J. Membr. Sci., 189 (2001) 1-21.

[16] N. Stafie, D.F. Stamatialis, M. Wessling, Insight into the transport of hexane-solute systems through tailor-made composite membranes, J. Membr. Sci., 228 (2004) 103-116.

[17] N. Stafie, D.F. Stamatialis, M. Wessling, Effect of PDMS cross-linking degree on the permeation performance of PAN/PDMS composite nanofiltration membranes, Sep. Purif. Technol., 45 (2005) 220-231.

[18] D.F. Stamatialis, N. Stafie, K. Buadu, M. Hempenius, M. Wessling, Observations on the permeation performance of solvent resistant nanofiltration membranes, J. Membr. Sci., 279 (2006) 424-433.

[19] A.V. Volkov, D.F. Stamatialis, V.S. Khotimsky, V.V. Volkov, M. Wessling, N.A. Plate, Poly[1-(trimethylsilyl)-1-propyne] as a solvent resistance nanofiltration membrane material, J. Membr. Sci., 281 (2006) 351-357.

[20] S. Darvishmanesh, J. Degrève, B. Van Der Bruggen, Mechanisms of solute rejection in solvent resistant nanofiltration: The effect of solvent on solute rejection, Phys. Chem. Chem. Phys., 12 (2010) 13333-13342.

[21] P.P. I. Voigt, T. Holborn, G. Dudziak, M. Mutter and A. Nickel, Ceramic nanofiltration membranes for applications in organic solvents, in: 9th Aachen Membrane Colloquium, Aachen, Germany, (2003), pp. pOP 20-21-OP 20-11.

[22] H.J. Zwijnenberg, A standardized characterization method for solvent resistant nanofiltration membrane modules., in: ICOM 2005, Seoul, Korea, (2005) Fr12B-3, pp I-481-482.

[23] Y.H. See Toh, X.X. Loh, K. Li, A. Bismarck, A.G. Livingston, In search of a standard method for the characterisation of organic solvent nanofiltration membranes, J. Membr. Sci., 291 (2007) 120-125.

[24] S.M. Dutczak, M.W.J. Luiten-Olieman, H.J. Zwijnenberg, L.A.M. Bolhuis-Versteeg, L. Winnubst, M.A. Hempenius, N.E. Benes, M. Wessling, D. Stamatialis, Composite capillary membrane for solvent resistant nanofiltration, J. Membr. Sci., 372 (2011) 182-190.

[25] M.A.M. Beerlage, M.L. Heijnen, M.H.V. Mulder, C.A. Smolders, H. Strathmann, Non-aqueous retention measurements: Ultrafiltration behaviour of polystyrene solutions and colloidal silver particles, J. Membr. Sci., 113 (1996) 259-273.

[26] N. Stafie, Poly(dimethyl siloxane) – based composite nanofiltration membranes for non-aqueous applications, Ph.D. thesis, University of Twente, Enschede, The Netherlands, (2004).

[27] J. De Jong, N.E. Benes, G.H. Koops, M. Wessling, Towards single step production of multi-layer inorganic hollow fibers, J. Membr. Sci., 239 (2004) 265-269.

[28] H.-G. Elias, An Introduction to Plastics, Wiley-VCH, Weinheim, 2003.

[29] J.E. Mark, Polymer Data Handbook, Oxford University Press, Inc., Oxford, 1999.

[30] F. Abe, Y. Einaga, H. Yamakawa, Intrinsic viscosity of oligo- and polyisobutylenes: treatments of negative intrinsic viscosities, Macromolecules, 24 (1991) 4423-4428.

[31] M. Yamada, M. Osa, T. Yoshizaki, H. Yamakawa, Excluded-volume effects on the mean-square radius of gyration of oligo- and polyisobutylenes in dilute solution, Macromolecules, 30 (1997) 7166-7170.

[32] F. Abe, Y. Einaga, T. Yoshizaki, H. Yamakawa, Excluded-volume effects on the mean-square radius of gyration of oligo- and polystyrenes in dilute solutions, Macromolecules, 26 (1993) 1884-1890.

[33] J.P. Robinson, E.S. Tarleton, K. Ebert, C.R. Millington, A. Nijmeijer, Influence of cross-linking and process parameters on the separation performance of poly(dimethylsiloxane) nanofiltration membranes, Ind. Eng. Chem. Res., 44 (2005) 3238-3248.

[34] E.S. Tarleton, J.P. Robinson, C.R. Millington, A. Nijmeijer, Non-aqueous nanofiltration: Solute rejection in low-polarity binary systems, J. Membr. Sci., 252 (2005) 123-131.

[35] R. Baker, Membrane Technology and Applications, 2nd Edition John Wiley & Sons, Ltd, 2004.

[36] I. Teraoka, Polymer solutions in confining geometries, Prog. Polym. Sci., 21 (1996) 89-149.

Chapter IV

New crosslinking method of polyamide-imide membranes for applications in harsh polar aprotic solvents

S.M. Dutczak, P.F. Cuperus, M. Wessling and D. Stamatialis

Abstract

We report for the first time successful crosslinking of polyamide-imide (Torlon®) based membranes using di-isocyanates. The crosslinked membranes are resistant to harsh polar aprotic solvents like N- methyl pyrrolidone (which are solvents of the non crosslinked membranes) and have very good mechanical properties. Besides, in contrast to to the state-of-the-art polyimide crosslinked membranes, the created covalent bond is thermally stable enabling applications at elevated temperatures. The transport characteristics of the new membranes (permeance and molecular weight cut off - MWCO) can be tailored via the crosslinking process.

1. Introduction

Solvent resistant nanofiltration (SRNF) attracts lot of attention due to its simplicity and great energy efficiency. Literature already reports numerous successful applications in many branches of industry ranging from petrochemistry [1], through pharmaceutical manufacturing [2-5], to catalytical processes [6-9]. The last years, lot of effort has been spent on development and improvement of membrane stability in various solvents [10-13]. Most of the membranes are either dense PDMS composites [14-22] or porous integrally skinned made of polyimides (PI) [10, 23] or polyamide-imide (PAI) [12]. Generally PI and PAI membranes are prepared by phase inversion process from solutions in polar aprotic solvents [5]. Therefore they cannot be used for separations in such solvents (e.g. N-methyl pyrrolidone (NMP), di-methyl sulfoxide (DMSO), di-methyl formamide (DMF) or di-methyl acetamide (DMAc)). To overcome this limitation and improve their stability, state-of-the art PI membranes are crosslinked by diamines in an imide-ring opening reaction [24] either during phase separation [12] or in post casting process [10]. The covalent bond created there is not thermally stable and at temperatures above 100^{o}C re-imidization might occur leading to loss of membrane stability [10, 25]. Moreover, long exposure to the diamine crosslinking solution may cause deterioration of the membrane or even membrane dissolution [26]. Particularly vulnerable to this are the PAIs.

In this work we report a new method of crosslinking of PAI membranes using di-isocyanates. The resulting membranes are resistant to NMP, have good mechanical properties and have potential to be used in separation processes at elevated temperature.

2. Experimental

2.1. Materials

Toluene, methanol and tetrahydrofuran (THF) all analytical grade, were purchased from Merck (The Netherlands). Styrene (ReagentPlus ≥99%), sec-butyllithium solution 1.4 M in cyclohexane, 6-Hexamethylene Diisocyanate (HMDI) (purum, ≥98.0%), triethylene diamine (TEA) (≥99%), Tin 2-ethylhexanoate (~95%) were purchased from Sigma Aldrich (The Netherlands). 1-Methyl-2-pyrrolidinone (NMP), extra pure, was purchased from Acros Organics. Acetone (technical grade) was purchased from Assink (Hengelo, The Netherlands). All chemicals were used as supplied without additional purification.

2.2. Crosslinking

Commercial Torlon® based membranes (obtained from SolSep B.V.) were used for cross-linking. The membranes were first dried at 150^{o}C for 12 h to remove water and then immersed into the cross-linking solution containing 70 wt% (v/v) tetrahydrofuran (THF), 14% (v/v) hexamethylene diisocyanate (HMDI) as crosslinking agent, a mixture of catalysts: 7% (v/v) triethylene diamine (TEA), 5% (v/v) NMP, and 4% (v/v) tin 2-ethylhexanoate as a co-catalyst, for 13 days at 50^{o}C. The reaction was performed in a closed container to ensure water free environment. Then the membranes were removed from the solution and rinsed carefully for 48 h in THF, then 8 h in methanol and finally 8 h in acetone. The resulting membranes were dried at ambient temperature.

2.3. Attenuated Total Reflectance Fourier Transform Infrared Spectroscopy (ATR-FTIR)

The FT-IR spectra for the crosslinked and non-crosslinked membranes were recorded over a scanning range of 650-4000 cm^{-1} at room temperature, using a Perkin Elmer Spectrum 100 FTIR spectrometer equipped with universal ATR

polarization accessory. All samples before measurements were dried in a vacuum oven at 30°C for 12 h.

2.4. Permeation measurements

All permeation experiments were performed in custom made cross-flow high pressure permeation set up in a total recycle mode at a crossflow velocity of the feed solution 1 m/s. The temperature of the feed solution was controlled at 18°C. The membrane area was 9.6 x10^{-4} m^2. Before starting the flux or retentions measurements, the membrane was always pressurized at the test pressure for minimum 2h to reach the steady state conditions. The flux through the membrane (J, in l $m^{-2}h^{-1}$) was calculated using the following equation:

$$J = \frac{V}{A \times t} \quad (1)$$

where V is the permeate volume (l), A the membrane area (m^2) and t is the permeation time (h). The permeance coefficient, P (l $m^{-2}h^{-1}bar^{-1}$), was calculated from the slope of the flux versus trans membrane pressure (TMP) graph:

$$P = \frac{J}{\Delta P} \quad (2)$$

The membrane retention R, for the PS oligomers was calculated from permeate and feed samples with the following equation:

$$R_{i-PS}(\%) = \left(1 - \frac{C_{P,i}}{C_{F,i}}\right) \times 100\% \quad (3)$$

where $C_{P,i}$ and $C_{F,i}$ are the concentrations of the individual PS oligomers in the permeate and the feed stream respectively.

Details of the cross-flow set up and the detailed description of MWCO determination using broad molecular weight polystyrene (300-6000 g mol^{-1}) are described elsewhere [13].

3. Results and discussion

3.1. Crosslinking of polyamide – imide (Torlon®)

Commercial polyamide-imide (Torlon®) based membranes, kindly provided by SolSep B.V. (Apeldoorn – The Netherlands), were crosslinked using 1,6-Hexamethylene Diisocyanate (HMDI). In our opinion crosslinking happens via reaction of amide group of Torlon and isocyanate group of HMDI [27] (see Fig. 1).

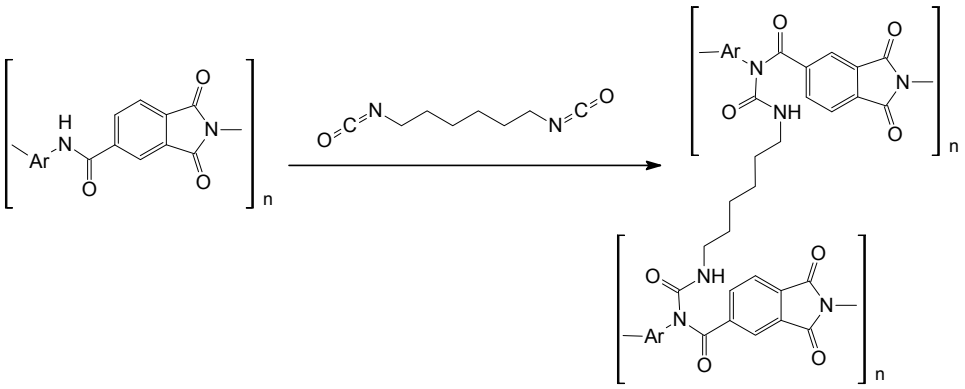

Figure 1 Crosslinking of polyamide-imide by HMDI

During crosslinking, one amide group is consumed and a new one is created, thus, we found no difference between the FTIR spectra of non crosslinked and crosslinked membrane (see Figure 2), in contrast to an imide open-ring crosslinking where there is distinct change in the spectrum [28].

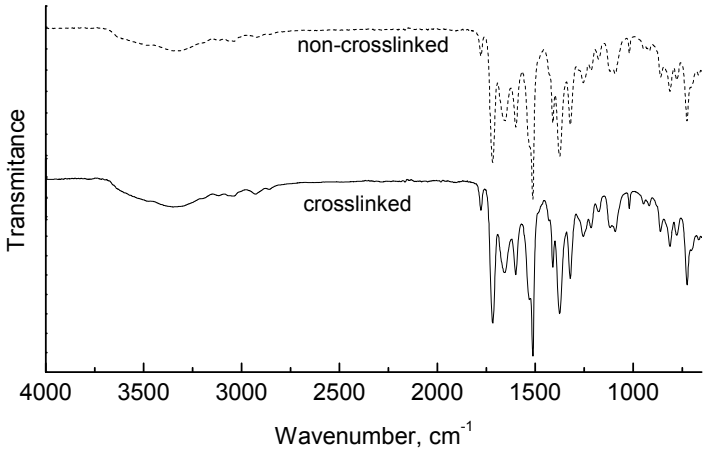

Figure 2 FTIR spectra of non-crosslinked and crosslinked Torlon

Direct evidence of the membrane crosslinking is the fact that it does not dissolve in NMP, which is solvent for the non crosslinked membrane. During our studies we also found out that addition of small amount of NMP into a crosslinking solution greatly increases the crosslinking reaction rate. We think that NMP, besides swelling the membrane and facilitating diffusion of HMDI into matrix, as a tertiary amine also acts as a catalyst for the crosslinking reaction [27]. In fact when the membrane is crosslinked without NMP, crosslinking is incomplete and the produced membranes partly dissolve during filtration in NMP. Membranes crosslinked using NMP are flexible and easy to handle.

3.2. Membrane performance in toluene and NMP

In order to evaluate the performance of the crosslinked membrane we performed the following filtration cycle: i) pure acetone ii) 0.3 % w/w acetone / polystyrene (PS) to obtain MWCO curves [13] iii) pure NMP and finally iv) 0.3% w/w acetone-PS to evaluate influence of NMP on MWCO. For the non crosslinked

membrane, we could only perform steps i) to iii) because it dissolves in NMP. All filtration experiments were carried out using the same sets of membranes.

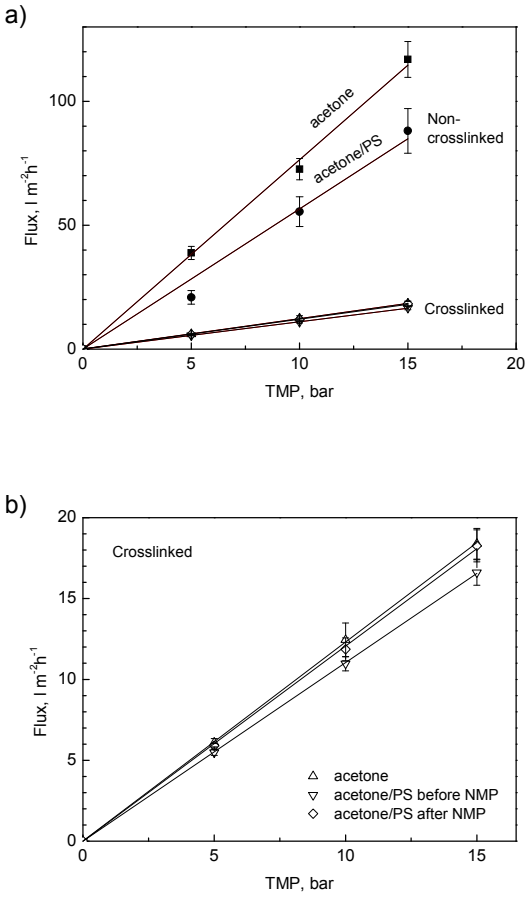

Figure 3 (a) Transport of acetone and acetone / PS mixtures through non crosslinked and crosslinked membranes. (b) Zoom in to the results of the crosslinked membranes.

Figure 3a presents results of all permeation experiments. For both non crosslinked and crosslinked membranes the flux increases linearly as a function of pressure indicating the absence of membrane compaction (and for the case of mixtures) concentration polarization phenomena. For the crosslinked membrane, permeance of pure acetone is similar to that for acetone / PS mixture (1.2 ± 0.1,

l $m^{-2}h^{-1}bar^{-1}$) and much lower than those of the non crosslinked ones; (7.6 ± 0.1 and 5.7 ± 0.3 l $m^{-2}h^{-1}bar^{-1}$ for acetone and PS /acetone, respectively).

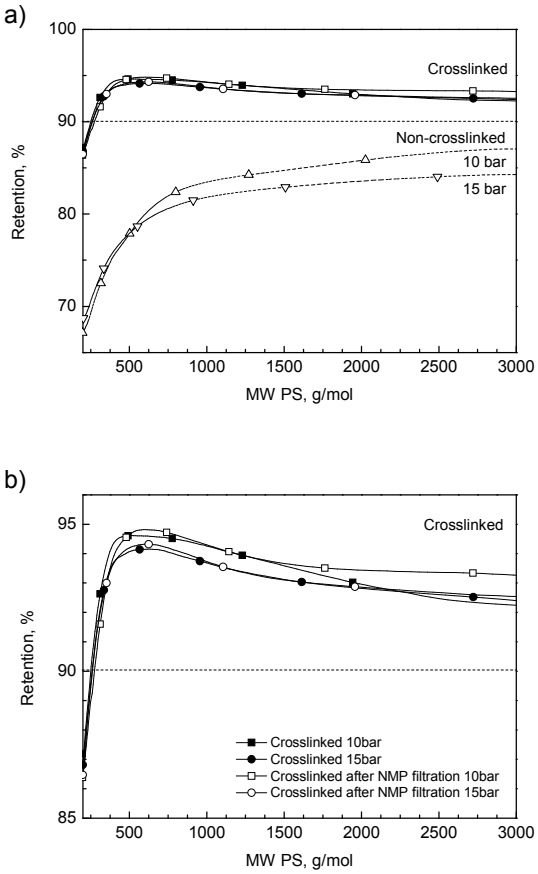

Figure 4 (a) Retention curves of polystyrene (PS) for the non crosslinked and crosslinked membranes before and after filtration. (b) Zoom into the results of the crosslinked membranes.

The NMP permeance for the crosslinked membrane is rather low (0.1, l $m^{-2}h^{-1}bar^{-1}$) and the structure of crosslinked membrane remains unchanged after NMP filtration. In fact, for this membrane, filtration of acetone / PS mixture after NMP filtration gives exactly the same flux as prior to NMP filtration (1.2, l $m^{-2}h^{-1}bar^{-1}$, Fig.3b).

Figure 4a compares the retention curves of PS in acetone for crosslinked and non crosslinked membranes. It was not possible to determine MWCO for non crosslinked membrane since maximum retention of PS was only 87%. The PS

retention by the crosslinked membrane is much higher (up to 95%) and the membrane MWCO is 260 g mol^{-1}. The estimated MWCO of the crosslinked membrane is the same before and after NMP filtration (Fig.4b), showing again the membrane stability in NMP. The filtration experiments clearly show that crosslinking causes membrane densification (decrease in membrane permeance and MWCO). We think that this densification can be controlled via tailoring of the crosslinking conditions. Because during crosslinking one amide group is consumed and another one is created, the reaction can continue till all diisocyanate is consumed or there is too much steric hindrance. Thus, in principle for high diisocyanate concentrations and longer crosslinking time denser membranes (with lower MWCO) can be produced. Our future work will focus on investigating of crosslinking of different PI and PAI's and the role of various polyisocyanates as well as the effect of crosslinking conditions on membrane structure and performance. We will also evaluate membrane thermal stability by conducting separations at elevated temperatures.

4. Conclusions

The new method of crosslinking of polyamide-imide membranes by diisocyanates proposed here is a very effective way to prepare membranes for filtration of polar aprotic solvents. By varying the crosslinking time it seems possible to tailor the membrane MWCO: longer crosslinking time corresponds to tighter (lower MWCO) membrane.

Acknowledgments

S. Dutczak would like to acknowledge Dutch Technology Foundation (STW) (project no 07349) for the financial support and Catherine R. Tanardi, Lydia Bolhuis-Versteeg for assistance with measurements.

References

[1] L.S. White, C.R. Wildemuth, Aromatics enrichment in refinery streams using hyperfiltration, Ind. Eng. Chem. Res., 45 (2006) 9136-9143.

[2] J.P. Sheth, Y. Qin, K.K. Sirkar, B.C. Baltzis, Nanofiltration-based diafiltration process for solvent exchange in pharmaceutical manufacturing, J. Membr. Sci., 211 (2003) 251-261.

[3] J.C.T. Lin, A.G. Livingston, Nanofiltration membrane cascade for continuous solvent exchange, Chem. Eng. Sci., 62 (2007) 2728-2736.

[4] D. Shi, Y. Kong, J. Yu, Y. Wang, J. Yang, Separation performance of polyimide nanofiltration membranes for concentrating spiramycin extract, Desalination, 191 (2006) 309-317.

[5] P. Vandezande, L.E.M. Gevers, I.F.J. Vankelecom, Solvent resistant nanofiltration: Separating on a molecular level, Chem. Soc. Rev., 37 (2008) 365-405.

[6] A. Livingston, L. Peeva, S. Han, D. Nair, S.S. Luthra, L.S. White, L.M. Freitas Dos Santos, Membrane separation in green chemical processing: Solvent nanofiltration in liquid phase organic synthesis reactions, in: Ann. N. Y. Acad. Sci., 2003, pp. 123-141.

[7] J.T. Scarpello, D. Nair, L.M. Freitas dos Santos, L.S. White, A.G. Livingston, The separation of homogeneous organometallic catalysts using solvent resistant nanofiltration, J. Membr. Sci., 203 (2002) 71-85.

[8] A. Livingston, L. Peeva, S. Han, D. Nair, S.S. Luthra, L.S. White, L.M. Freitas Dos Santos, Membrane Separation in Green Chemical Processing, Ann. N. Y. Acad. Sci., 984 (2003) 123-141.

[9] S.S. Luthra, X. Yang, L.M. Freitas dos Santos, L.S. White, A.G. Livingston, Homogeneous phase transfer catalyst recovery and re-use using solvent resistant membranes, J. Membr. Sci., 201 (2002) 65-75.

[10] Y.H. See Toh, F.W. Lim, A.G. Livingston, Polymeric membranes for nanofiltration in polar aprotic solvents, J. Membr. Sci., 301 (2007) 3-10.

[11] K. Vanherck, P. Vandezande, S.O. Aldea, I.F.J. Vankelecom, Cross-linked polyimide membranes for solvent resistant nanofiltration in aprotic solvents, J. Membr. Sci., 320 (2008) 468-476.

[12] K. Vanherck, A. Cano-Odena, G. Koeckelberghs, T. Dedroog, I. Vankelecom, A simplified diamine crosslinking method for PI nanofiltration membranes, J. Membr. Sci., 353 (2010) 135-143.

[13] S.M. Dutczak, M.W.J. Luiten-Olieman, H.J. Zwijnenberg, L.A.M. Bolhuis-Versteeg, L. Winnubst, M.A. Hempenius, N.E. Benes, M. Wessling, D. Stamatialis, Composite capillary membrane for solvent resistant nanofiltration, J. Membr. Sci., 372 (2011) 182-190.

[14] S. Aerts, A. Vanhulsel, A. Buekenhoudt, H. Weyten, S. Kuypers, H. Chen, M. Bryjak, L.E.M. Gevers, I.F.J. Vankelecom, P.A. Jacobs, Plasma-treated PDMS-membranes in solvent resistant nanofiltration: Characterization and study of transport mechanism, J. Membr. Sci., 275 (2006) 212.

[15] K. Ebert, J. Koll, M.F.J. Dijkstra, M. Eggers, Fundamental studies on the performance of a hydrophobic solvent stable membrane in non-aqueous solutions, J. Membr. Sci., 285 (2006) 75-80.

[16] L.E.M. Gevers, S. Aldea, I.F.J. Vankelecom, P.A. Jacobs, Optimisation of a lab-scale method for preparation of composite membranes with a filled dense top-layer, J. Membr. Sci., 281 (2006) 741-746.

[17] N. Stafie, Poly(dimethyl siloxane) – based composite nanofiltration membranes for non-aqueous applications, Ph.D. thesis, University of Twente, Enschede, The Netherlands, (2004).

[18] N. Stafie, D.F. Stamatialis, M. Wessling, Insight into the transport of hexane-solute systems through tailor-made composite membranes, J. Membr. Sci., 228 (2004) 103-116.

[19] N. Stafie, D.F. Stamatialis, M. Wessling, Effect of PDMS cross-linking degree on the permeation performance of PAN/PDMS composite nanofiltration membranes, Sep. Purif. Technol., 45 (2005) 220-231.

[20] D.F. Stamatialis, N. Stafie, K. Buadu, M. Hempenius, M. Wessling, Observations on the permeation performance of solvent resistant nanofiltration membranes, J. Membr. Sci., 279 (2006) 424-433.

[21] E.S. Tarleton, J.P. Robinson, C.R. Millington, A. Nijmeijer, M.L. Taylor, The influence of polarity on flux and rejection behaviour in solvent resistant nanofiltration - Experimental observations, J. Membr. Sci., 278 (2006) 318-327.

[22] E.S. Tarleton, J.P. Robinson, M. Salman, Solvent-induced swelling of membranes - Measurements and influence in nanofiltration, J. Membr. Sci., 280 (2006) 442-451.

[23] Y.H. See-Toh, F.C. Ferreira, A.G. Livingston, The influence of membrane formation parameters on the functional performance of organic solvent nanofiltration membranes, J. Membr. Sci., 299 (2007) 236-250.

[24] Y. Liu, R. Wang, T.-S. Chung, Chemical cross-linking modification of polyimide membranes for gas separation, J. Membr. Sci., 189 (2001) 231-239.

[25] L. Shao, T.-S. Chung, S.H. Goh, K.P. Pramoda, Polyimide modification by a linear aliphatic diamine to enhance transport performance and plasticization resistance, J. Membr. Sci., 256 (2005) 46-56.

[26] F. Santoso, W. Albrecht, M. Schroeter, T. Weigel, D. Paul, R. Schomäcker, A novel technique for preparation of aminated polyimide membranes with microfiltration characteristics, J. Membr. Sci., 223 (2003) 171-185.

[27] K. Ashida, Polyurethane and Related Foams: Chemistry and Technology, CRC Taylor & Francis, Boca Raton-London-New York, 2006.

[28] K.K. Kopec, S.M. Dutczak, M. Wessling, D.F. Stamatialis, Chemistry in a spinneret - On the interplay of crosslinking and phase inversion during spinning of novel hollow fiber membranes, J. Membr. Sci., 369 (2011) 308-318.

Chapter V

Chemistry in a spinneret to fabricate hollow fibers for organic solvent filtration

S.M. Dutczak, C.R. Tanardi, K.K. Kopeć, M. Wessling, D. Stamatialis

Submitted for publication in Sep. Purif. Technol.

Abstract

Organic solvent filtration (OSF) is a very efficient separation technique with high potential in many branches of industry. Currently the choice of the commercial membranes is limited only to a few flat sheet membranes and spiral wound modules. It is generally known that a membrane in hollow fiber form has several advantages, over a flat configuration, such as high surface to volume ratio and no need of spacers. Consequently more compact and simpler modules and easy to scale up can be built.

In this work we explore a new technique called “chemistry in a spinneret”, to fabricate a hollow fiber (HF) for OSF. This technique combines the membrane formation and crosslinking reaction into a single step process. P84 (Evonik) polyimide was chosen as a membrane forming polymer and poly(ethylene imine) (PEI), dissolved in the bore liquid, as a crosslinking agent. In order to achieve the best balance between membrane stability and separation characteristics, the composition of the bore liquid was systematically varied, including solvent / non-solvent ratio and PEI concentration.

The crosslinked membranes have MWCO in the range of 2500 – 3500 g mol^{-1} and toluene permeance in the range of 0.2 - 1.1 l m^{-2} h^{-1} bar^{-1}. The most stable crosslinked membrane maintains 80% of its mass after 11 days immersion in N-methyl-2-pyrrolidinone. Due to crosslinking, the HFs become more hydrophilic and therefore attractive for separations in alcohol systems. Preliminary results are in fact presented here using an ethanol / polyethylene glycol model system.

1. Introduction

Organic solvent filtration (OSF) is a simple yet effective, separation technique with high potential in many branches of industry. The already reported successful applications are ranging from petrochemistry [1] through pharmaceutical manufacturing [2-6], to catalytic processes [7-9]. The polymeric membranes described in the literature are generally either asymmetric integrally skinned made of polyimides (PI) [10] or thin film composites comprising a poly(dimethylsiloxane) (PDMS) separating layer on a polyacrylonitrile (PAN) [11-18] or PI porous support [19]. The asymmetric integrally skinned PI membranes are usually prepared by phase inversion from solutions in polar aprotic solvents [6]. Consequently this type of membranes cannot be used directly for separations in such solvents (e.g. N-methyl pyrrolidone (NMP), di-methyl sulfoxide (DMSO), di-methyl formamide (DMF) or di-methyl acetamide (DMAc)). This limitation can be surmounted by a diamine crosslinking step involving an imide-ring opening reaction [20]. The crosslinking can be accomplished either in post casting process [21] or during phase separation [22].

It is generally accepted that a hollow fiber (HF) membrane has several advantages over a flat sheet membrane. A higher surface to volume ratio of HF membrane enables building of more compact modules. The module design there is simpler since there is no spacer. Besides, scaling up of HF membrane module is easier comparing to the flat membrane configuration. Despite all these advantages there are no such membranes commercially available in the OSF field. The literature is also very scarce on this topic. Only recently X. Loh et al. developed polyaniline (PANI) hollow fibers with good stability in dimethyl formamide and acetone [23]. Recently, we reported [24] a new HF fabrication method, called “chemistry in a spinneret”, in which membrane formation and crosslinking are integrated into a single step process. By careful control of the interplay between the phase inversion and the chemical crosslinking one can influence the final morphology and chemistry of the HF making “chemistry in a spinneret” a very attractive method for preparation of membranes for OSF. To this end, in this work we explore its application for fabrication of OSF using P84 polyimide (Evonik

Industries) as a membrane forming polymer and poly(ethylene imine) (PEI) as crosslinking agent. The composition of the bore liquid was systematically varied, including solvent / non-solvent ratio and PEI concentration, in order to achieve the best balance between membrane stability and separation characteristics. All HF membranes were methodically studied including morphology using SEM imaging and permeation properties (permeance / MWCO) using a high pressure cross flow set-up.

2. Experimental

2.1. Materials

Evonik Industries P84 polyimide (325 mesh, STD) was purchased from HP Polymer GmbH, Austria. N-methyl-2-pyrrolidinone (NMP, 99% extra pure) was supplied by Acros Organics (Belgium). Poly(ethylene imine) (PEI, M_w ~ 25000 g mol^{-1}; M_n ~ 10000 g mol^{-1}; containing 34% primary amines, 40% secondary amines and 26% tertiary amines; water-free) were supplied by Sigma-Aldrich (The Netherlands). Broad molecular weight polystyrene (PS) was synthesized according to procedure described in [25] and poly(ethylene glycol)'s (PEG) of molecular weights 200, 600, 1500 and 3000 g mol^{-1} were supplied by Sigma-Aldrich, The Netherlands. Toluene, ethanol and glycerol all of analytical grade, were purchased from Merck, Germany. Technical ethanol and n-hexane, used for hollow fibers fabrication, were purchased from Assink Chemie, The Netherlands. Two component epoxy resin Araldite® 2014-1 (Viba, The Netherlands) was used as membrane potting material for membrane module fabrication. All chemicals were used as received without further purification.

2.2. Fabrication of hollow fiber membranes

Nine batches of the hollow fibers named B1-B9 were produced by wet immersion precipitation spinning using a triple orifice spinneret. P84 polyimide was

dried overnight at 150°C. The polymer dope solution was prepared by mixing NMP (66% w/w) with glycerol (10% w/w) in a glass flask followed by addition of P84 powder (24% w/w). The solution was stirred for 48 h at 55°C, next it was filtered through a 15 μm mesh Bekipor ST 15 AL 3 metal filter (Bekaert) at 60°C and kept in the spinning tank at 55°C for 48 h for degassing. Before spinning the polymer solution was cooled down to 22°C. Both bore and shell liquids were stirred continuously at room temperature for 24 h and left for degassing for 12 h. Coagulation bath (external coagulant) was filled up with tap water at room temperature. The dope and shell liquids compositions and spinning process parameters were kept constant and only the bore liquid composition was varied (for details see Table 1). The dope solution, the bore and shell liquids were simultaneously extruded through a triple spinneret. The extruded fiber, after a brief residence in the air gap, was immersed in a coagulation bath. The take-up velocity was regulated by a pulling wheel, rotating at an adjustable speed. The collected fiber was cut into approximately one meter long pieces and immersed in a flowing water bath for 72 hours to remove residual solvents and excess of crosslinking agent. In order to prevent pore collapse upon drying the fibers were first immersed in ethanol for 24 h, next in n-hexane for 24 h and finally dried in the air at ambient conditions.

Table 1 Membrane preparation parameters

Polymer dope: 24 % (w/w) P84, 10 % (w/w) glycerol, 66 % (w/w) NMP Shell liquid: 75 % (w/w) NMP, 25 % (w/w) distilled water External coagulant: tap water				
Fibers	Bore liquid, % (w/w)			Bore liquid NMP/water
	PEI	NMP	water	
B1	20	68.5	11.5	6/1
B2	20	66.7	13.3	5/1
B3	20	64	16	4/1
B4	20	60	20	3/1
B5	20	57.1	22.9	2.5/1
B6	20	53.3	26.7	2/1
B7	20	40	40	1/1
B8	23	51.3	25.8	2/1
B9	15	63.8	21.3	3/1
Spinning parameters	Dope solution speed,		ml/min	3.0
	Bore liquid speed,		ml/min	1.4
	Shell liquid speed,		ml/min	0.8
	Air gap length,		cm	2.5
	Take-up speed,		m/min	2.2
	Temperature,		°C	22
	Humidity,		%	40

2.3. Scanning electron microscopy

The HF were fractured in liquid nitrogen and mounted onto holders. After drying in a vacuum oven at 30°C for 12 hours, the samples were sputtered with gold (4 minutes, 13 mA) using a Blazers Union SCD 040 sputtering device. SEM images of the spun HF membranes were made using Jeol JSM5600LV scanning electron microscope (SEM) at a 5 kV accelerating voltage and working distance of 24 mm.

2.4. Module preparation and filtration experiments

Each module contained two randomly selected fibers (33 cm each) potted with Araldite epoxy resin. The resin was allowed to set for at least 24 hours before the module was used for filtration. The permeation experiments were performed in a custom made cross-flow set-up in a total recycle mode. The detailed description of the filtration set up can be found elsewhere [25]. In order to ensure fully turbulent flow (Re ≈ 11700) and consequently minimize effects of concentration polarization, all measurements were performed at high cross-flow velocity of about 10 m s^{-1}. Before the first permeation measurement, each new membrane was pre-compacted for 4 hours at 20 bar without permeate being collected. Prior to the first measurement, the system was stabilized at a desired pressure for two hours. The toluene permeation was performed in the order 5, 10, 20, 15 and then 7.5 bar in case of ethanol the order was 20, 15, 10 and 5 bar. The permeance of membranes (P, l m^{-2} h^{-1} bar^{-1}) was calculated from the slope of the flux versus trans membrane pressure (TMP) plot.

2.5. Molecular weight cut-off (MWCO) measurements

The MWCO reported in this work was obtained from filtration experiments at 7.5 bar using PS in toluene (0.3 % w/w, MW 300-15000 g mol^{-1}) and PEG in ethanol solutions (0.3 % w/w, MW 100-4000 g mol^{-1}) (Fig.1).

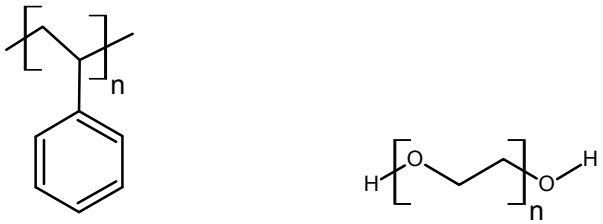

(a) (b)

Figure 1 Chemical structures of (a) PS and (b) PEG.

For all collected PEG/ethanol samples a solvent swap was performed; ethanol was evaporated and exchanged for a mobile aqueous phase (aq. 0.05 M $NaNO_3$ and 0.05 g l^{-1} NaN_3). All samples of oligomers were analyzed using an Agilent Technologies 1200 Series GPC system with a Shodex RI-71 refractive index detector. For PS separation a PSS SDV 1000 Å column and toluene as a mobile phase were used. For the PEG analysis two, PSS Suprema 100 Å columns were used. The mobile phase was aqueous solution of $NaNO_3$ (0.05 M) and NaN_3 (0.05 g l^{-1}). The detailed analysis of PEG oligomers was done following the procedure described by Dalwani et al. [26].

2.6. Mass loss experiments

The stability of the crosslinked fibers in NMP was evaluated by quantitative mass loss analysis. Six fibers were selected from each batch. Pieces of 5 cm pieces were cut from the middle of each fiber and dried in a vacuum oven at 150°C for 24 hours to remove water. Then, the samples were left in a desiccator to cool down and the weight of each fiber was obtained using analytical balance (Mettler Toledo AE240). After that, the samples were separately immersed in NMP for eleven days. The residual samples were rinsed first in water for 24 hours and afterwards in ethanol for 5 days. After drying in a vacuum oven at 150°C for 3 days, the samples were weighed again and the mass loss was calculated.

2.7. Attenuated Total Reflectance Fourier Transform Infrared Spectroscopy (ATR-FTIR)

Changes between the crosslinked and non-crosslinked P84 membranes were analyzed using a Perkin Elmer Spectrum 100 FTIR spectrometer equipped with universal ATR polarization accessory. The samples of crosslinked P84, were prepared by removing non-crosslinked part of a membrane in NMP followed by rinsing in water and ethanol. A P84 powder was used as the non-crosslinked samples. All samples before measurements were dried in a vacuum oven at 30°C for 12 h. The FT-IR spectra were recorded over a scanning range of 650-4000 cm^{-1}

with a resolution of 1.0 cm^{-1} at room temperature. The changes of typical imide and amide bands were used to identify the changes in polymer structure [22].

2.8. Contact angle measurements

In order to investigate influence of PEI crosslinking on the membrane hydrophilicity, water contact angles were measured. For this, flat membranes of non-crosslinked P84 membranes were prepared by casting the dope solution (24% w/w P84, 10% w/w glycerol, 66% w/w NMP) onto a silicon wafer followed by immediate immersion into a water bath at room temperature. The flat crosslinked P84 membranes were obtained by immersion of the cast polymer in a bath containing the bore liquid for preparation of B4 fiber (20% PEI, NMP/water = 3/1) for 30 seconds, followed by immersion in a water bath. After precipitation, the 200 μm-thick membranes were kept in running water bath for 72 hours to remove any residual solvents and excess of PEI. The membranes were then rinsed with Millipore water and air-dried. Prior to contact angle measurements, the membranes were kept in a vacuum oven at 30°C for 2 hours. The static contact angle measurements were performed on a Dataphysics contact angle system OCA 20 at room temperature. For this, 10 μl of deionized water droplets were placed onto the membrane surface by a computer controlled syringe. After 5 seconds, contact angle of the water drop was recorded and analyzed using SCA20 software. Measurements were repeated eight to ten times for every membrane.

3. Results and discussion

3.1. The formation of crosslinked P84

Figure 2 shows the normalized, to the highest peak, FTIR spectra for the crosslinked and non-crosslinked P84.

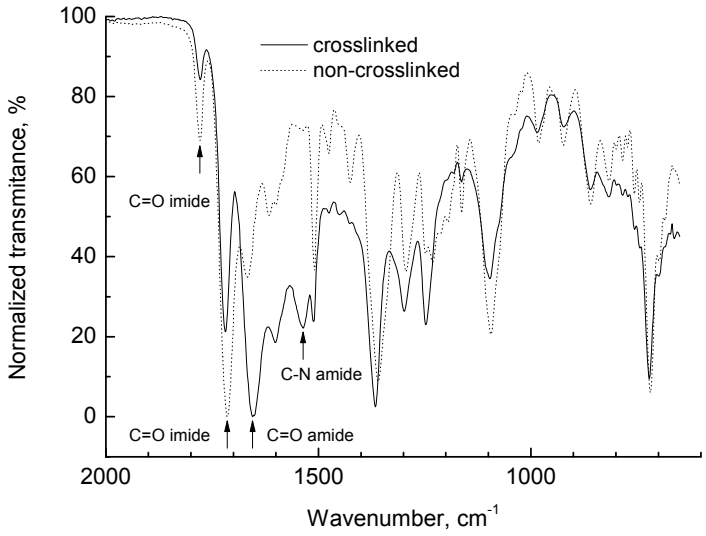

Figure 2 FTIR spectra of P84 hollow fiber membranes (non- crosslinked and crosslinked).

FTIR spectrum was recorded for each batch of HF. Since no significant difference in spectra among the crosslinked HF samples was observed, Figure 2 presents spectrum of B6 as an example. For crosslinked P84 membrane, the typical imide peaks at 1778 cm^{-1} (symmetric C=O stretching) and 1714 cm^{-1} (asymmetric C=O stretching) decrease in comparison to non-crosslinked P84. Besides, the typical amide peaks, a result of crosslinking reaction between P84 and PEI, increase at 1655 cm^{-1} (C=O stretching) and 1536 cm^{-1} (C-N stretching). These results indicate that crosslinking reaction between imide groups of P84 and amine groups of PEI occurs, resulting in amide bonds formation (see Fig.3).

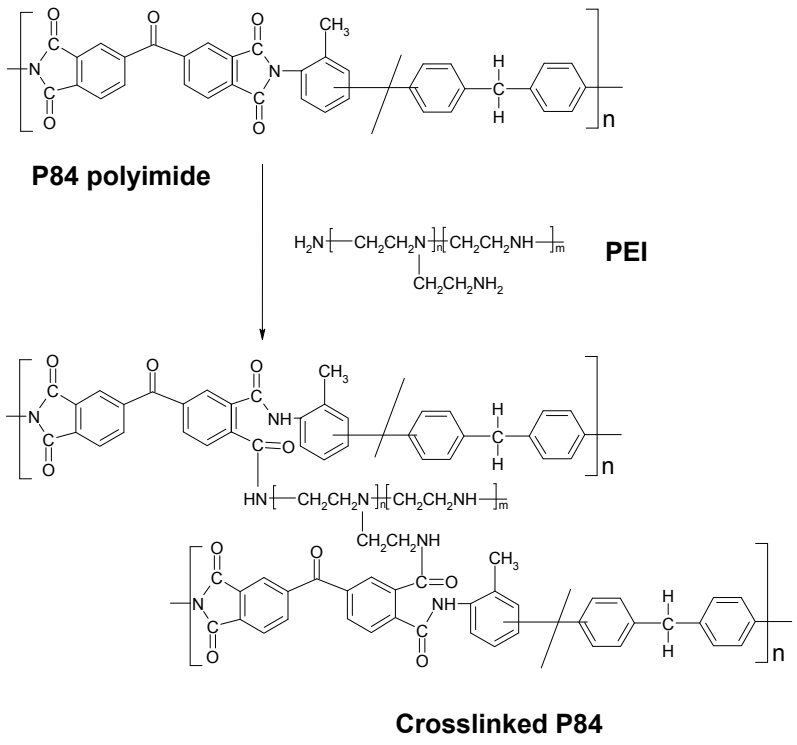

Figure 3 Crosslinking reaction between the carbonyl groups of P84 and the amine groups of PEI [24].

3.2. Water contact angle measurement

The water contact angle of non-crosslinked and crosslinked P84 membranes are 75 ± 1° and 61 ± 2°, respectively, showing that crosslinking results in more hydrophilic membrane. This is probably due to the free amine groups (secondary and tertiary) of PEI introduced during crosslinking (see Fig.3). As shown in Figure 3, crosslinking reaction occurs between carbonyl groups of P84 imide ring and primary (-NH_2) or secondary (=NH) amine groups of PEI, resulting in the formation of amide bonds (NH-C=O). It seems that due to less steric hindrance, reaction of primary amine groups with an imide ring is preferable. These free amine

groups besides increasing hydrophilicity of the membrane, also introduce positive charge at the membrane surface [24].

3.3. Organic solvent filtration hollow fibers fabrication and optimization

Figure 4 shows the morphology of the produced HF and Table 2 presents the results of their characterization. All fibers have rather spongy, macrovoid free structure (Fig.4a, b) with a well centered bore. The surface of the selective layer in case of fibers with high NMP / water ratio (B1-B2) is smoother than that with low NMP concentration (B6-B7). The fibers where high NMP concentration in bore liquid was used (B1-B3), have two distinct layers: a dense inner layer and a porous sponge substructure. With decrease of NMP concentration, the thickness of the inner dense layer reduces and already at the NMP / water ratio 3:1 it seems that the fiber is completely porous (Fig.4, B4). The fibers B1, B2 and B3 dissolve almost completely in NMP (see mass loss, Table 2), leaving only a thin gel-like green inner layer, suggesting that only a thin inner layer of these fibers is crosslinked. Similar observations on the influence of NMP /water ratio in the bore liquid on the morphology of P84 - PEI crosslinked HF was recently demonstrated by Kopeć et al. [24]. They report that, the membrane formation on the bore side is controlled by the interplay of crosslinking and the phase separation. If the phase separation occurs faster than crosslinking, a porous structure is formed. If crosslinking is faster than phase separation, a dense inner layer is formed. On the shell side, the structure formation is a result of only phase inversion. The thickness of the inner dense layer is determined by the diffusion rate of these two fronts, coagulation from the outside and crosslinking from the inside of the fiber. The formation and the growth of the dense inner layer, stop at the point where these two fronts meet. In fact, a high NMP / water ratio in bore liquid generally results in a membrane structure with thin, crosslinked, dense inner layer, whereas a low NMP / water ratio results in a porous more crosslinked fiber. As the NMP / water ratio in the bore liquid decreases, phase inversion occurs faster. Consequently, the dense layer is not

B1 (a) B1 (b) B1 (c)

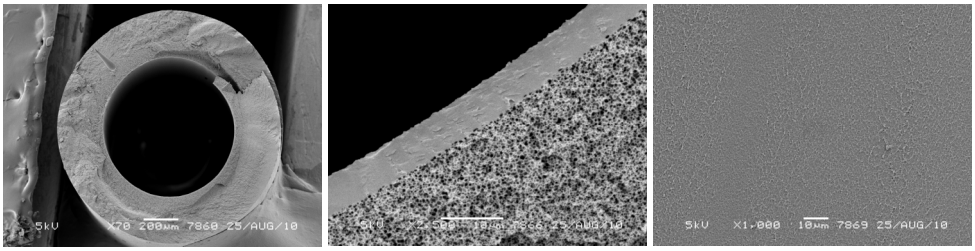

B2 (a) B2 (b) B2 (c)

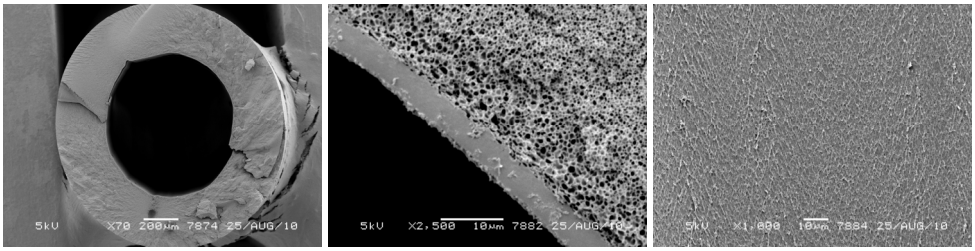

B3 (a) B3 (b) B3 (c)

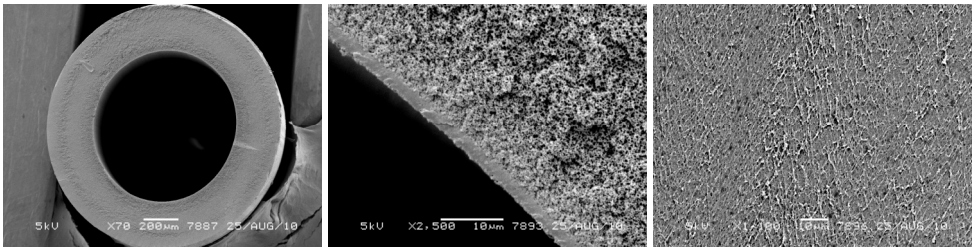

B4 (a) B4 (b) B4 (c)

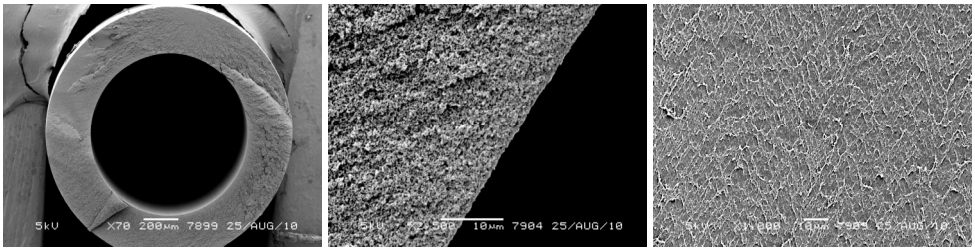

B5 (a) B5 (b) B5 (c)

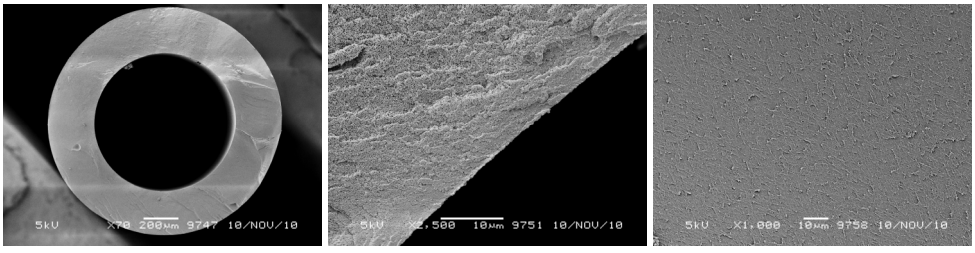

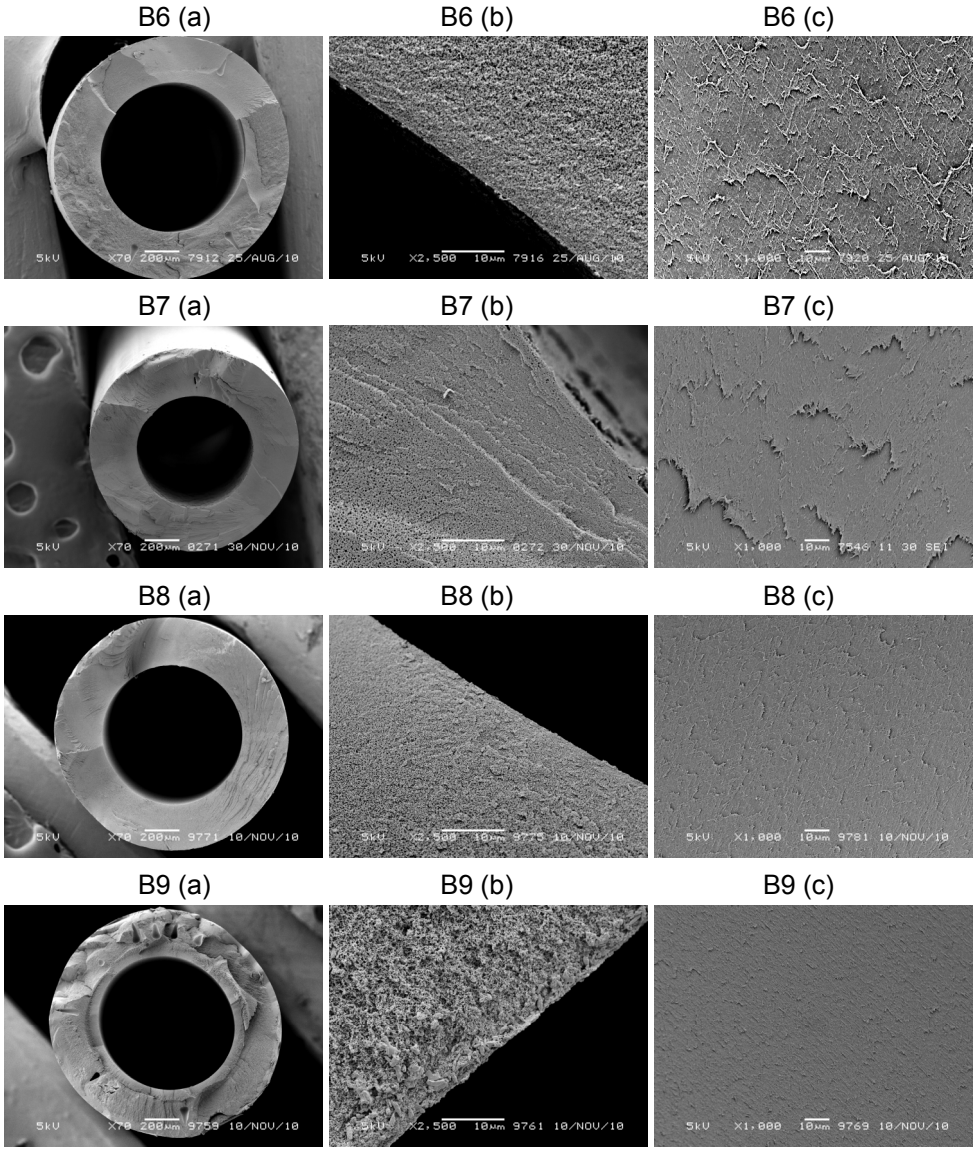

Figure 4 SEM images of all spun hollow fibers: (a) cross section, (b) cross section of the inner selective layer, (c) surface of inner selective layer.

formed because the crosslinking reaction between PEI and unsolidified P84 becomes slow compared to coagulation. The porous inner layer does not hinder further PEI diffusion into already solidified porous polymer matrix and crosslinking reaction can still proceed. This secondary crosslinking is much slower, as reported by Vanherck et al. [22] and seems to have no impact on membrane morphology.

Table 2 Characterization of hollow fibers

HF code	NMP:H_2O in bore liquid	PEI in bore liquid, % (w/w)	Layer(s) (SEM)	Mass loss, %	Permeance of toluene, l m^{-2} h^{-1} bar^{-1}	Toluene / PS	
						Permeance l m^{-2} h^{-1} bar^{-1}	MWCO g mol^{-1}
B1	6:1	20	2	99±0	0*	n.m	n.m
B2	5:1	20	2	98 ± 2	0*	n.m	n.m
B3	4:1	20	2	98 ± 1	0*	n.m	n.m
B4	3:1	20	1	83 ± 1	0*	n.m	n.m
B5	2.5:1	20	1	74±3	n.m	0.5±0.3	3300
B6	2:1	20	1	20 ± 3	1.5 ± 0.1	0.9±0.2	3300
B7	1:1	20	1	64 ± 8	24.5 ± 1	n.m	n.m
B8	2:1	23	1	43±6	n.m	0.2±0.1	2500
B9	3:1	15	1	61±4	n.m	1.1±0.3	3300

**No toluene permeation observed at 30 bar over 8 hours.*
n.m.- not measured

Table 2 shows that, as NMP / water ratio decreases, generally the fibers become more porous (B6 and B7 are permeable for toluene) and better crosslinked (lower mass loss in NMP). It seems that the more porous the inner layer is the higher diffusion rate of PEI through the fiber wall and thus better crosslinking. After phase inversion and until the bore liquid is fully washed away from the fiber, diffusion of PEI through the crosslinked layer and hence secondary crosslinking may be possible. This might explain very good crosslinking of B6 (longer contact time with PEI in the washing bath). The clean toluene permeance of this fiber was 1.5 ± 0.1 l m^{-2} h^{-1} bar^{-1}, in the order expected for nanofiltration membranes. However,

measurement using PS / toluene solution show that its MWCO is around 3300 g mol^{-1} (see Figure 5).

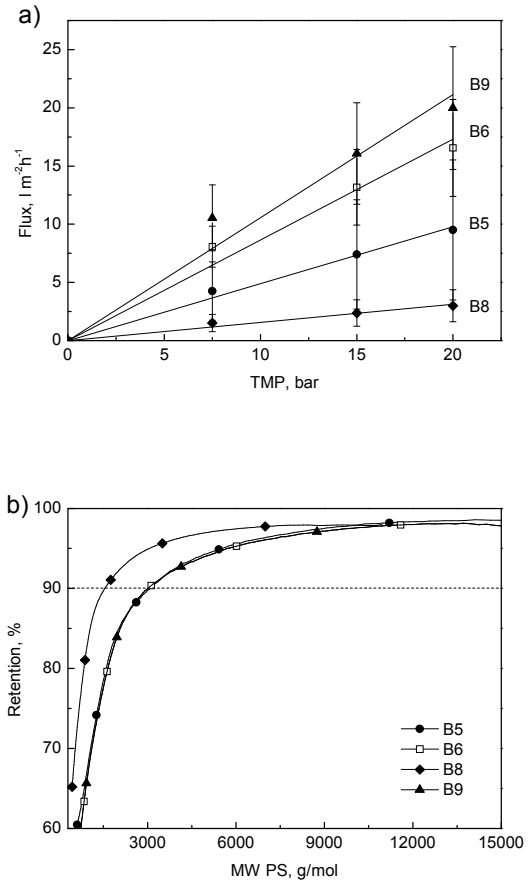

Figure 5 HF membranes B6, B5, B9 and B8: (a) flux of PS / toluene as a function of TMP, (b) PS retention at 7.5 bar.

Interestingly, when the NMP / water ratio was raised to 2.5:1 the membrane becomes denser concerning permeance (0.5 ± 0.3 l m^{-2} h^{-1} bar^{-1}) but its MWCO stays around 3300 g mol^{-1} (see Fig.5 and Table 3). It seems that in this case, the increase of NMP content in the bore liquid does not influence significantly the pore size distribution but results in decrease of the separation layer porosity. The MWCO of the crosslinked membrane decreases to 2500 g mol^{-1} and its permeance

to 0.2 ± 0.1 l m^{-2} h^{-1} bar^{-1} when 23% w/w PEI in the bore liquid is applied (fiber B8 in Fig.5 and Table 3). In this case, it seems that both porosity and the average pore size of the membranes decrease and as a result lower crosslinking occurs. (fiber B8 has higher mass loss (43 ± 6% w/w) compared to B6 (20 ± 3% w/w)). Finally, using lower PEI concentration in bore liquid slows down crosslinking leading to a more open membrane structure. In fact, the B9 membrane with NMP / water ratio 3:1 and 15% w/w of PEI has relatively high toluene / PS permeance of 1.1 l m^{-2} h^{-1} bar^{-1} (Fig.5a), however its MWCO remains around 3300 g mol^{-1} (Fig.5b). There, PEI diffusion into polymer matrix is rapid and somewhat better crosslinking is achieved (mass loss of B9 fiber is around 61% and lower than that of B4 (83%, see Table 2).

3.4. Membrane performance in ethanol

Due to increased hydrophilicity of the membranes, performance of two selected HF (B5 and B8) in a polar system was evaluated. As a model solvent ethanol waschosen because of its wide use in purification processes such as in food industry for extraction of oils and valuable bio-active compounds from raw plant materials, xanthophylls from corn and polyphenols from green tea [6] and as a substitute extractant for other organic solvents, e.g. hexane [27]. Poly(ethyleneglycol) (PEG) was selected as a model solute, since it is polar and hydrophilic. The MW range of PEG was restricted up to 4000 g mol^{-1} due to limitation in solubility of higher fractions in pure ethanol [28].

Figure 6a presents transport of ethanol and PEG / ethanol mixtures for those HF. The linear relation between the fluxes and trans membrane pressure shows that there is no membranes compaction within this pressure range. For both membranes, the permeance of pure ethanol and PEG / ethanol are very similar, indicating that there is no significant effect of concentration polarization.

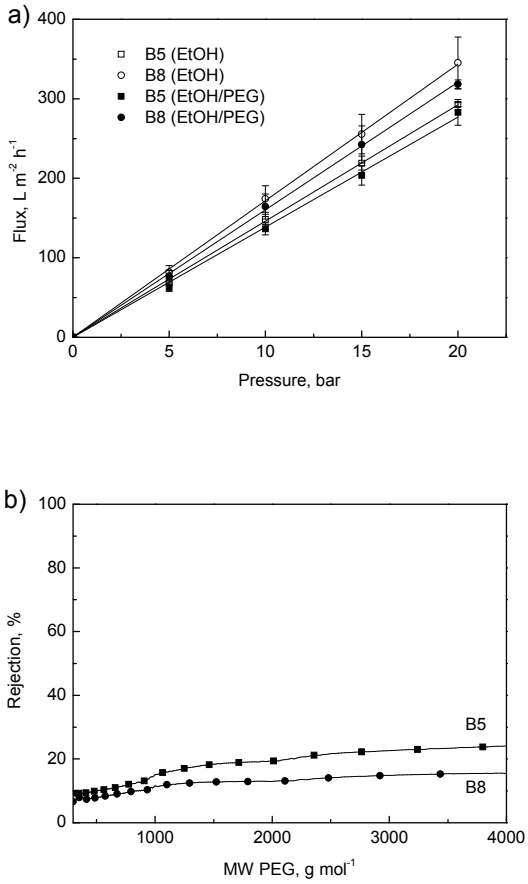

Figure 6 (a) Clean etOH and etOH/PEG permeance and (b) PEG rejection of B5 and B8 fibers.

For both membranes the permeance of PEG / ethanol are very high in comparison to toluene / PS mixture, probably due to membrane hydrophilicity (see Table 3). The PEG retention however for both membranes is low, 14-23% over the whole studied MW range (300-4000 g mol^{-1}) (Fig.6b). This may be due to higher interaction of the hydrophilic crosslinked membrane with ethanol and causing membrane swelling and / or due to the shape of the

Table 3 Comparison of the performances B5 and B8 fibers in EtOH / PEG and toluene / PS systems

HF membrane	B5		B8	
System	Permeance, l m^{-2} h^{-1} bar^{-1}	Retention at 3300 g mol^{-1}, %	Permeance, l m^{-2} h^{-1} bar^{-1}	Retention at 2500 g mol^{-1}, %
Toluene/PS	0.5 ± 0.3	90** (PS)	0.2 ± 0.1	90** (PS)
Ethanol/PEG	13.9 ± 0.8	23* (PEG)	16.0 ± 0.9	14* (PEG)
Ethanol	14.6 ± 0.2	-	17.2 ± 1.6	-

** Obtained at 5 bar; no rejection at higher pressures*

*** Obtained as the average of permeation at 7.5 and 15 bar*

PEG molecule itself. PEG has a linear structure and small chain diameter (see Fig.1). This makes PEG flexible, easy to deform and to fit into smaller pores whereas the more rigid and bulky polystyrene due to the presence of benzene rings in its chain [29] has higher retention.

4. Conclusions

In this study the concept of “chemistry in a spinneret” was explored towards fabrication of HF membranes for OSF. The HF were prepared using P84 polyimide as a base polymer and poly(ethylene imine) (PEI) as crosslinking agent. The interplay between crosslinking and the phase inversion during spinning process was studied by varying systematically the composition of bore liquid, i.e. (PEI), NMP and water concentrations. In general, the prepared HF membranes have MWCO (measured in the polystyrene/toluene system) in the range 2500-3500 g mol^{-1} whereas toluene permeances are relatively low; ranging from 0.2 - 1.1 l m^{-2} h^{-1} bar^{-1}. The membranes are partially stable in N-methyl-2-pyrrolidinone (NMP), the most stable one maintains 80% of its mass after 11 days immersion in NMP. Due to crosslinking, the HFs become more hydrophilic and therefore have high ethanol / PEG permeance and low PEG retention. Future research in this field should focus on the development and characterization of P84 / PEI membranes for polar organic solvents.

5. Acknowledgments

Dutch Technology Foundation (STW) (project no 07349) is gratefully acknowledged for the financial support.

References

[1] L.S. White, C.R. Wildemuth, Aromatics enrichment in refinery streams using hyperfiltration, Ind. Eng. Chem. Res., 45 (2006) 9136-9143.

[2] X. Cao, X.Y. Wu, T. Wu, K. Jin, B.K. Hur, Concentration of 6-aminopenicillanic acid from penicillin bioconversion solution and its mother liquor by nanofiltration membrane, Biotechnology and Bioprocess Engineering, 6 (2001) 200-204.

[3] J.P. Sheth, Y. Qin, K.K. Sirkar, B.C. Baltzis, Nanofiltration-based diafiltration process for solvent exchange in pharmaceutical manufacturing, J. Membr. Sci., 211 (2003) 251-261.

[4] J.C.T. Lin, A.G. Livingston, Nanofiltration membrane cascade for continuous solvent exchange, Chem. Eng. Sci., 62 (2007) 2728-2736.

[5] D. Shi, Y. Kong, J. Yu, Y. Wang, J. Yang, Separation performance of polyimide nanofiltration membranes for concentrating spiramycin extract, Desalination, 191 (2006) 309-317.

[6] P. Vandezande, L.E.M. Gevers, I.F.J. Vankelecom, Solvent resistant nanofiltration: Separating on a molecular level, Chem. Soc. Rev., 37 (2008) 365-405.

[7] J.T. Scarpello, D. Nair, L.M. Freitas dos Santos, L.S. White, A.G. Livingston, The separation of homogeneous organometallic catalysts using solvent resistant nanofiltration, J. Membr. Sci., 203 (2002) 71-85.

[8] A. Livingston, L. Peeva, S. Han, D. Nair, S.S. Luthra, L.S. White, L.M.F.D. Santos, Membrane Separation in Green Chemical Processing: Solvent Nanofiltration in Liquid Phase Organic Synthesis Reactions, Ann. Ny. Acad. Sci., 984 (2003) 123–141.

[9] S.S. Luthra, X. Yang, L.M. Freitas dos Santos, L.S. White, A.G. Livingston, Homogeneous phase transfer catalyst recovery and re-use using solvent resistant membranes, J. Membr. Sci., 201 (2002) 65-75.

[10] Y.H. See-Toh, F.C. Ferreira, A.G. Livingston, The influence of membrane formation parameters on the functional performance of organic solvent nanofiltration membranes, J. Membr. Sci., 299 (2007) 236-250.

[11] S. Aerts, A. Vanhulsel, A. Buekenhoudt, H. Weyten, S. Kuypers, H. Chen, M. Bryjak, L.E.M. Gevers, I.F.J. Vankelecom, P.A. Jacobs, Plasma-treated PDMS-membranes in solvent resistant nanofiltration: Characterization and study of transport mechanism, J. Membr. Sci., 275 (2006) 212.

[12] K. Ebert, J. Koll, M.F.J. Dijkstra, M. Eggers, Fundamental studies on the performance of a hydrophobic solvent stable membrane in non-aqueous solutions, J. Membr. Sci., 285 (2006) 75-80.

[13] N. Stafie, Poly(dimethyl siloxane) – based composite nanofiltration membranes for non-aqueous applications, Ph.D. thesis, University of Twente, Enschede, The Netherlands, (2004).

[14] N. Stafie, D.F. Stamatialis, M. Wessling, Insight into the transport of hexane-solute systems through tailor-made composite membranes, J. Membr. Sci., 228 (2004) 103-116.

[15] N. Stafie, D.F. Stamatialis, M. Wessling, Effect of PDMS cross-linking degree on the permeation performance of PAN/PDMS composite nanofiltration membranes, Sep. Purif. Technol., 45 (2005) 220-231.

[16] D.F. Stamatialis, N. Stafie, K. Buadu, M. Hempenius, M. Wessling, Observations on the permeation performance of solvent resistant nanofiltration membranes, J. Membr. Sci., 279 (2006) 424-433.

[17] E.S. Tarleton, J.P. Robinson, C.R. Millington, A. Nijmeijer, M.L. Taylor, The influence of polarity on flux and rejection behaviour in solvent resistant

nanofiltration--Experimental observations, J. Membr. Sci., 278 (2006) 318-327.

[18] E.S. Tarleton, J.P. Robinson, M. Salman, Solvent-induced swelling of membranes - Measurements and influence in nanofiltration, J. Membr. Sci., 280 (2006) 442-451.

[19] L.E.M. Gevers, S. Aldea, I.F.J. Vankelecom, P.A. Jacobs, Optimisation of a lab-scale method for preparation of composite membranes with a filled dense top-layer, J. Membr. Sci., 281 (2006) 741-746.

[20] Y. Liu, R. Wang, T.-S. Chung, Chemical cross-linking modification of polyimide membranes for gas separation, J. Membr. Sci., 189 (2001) 231-239.

[21] Y.H. See Toh, F.W. Lim, A.G. Livingston, Polymeric membranes for nanofiltration in polar aprotic solvents, J. Membr. Sci., 301 (2007) 3-10.

[22] K. Vanherck, A. Cano-Odena, G. Koeckelberghs, T. Dedroog, I. Vankelecom, A simplified diamine crosslinking method for PI nanofiltration membranes, J. Membr. Sci., 353 (2010) 135–143.

[23] X.X. Loh, M. Sairam, J.H.G. Steinke, A.G. Livingston, A. Bismarck, K. Li, Polyaniline hollow fibers for organic solvent nanofiltration, Chem. Commun., (2008) 6324-6326.

[24] K.K. Kopec, S.M. Dutczak, M. Wessling, D.F. Stamatialis, Chemistry in a spinneret - On the interplay of crosslinking and phase inversion during spinning of novel hollow fiber membranes, J. Membr. Sci., (2011).

[25] S.M. Dutczak, M.W.J. Luiten-Olieman, H.J. Zwijnenberg, L.A.M. Bolhuis-Versteeg, L. Winnubst, M.A. Hempenius, N.E. Benes, M. Wessling, D. Stamatialis, Composite capillary membrane for solvent resistant nanofiltration, J. Membr. Sci., 372 (2011) 182-190.

[26] M. Dalwani, N.E. Benes, G. Bargeman, D. Stamatialis, M. Wessling, A method for characterizing membranes during nanofiltration at extreme pH, J. Membr. Sci., 363 (2010) 188-194.

[27] A.V. Volkov, G.A. Korneeva, G.F. Tereshchenko, Organic solvent nanofiltration: prospects and application, Russ. Chem. Rev., 77 (2008) 983-993.

[28] B.O. Haglund, R. Svensson, A thermoanalytic method for the study of the solubility of polyethylene glycols in ethanol and water, J. Therm. Anal., 35 (1989) 391-395.

[29] F.W. Billmeyer, Textbook of Polymer Science, John Wiley & Sons, Inc., Singapore, 1994.

Chapter VI

Conclusions and outlook

S.M. Dutczak, M. Wessling, D. Stamatialis

In this thesis we presented the development of novel membranes, with target molecular weight cut-off lower than 500 g mol^{-1}, for organic solvent filtration (OSF). New membranes were prepared by either coating a PDMS layer on a ceramic capillary or hollow fiber support (Chapter 2), or diisocyanate crosslinking of commercial polyamide-imide flat nanofiltration (NF) membranes (Chapter 4) or spinning of polyimide hollow fibers (HF) using chemistry in a spinneret concept (Chapter 5). In all chapters, the membranes were characterized by solvent permeation and molecular weight cut-off (MWCO) studies. In Chapter 3 we therefore highlighted the importance of the careful selection of the solute and process conditions for the MWCO determination of the newly developed membranes.

In **Chapter 2** composite membranes were prepared by coating a tailor made PDMS top layer on a commercial capillary Hyflux InoCep M20 α-alumina support. If PDMS is applied on α-alumina support of large pore size (800 nm), the coating solution intrudes significantly in the porous support blocking pores and decreases the toluene permeance significantly. A membrane with good flux of toluene (1.6 l $m^{-2}h^{-1}bar^{-1}$) and low MWCO (500 g mol^{-1}) was prepared on a support with relatively small pore size of about 20 nm.

In this respect, further development of the composite membrane should focus on preparation of thinner coatings by using either lower polymer concentrations or lower solution viscosities. Besides, to improve productivity, a ceramic support of smaller diameter or even a HF could be used. In fact, in Chapter 3 we presented some preliminary results of α-alumina/PDMS HF composites. HF supports there had relatively big pores (250 nm), therefore these composites had low toluene permeance (0.8 - 1.1, l $m^{-2}h^{-1}bar^{-1}$) due to intrusion of PDMS coating into the support. To broaden the application range, besides PDMS based hydrophobic coatings, one could prepare membranes using more hydrophilic polymers such as polyethylene oxide-poly(dimethyl siloxane) (PEO-PDMS) [1] or sulphonated poly(ether ether ketone) (S-PEEK) [2] for applications in polar solvents.

In **Chapter 3** main focus was on effects of process conditions and phenomena such as: concentration polarization; interactions between solvent, solute, and membrane; shape and flexibility of solute, on molecular weight cut off (MWCO) characterization of solvent resistant nanofiltration membranes. Our results demonstrate that for the α-alumina / PDMS composite membranes, there was very little effect of flux on retention and the membrane's MWCO was predominantly affected by solute-membrane and solvent-membrane interactions. In case of a rigid porous zirconia membrane, a significant effect of applied pressure was observed, in particular for the flexible solute - polyisobutylene (PIB). The variations in MWCO with pressure there indicated combined effects of concentration polarization and shear induced deformation of the flexible solute. Our results clearly showed that the selection of the proper solvent - solute system and the process conditions for the retention measurements as well as the interpretation of MWCO data in organic solvents require great caution.

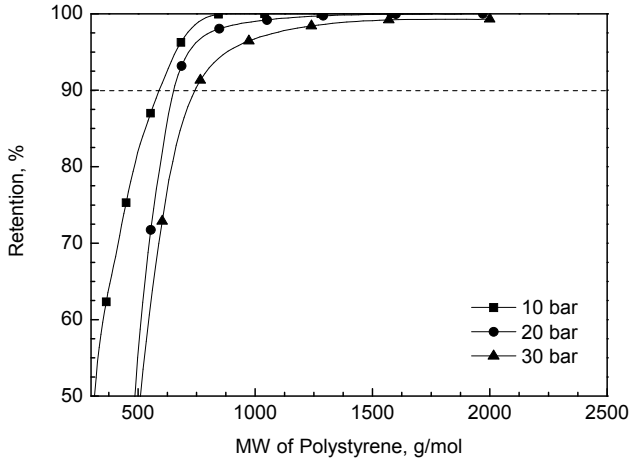

Figure 1 Composite α-alumina / PDMS HF (PDMS top layer thickness ~13 μm) PS retention in chloroform.

Besides, the MWCO characterization with polystyrene (PS) in toluene (Chapter 2-5) or polyisobutylene in toluene or n-hexane (Chapter 3) we also

investigated rejection of PS in chloroform using α-alumina / PDMS HF. The permeance of chloroform, its viscosity as well as PDMS swelling degree in this solvent ($SD_{chloroform}$ ≈ 130 % v/v, $\nu_{chloroform}$ = 0.57 mPa s and $P_{chloroform}$ = 0.8 ± 0.1, l m^{-2} h^{-1} bar^{-1}) matched almost exactly those in toluene ($SD_{toluene}$ ≈ 131 % v/v, $\nu_{toluene}$ = 0.59 mPa s and $P_{toluene}$ = 0.8 ± 0.1, l m^{-2} h^{-1} bar^{-1}). As a result, transport of PS in those two systems through PDMS membrane was similar and MWCO in chloroform (600 g mol^{-1}, see Fig.1a) did not differ significantly from MWCO in toluene (500 g mol^{-1}).

In **Chapter 4** we reported a new crosslinking method of polyamide-imide (Torlon®) membranes for applications in harsh polar aprotic solvents. A commercial NF polyamide-imide was crosslinked using 1,6-Hexamethylene Diisocyanate (HMDI). The resulting membranes were resistant to NMP and the created covalent bonds are expected to be thermally stable enabling separation at elevated temperature. Besides, it seems possible to tailor the MWCO of the membrane by varying the crosslinking time: longer crosslinking time corresponds to tighter (lower MWCO) membrane.

Further research should focus on crosslinking of Torlon® by different polyisocyanates in order to shorten the reaction time and tailor MWCO. It is also important to evaluate membrane thermal stability by conducting actual separations at elevated temperatures.

In **Chapter 5** we explored “chemistry in a spinneret” to develop crosslinked P84 fibres. This new spinning technique [3], combines the membrane formation and crosslinking reaction into a single step process. The interplay between crosslinking and phase inversion during membrane formation was studied by methodical change of bore liquid composition (solvent / nonsolvent ratio and crosslinker (PEI) concentration). The prepared membranes had MWCO in the range 2500-3500 g mol^{-1} and the toluene / PS permeance ranging from 0.2 - 1.1 l m^{-2} h^{-1} bar^{-1}. Due to crosslinking, the HFs became more hydrophilic and therefore had high ethanol / PEG permeance (14.6-17.2 l m^{-2} h^{-1} bar^{-1}) and low rejection of PEG (14- 23 % of 4000 g mol^{-1}). The most stable membrane lost 20% of its mass after 11 days immersion in NMP.

To improve crosslinking of this membrane, one could add PEI in the bore as well as shell liquid. In this way the crosslinking is expected to occur from both sides of the fiber wall. Table 1 presents some preliminary results on this.

Table 1 Crosslinking from bore and shell side; spinning parameters and membrane performance summary

Spinning parameters	
Air gap, cm	10
Bore liquid, % (w/w)	20 % PEI, NMP/H_2O = 2/1
Shell liquid, % (w/w)	25 % PEI, NMP/H_2O = 1/1
Polymer dope, % (w/w)	24 % P84, 10 % glycerol, 66 % NMP
Performance	
Toluene / PS permeance, l m^{-2} h^{-1} bar^{-1}	1.5 ± 0.2
PS MWCO, g mol^{-1}	4200
Mass loss, %	19 ± 8 %

Unfortunately, addition of PEI in the shell liquid did not result in a more crosslinked membrane. Besides, despite increasing the air gap to prolong the contact of PEI with the forming fibre, there was no improvement in fiber stability (no difference in mass loss). PEI may not be reactive enough and / or does not diffuse quickly enough into the polymer matrix to crosslink the fiber.

Table 2 EDA crosslinking op P84 – spinning compositions and membrane performance

Code	Bore liquid, % (w/w)		Performance	
	EDA	PEG-400	Toluene permeance l $m^{-2}h^{-1}bar^{-1}$	Comments
E1	0	100	26	10% Retention of 10.000 g mol^{-1} PS
E2	2	98	0.6	20% Retention of 10.000 g mol^{-1} PS
E3	5	95	No	no flux up to 30bar
E4	20	80	n.m.	delaminating, brittle, difficult to handle

Polymer dope: 22 % (w/w) P84, 12 % (w/w) glycerol, 66 % (w/w) NMP
Shell liquid: 75 % (w/w) NMP, 25 % (w/w) water

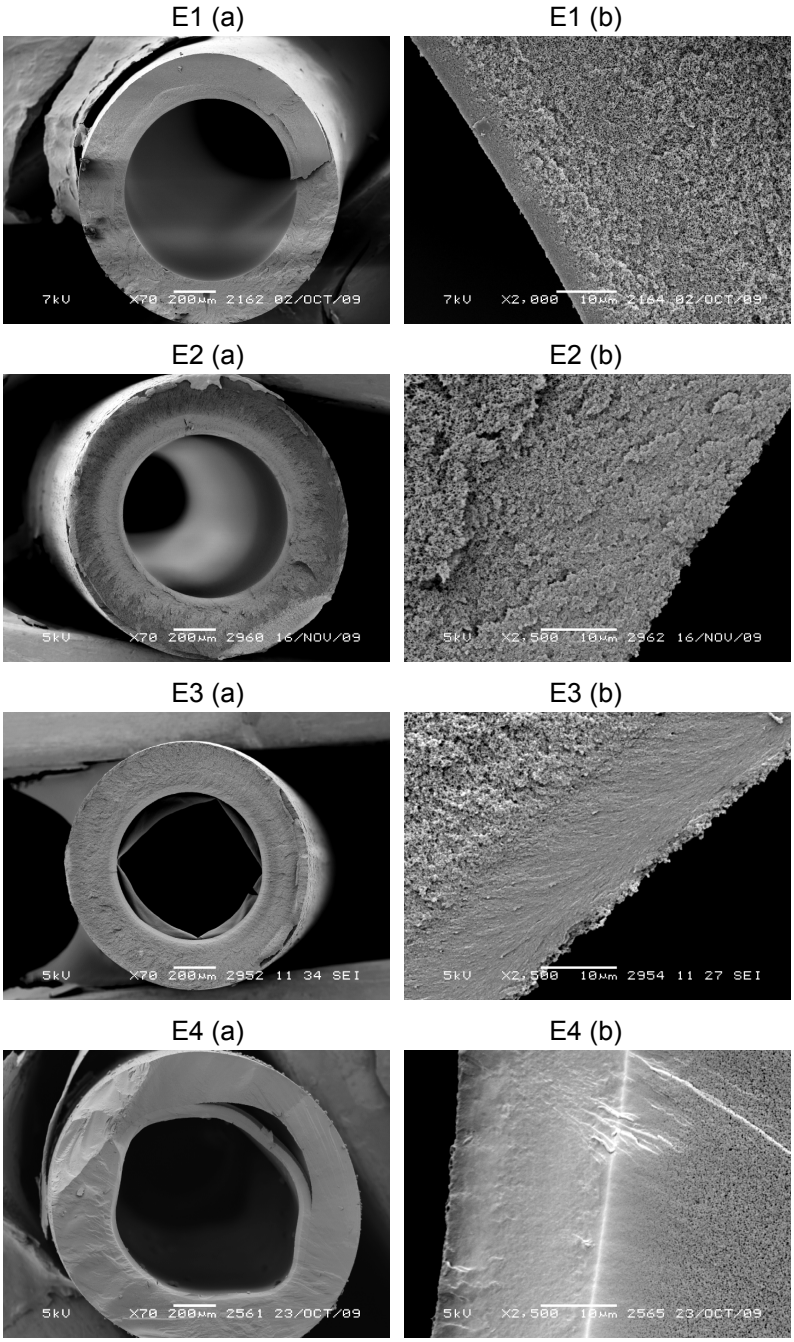

Figure 2 EDA-crosslinking: (a) cross section, (b) cross section of the inner selective layer (Bore liquids % w/w: E1: 100% PEG, E2: 98% PEG, 2% EDA, E3: 95% PEG + 5% EDA, E4: 80% PEG + 20% EDA).

To successfully crosslink the fiber from the outside one could use more reactive polyamine of lower MW. Preliminary experiments with ethylene diamine (EDA, MW = 61.1 g mol^{-1}, see Table 2) showed that EDA is very reactive and even at its low concentrations in bore liquid dramatically densifies the separation layer (Fig.2 E2). As a result, the toluene permeance decreased from 26.0 l $m^{-2}h^{-1}bar^{-1}$ (0% EDA) to 0.6 l $m^{-2}h^{-1}bar^{-1}$ (2 % w/w EDA). At the same time, the retention of 10.000 g mol^{-1} PS increased only from 10% to 20%. Further increase of EDA concentration up to 5 % w/w (Fig.2 E3) resulted in a membrane with no toluene flux. When 20% w/w of EDA in bore liquid was used, delamination of the crosslinked layer occurred (Fig.2 E4) and the fiber became brittle and difficult to handle.

References

[1] N. Stafie, Poly(dimethyl siloxane) – based composite nanofiltration membranes for non-aqueous applications, Ph.D. thesis, University of Twente, Enschede, The Netherlands, (2004).

[2] T. He, M. Frank, M.H.V. Mulder, M. Wessling, Preparation and characterization of nanofiltration membranes by coating polyethersulfone hollow fibers with sulfonated poly(ether ether ketone) (SPEEK), J. Membr. Sci., 307 (2008) 62-72.

[3] K.K. Kopec, S.M. Dutczak, M. Wessling, D.F. Stamatialis, Chemistry in a spinneret - On the interplay of crosslinking and phase inversion during spinning of novel hollow fiber membranes, J. Membr. Sci., 369 (2011) 308-318.

Summary

This thesis describes preparation and characterization of membranes for organic solvent filtration (OSF). The main aim was developing membranes for solvent resistant nanofiltration (SRNF) with molecular weight cut-off below 500 g mol^{-1}. In Chapters 2 – 5, we prepare and characterize various membranes by either coating a polymeric layer on capillary / hollow fibre supports, crosslinking of commercial polyamide-imide membranes or spinning integrally skinned polyimide hollow fibres (HF) using chemistry in a spinneret process. In Chapter 3 we draw attention to important aspects of MWCO characterization in organic solvents such as selection of a proper solute and process conditions.

Chapter 2, "Composite capillary membrane for solvent resistant nanofiltration", describes the preparation and characterization of capillary α-alumina / poly(dimethylsiloxane) (PDMS) composite membranes. Viscosity and concentration of PDMS coating solutions are tailored to obtain thin coatings and limit pore intrusion. As a support, a commercial α-alumina capillary, with pore size of 800 nm on the outside and 20 nm on the inside, is used. The best composite capillary membrane is prepared by coating on the inside of the capillary. This membrane has stable performance for over 40 h in toluene, toluene permeance of 1.6 l $m^{-2}h^{-1}bar^{-1}$ and MWCO of 500 g mol^{-1}.

Chapter 3, "Important factors influencing molecular weight cut-off determination of membranes in organic solvents", discusses effects of solvent, solute, membrane properties, and of applied process conditions, on molecular weight cut off (MWCO) characterization. For this study a rigid porous membrane (hydrophobized zirconia) and a rubbery dense membrane (α-alumina / PDMS composite) are used. Behaviour of two solutes a stiff (polystyrene) and a flexible (polyisobutylene) is studied in a rather low (toluene) and high flux (n-hexane) solvents. The results show that, under applied experimental conditions, the MWCO of the PDMS membrane is mostly affected by solute-membrane and solvent-

membrane interactions. For the porous zirconia membrane the effects of concentration polarization and shear induced solute deformation are significant. For this membrane the retention of flexible PIB decreases dramatically at higher fluxes, whereas retention of the more rigid PS stays relatively constant. The results unmistakably show that the selection of solute markers and the interpretation of MWCO data in organic solvents require extreme caution.

Chapter 4, "New crosslinking method of polyamide-imide membranes for applications in harsh polar aprotic solvents", shows an easy crosslinking method of polyamide-imide (Torlon®) based membranes, using hexamethylene di-isocyanate. The crosslinked membranes are stable in N-methyl pyrrolidone which is a solvent of the non-crosslinked membrane. The created covalent bond there is thermally stable in contrast to state-of-the-art diamine crosslinked polyimide membranes. For this reason the crosslinked membrane can be potentially employed for high temperature applications. Besides, via the crosslinking process, separation characteristics of the new membrane can be tailored.

Chapter 5, "Chemistry in a spinneret to fabricate hollow fibres for organic solvent filtration", explores a new hollow fibre spinning method called "chemistry in a spinneret" to fabricate a membrane for organic solvent filtration (OSF). This method integrates the membrane formation and crosslinking reaction into a single step. The membranes studied in this chapter are based on P84 (Evonik) polyimide as a membrane forming polymer while the crosslinkeerpoly(ethylene imine) (PEI) is dissolved in the bore liquid. The prepared fibres have MWCO between 2500 – 3500 g mol^{-1} and toluene permeance in the range of 0.2 - 1.1 l m^{-2} h^{-1} bar^{-1}. The most stable membrane loses 20% of its mass after 11 days immersion in N-methyl-2-pyrrolidinone. The PEI crosslinking results in hydrophilization of the fibres and therefore makes them attractive for separations in alcohol systems. In fact, these fibres have high ethanol permeances (14.6 - 17.2 l m^{-2} h^{-1} bar^{-1}) and low rejections of polyethylene glycol (PEG) (14-23% of 4000 g mol^{-1}).

Chapter 6 discusses the main conclusions of this thesis and presents some reflections and outlook for future work.

Samenvatting

Dit proefschrift beschrijft de bereiding en karakterisering van membranen, die gebruikt worden voor filtratie van organische oplosmiddelen. De belangrijkste doelstelling is de ontwikkeling van membranen die bestand zijn tegen verschillende organische oplosmiddelen en toegepast kunnen worden voor (nano)filtratie van moleculen met een molecuulgewicht kleiner dan 500 g mol^{-1}, oftewel een "Molecular Weight Cut Off" (MWCO) < 500 g mol^{-1}. In de hoofdstukken 2-5 worden de bereiding en karakterisering beschreven van verschillende membranen via coaten van een polymere laag op een capillair / holle vezel of door crosslinking van commerciële polyamide-imide membranen of via het integraal spinnen van een polyimide holle vezel met verschillende structuren in de binnen en buiten laag van de vezel door gebruik te maken van het "chemie in een spinneret" proces.

Hoofdstuk 2, "Composiet capillair membranen welke bestand zijn tegen organische oplosmiddelen", beschrijft de bereiding en karakterisering van α-alumina vezel / Poly(dimethylsiloxane) (PDMS) composiet membranen. De viscositeit en de concentratie van de PDMS coatings oplossing zijn zodanig ingesteld om een dunne coating van een te realiseren met beperkte pore indringing in het support. Als support wordt een commercieel verkrijgbare α–alumina vezel (capillair) gebruikt met een porie diameter van 800 nm aan de buitenkant en een porie diameter of 20 nm aan de binnenkant. Het beste composiet membraan is bereid door het coaten van een PDMS laag aan de binnenkant van het alumina capillair. Dit membraan is voor meer dan 40 uur stabiel in tolueen, heeft een tolueen permeatie van 1.6 l m^{-2} h^{-1} bar^{-1} en een MWCO van 500 g mol^{-1}

Hoofdstuk 3, "Belangrijke factoren die de MWCO bepaling beïnvloeden van membranen in organische oplosmiddelen", beschrijft het effect van vier factoren op de MWCO karakteristieken nl het oplosmiddel, de te scheiden moleculen, membraan eigenschappen en de toegepaste procescondities. Voor deze studie is een rigide poreus membraan (hydrofoob zirconia) en een

rubberachtig dicht membraan (een α –alumina/PDMS composiet) gekozen. Het scheidings gedrag van twee polymere moleculen is geanalyseerd; een rigide molecuul (polystyreen: PS) en een flexibel molecuul (polyisobutylene: PIB) zijn bestudeerd in een oplosmiddel met lage flux (tolueen) en in een oplosmiddel met hoge flux (hexaan). De resultaten laten zien dat, onder de gekozen experimentele omstandigheden, de MWCO van het PDMS membraan het meeste beïnvloed wordt door interacties tussen de moleculen en membraan en de interactie tussen het oplosmiddel en membraan. Voor het poreuze zirconia membraan is er een significant effect van polarisatie condensatie en door afschuifspanning geïnduceerde vervorming van het molecuul. De retentie van het flexibele PIB molecuul neemt sterk af bij hogere fluxen, terwijl de retentie van het meer rigide PS molecuul constant blijft voor dit membraan. De resultaten laten duidelijk zien dat de selectie van de gekozen moleculen en de interpretatie van de MWCO data in organische oplosmiddelen extreme voorzichtigheid gebieden.

Hoofdstuk 4, "Nieuwe methodes voor crosslinking van polyamide-imide membranen voor toepassingen in extreme polaire oplosmiddelen", geeft een eenvoudige crosslinking methode voor de bereiding van polyamide-imide (torlon®) gebaseerde membranen door gebruik te maken van hexamethylene di-isocyanate. De gecrosslinkte membranen zijn stabiel in N-methyl pyrolidone dat het oplosmiddel is voor niet gecrosslinkte polyimide membranen. De gecreëerde covalente bindingen zijn thermisch stabiel, dit in tegenstelling tot de state-of-the-art diamine gecrosslinkte polyimide membranen. Hierdoor kunnen deze gecrosslinkte membraan mogelijk gebruikt worden voor toepassingen bij hoge temperaturen. Daarnaast kunnen de scheidingskarakteristieken van deze nieuwe membranen worden aangepast via het crosslinking proces.

Hoofdstuk 5, "Chemie in een spinneret om holle vezels ter fabriceren voor filtratie van organisch oplosmiddelen', verkent een nieuw holle vezel spinning methode genaamd "chemie in een spinneret" om een membraan voor organisch oplosmiddel filtratie (OSF) te fabriceren. Deze methode integreert de membraan vormings- en croslinkingsreactie in een enkele stap. De bestudeerde membranen in dit hoofdstuk zijn gebaseerd op de P84 (Evonik) polyimide als een

membraanvormend polymeer, terwijl de crosslinker poly (ethyleen imine) (PEI) is opgelost in de boor vloeistof. De bereide vezels vertonen een MWCO tussen 2500 - 3500 g mol-1 en een tolueen flux in de range van 0,2 - 1,1 l m^{-2} h^{-1} bar^{-1}. Het meest stabiele membraan verliest 20% van zijn massa na 11 dagen onderdompeling in N-methyl-2-pyrrolidinon. De PEI crosslinking resulteert in het hydrofoob maken van de vezels en maakt ze daardoor aantrekkelijk voor scheidingen in alcohol-systemen. In feite hebben deze vezels hoge ethanol permeatie (14.6 tot 17.2 l m-2 h^{-1} bar^{-1}) en een lage retentie van polyethyleenglycol (PEG) (14-23% van de 4000 g mol^{-1}).

Hoofdstuk 6 behandelt de belangrijkste conclusies van dit proefschrift en presenteert een aantal reflecties en vooruitzichten voor toekomstige werkzaamheden.

Acknowledgment

It has been a while since I started PhD, the scientific adventure of my life. Now, when the journey came to the end and I hold this book proudly in my hand, I would like to look back and express my gratitude to all the people who contributed to this work.

I owe my deepest gratitude to my promotor Prof. Matthias Wessling for giving me the opportunity to work on this interesting and challenging project. Thank you for your trust in my work, encouragement and all your support.

I wish to thank Dimitris, my assistant promotor. It would not have been possible to write this thesis without your guidance, support, motivation, endless scientific discussions and thousands of your corrections.

I would like to thank Prof. Jordan, my MSc promotor at Fachhochschule Münster. Five years ago you introduced me in membranes and now, it is a great honour for me that you agreed to be a member of my PhD graduation committee.

The next person, Bernd Krause, my supervisor during MSc project at Gambro Dialysatoren GmbH, is actually the one who has given me the final push to start PhD. Bernd, without you most likely I would not be here. Thank you!

Karina, my “favourite colleague” and friend! Yes, you are right, it is actually not clear who pulled / pushed whom during last six years. What is sure is that we both have managed! Thank you for all your support, motivation, endless hours of discussions (those scientific and less scientific) and kilometres of hollow fibres spun together ;). I am so happy to have you as my paranymph today. Thank you!

The MTG, IM and SFI.
First of all Greet, you are the basis of the MTG! It is still amazing for me how do you manage to find time for all of us. Thank you for all your help. Mieke and Louis, it was a great pleasure to work with you on this project. Special thanks to you both for translation of the “Samenvatting”. Lydia, I really appreciate your work you have done for me. I hope that you do not have nightmares because of “this stupid PDMS which gelated again”.
Harmen, we have spent so much time with each other and I enjoyed every minute of it. Thank you for all the scientific and non-scientific discussions. You were actually my SRNF and RI&E teacher. Now, with only one look at the set up, I can tell what will “possibly go wrong”.

Special thanks to my office colleagues, without you the PhD life would not have been so colourful. In Langezijds I shared the room with Katia, Srivatsa, Saiful, Clara; and in Meander with Saiful, Jorrit, Schwan, Hans, Mayur, Irdham, Sinem and Erik. Mayur, we are the best extreme-SRNF team ever! I enjoyed all the time we have spent together (NAMS, ICOM, OSN Leuven, OSN London). Thank you for being my paranymph.

John, I am so grateful for all your assistance in rebuilding my set ups. I have learned a lot from you and still believe that one day we will manage to go fishing together. My next thanks go to the most confusing office: Harmen, Herman, Erik I and Erik II. Herman, you were my great SEM and spinning teacher. Erik I (R.), I really appreciate your help with spinning and GPC analysis.

Many thanks to my students Yuanyuan and Catherine and “part time” students: Nick and Nadia. Catherine I really owe you, ¼ of the experiments of this thesis is done by you. Good luck to all of you!

I would like to thank all the MTG, IM and SFI members, particularly: David, Wojtek, Olga, Beata, Bas, Izabela, Didi, Enver, Can, Elif, Joris, Anne Corine, Yusuf, Jeroen and Jumeng.

Many thanks go to the entire Polish community, by some called “Polish mafia”: Kasia and Krzysiu, Karina, Asia and Wojtek, Agata and Wilco (almost Polish), Magda and Artur, Asia M., Kasia and Grzesiu and of course Ikenna - the person from north of Poland :-).

Great thanks to all my EMI colleagues: Antoine, Marcel, Harmen, Herman, Erik Rolevink and Erik van de Ven and especially Zandrie for his understanding during final months of writing my doctoral thesis.

I would like to show my gratitude to Petrus for his significant input in the project. We understand each other very well and I think we were quite a good team. I really enjoyed collaboration with you.

David and Yujia my dear roommates! We have had so much fun together, shared happy and difficult moments but the most important we were always supporting each other (despite all those teasing activities). By now I consider you as a part of my family. Thank you for sharing probably the most wonderful time of my life.

It seems unbelievable but besides science there was still time left for some extra activities. Bas, Nick, Willem and David, the core people of S.V. Lichtgeraakt, It was always a joy to put some lead down the range with you.

Na koniec chciałbym podziękować najważniejszym osobom w moim życiu, mojej rodzinie. Urszulo, Maćku i Marto dziękuję Wam za to, że zawsze mogłem liczyć na Was i Waszą pomoc. Mamo, Tato dziękuję Wam za wiarę we mnie, za umożliwienie mi studiów i wyrozumiałość w początkach mojej kariery chemicznej. Jestem wdzięczny Wam za wsparcie we wszystkich moich decyzjach.

Specjalne podziękowania kieruję do mojej ukochanej żony Danusi. Dziękuję za to, że byłaś moim oparciem szczególnie w ostatnich miesiącach pisania pracy. Dziękuję, że cztery lata temu zdecydowałaś się dołączyć do mnie i zamieszkać w Steinfurcie. Wiem, że nie była to dla Ciebie łatwa decyzja i tym bardziej jestem Ci za to wdzięczny. Dzięki Tobie moje życie nabrało sensu. Kocham Cię!